RESOLUTION OF THE DIMER BRIDGE OF MINUTE VIRUS OF MICE:
ROLES OF THE VIRAL NS-1 PROTEIN AND A HOST CELL FACTOR

by

Qingquan Liu

B.Sc. (Hon), M.Sc., Beijing Normal University

A THESIS SUBMITTED IN PARTIAL FULFILMENT OF

THE REQUIREMENTS FOR THE DEGREE OF

Doctor of Philosophy

in

THE FACULTY OF GRADUATE STUDIES

Department of Biochemistry and Molecular Biology

We accept this thesis as conforming to the required standard

THE UNIVERSITY OF BRITISH COLUMBIA

September, 1996

In presenting this thesis in partial fufilment of the requirements for an advanced degree at The University of British Columbia, I agree that the library shall make it freely available for reference and study. I further agree that permission for extensive copying of this thesis for scholarly purposes may be granted by the Head of my Department or by his or her representatives. It is understood copying or publication of this thesis for financial gain shall not be allowed without my written permission.

Department of Biochemistry and Molecular Biology

The University of British Columbia

2075 Wesbrook Place

Vancouver, Canada

V6T 1W5

Date: September 15, 1996

Abstract

Previous characterization of the terminal sequences of the Minute Virus of Mice (MVM) genome demonstrated that the right hand palindrome contains two sequences, each the inverted complement of the other. However, the left hand palindrome was shown to exist as a unique sequence (Astell *et al.*, Virology 54:171-177, 1985). The Modified Rolling Hairpin Model (MRHM) for MVM replication provided an explanation for how the right hand palindrome could undergo hairpin transfer to generate two sequences while the left end palindrome within the dimer bridge could undergo asymmetric resolution and retain the unique left end sequence (Astell *et al.*, ibid). The MRHM proposed that an initiating nick occurs on the parental viral strand of the A-half of the dimer bridge while a subsequent nick cuts the B-half of the dimer bridge (on the progeny viral strand).

This thesis describes studies on the *in vitro* resolution of the wildtype dimer bridge sequence of MVM using recombinant (baculovirus) expressed NS-1, the major nonstructural protein of MVM, and a replication extract from mouse LA9 cells. The resolution products are consistent with those predicted by the MRHM, thus providing support for this replication mechanism. In addition, mutant dimer bridge clones were constructed and used in the resolution assay. The mutant structures included removal of the "bubble" asymmetry of the dimer bridge, inversion of the sequence which was proposed to include the initiating nick site, and a two bp deletion within the A-half between the "bubble" sequence and putative initiating nick site of the dimer bridge. The resolution patterns of these mutant dimer bridge structures suggest that the resolution procedure of the dimer bridge proposed in the MRHM is likely incorrect, although some sequences within the dimer

bridge are likely responsible for asymmetric resolution and thus conservation of the unique sequence of the left hand hairpin of the MVM genome (Liu *et al.*, 1994).

In parallel studies described by others, the B-half (but not the A-half) of the dimer bridge was shown to be nicked site-specifically by a HeLa cellular replication extract supplemented with a HeLa cell nuclear extract containing expressed NS-1 (Cotmore and Tattersall, EMBO J. 13:4145-4152, 1994). Furthermore, it was predicted that host factor [possibly the activating transcription factor (ATF)] is required for the NS-1 nicking. One reason for this prediction is that mutation of an important nucleotide (the first C) in the putative ATF binding site (CGTCA) greatly decreased the nicking efficiency of the B-half dimer bridge (Cotmore and Tattersall, ibid).

Data presented in this thesis confirm that the B-half (but not the A-half) of the MVM dimer bridge is nicked site-specifically when incubated with crude NS-1 protein (expressed in insect cells) and mouse LA9 cellular replication extract. When highly purified NS-1 is used in this nicking reaction, there is an absolute requirement for the LA9 cellular extract, suggesting a cellular factor (or factors) is (are) required.

A series of mutations were created in the putative <u>h</u>ost <u>f</u>actor <u>b</u>inding <u>r</u>egion or HFBR of the B-half dimer bridge. Nicking assays of these B-half mutants showed that two CG motifs displaced by 10 nucleotides are important for nicking. Gel mobility shift assays demonstrate that a host factor(s) can bind to the HFBR and efficient binding depends on the presence of both CG motifs. Competitor DNA containing the wildtype HFBR sequence is able to specifically inhibit nicking of the B-half indicating that the host factor(s) bound to the HFBR is (are) essential for site-specific nicking to occur. These

data also suggest that it is highly unlikely that ATF is the host factor required for NS-1 nicking (Liu and Astell, Virology, 1996, in press.).

Table of Contents

List of tables

List of figures

Abbreviations

aa	amino acid
AAV	adeno-associated virus
ABF1	ARS binding factor 1
ACS	ARS consensus sequence
ARS	autonomously replicating sequence
ATF	activating transcription factor
aux	auxiliary element
BRL	Bethesda Research Laborotaries
CHO	Chinese hamster ovary
DHFR	dihydrofolate reductase
DTT	dithiothreitol
DUE	DNA unwinding element
EP	early palindrome
HFBR	host factor binding region
hRPA	human replication protein A
IR	initiation region
MCM	minichromosome maintenance
MF1	maturation factor 1
m.o.i.	multiplicity of infection
mRF	monomer replicative form
MRHM	modified rolling hairpin model
MVM	minute virus of mice
MVMi	minute virus of mice, immunosuppressive strain
MVMp	minute virus of mice,

	prototypical strain
ORC	origin recognition complex
ori	origin
PAGE	polyacrylamide gel electrophoresis
PCNA	proliferating cell nuclear antigen
Pol	polymerase
PYR	pyrimidine tract
NS	nonstructural protein
nt	nucleotide(s)
RFC	replication factor C
RPA	replication protein A
SAR	scaffold attachment region
SDP-2	polyclonal antibodies against NS-1
ssDNA	single-stranded DNA
SV40	simian virus 40
T Ag	SV40 large tumor antigen
VP	viral protein
wt	wildtype

Acknowledgements

Firstly, I would like to thank Dr. Caroline R. Astell, my supervisor, for the opportunity to work in her lab, all kinds of instruction and help. I am also impressed by her great patience and consideration. I owe thanks to Dr. Peter E. Candido and Michel Roberge, my committee members, for their useful advice and precious time spend on helping me. I also wish to express my deep appreciation for the support from my wife, Shili Duan. It is unfair if here I do not mention my baby daughter, Holly X. Liu, for her keeping quiet when I worked at home.

Thanks also go to Carl B. Yong for the preparation of recombinant baculovirus stocks containing either wild type or mutant NS-1 genes and culturing the Sf9 cells, Dr. Hitesh Jindal for AC6 antibody used in the purification of NS-1, Dr. E. A. Faust (McGill) for polyclonal antibodies to NS-1, Dr. R. Molday for antibodies to bovine rhodopsin, Gary Wilson for the stock Sf9 cells, and Dr. John J. Keity (University of Massachusetts Medical Center), Dr. Laurie H. Glimchev (Harvard School of Public Health), and Dr. Günther Schütz (German Cancer Research Center) for cDNA clones encoding murine ATF proteins. The helpful discussions from Dr. Patrick Tam, John Brunstein and Colin Harris, and the smiling faces from other members of Dr. Astell's lab will also be remembered.

I. Introduction

1.1. The significance of the studies of MVM

Studies on different viruses, all obligate intracellular parasites, are strikingly important for the elucidation of various aspects of the biochemistry and molecular biology of their host organisms. It is believed that the examination of each step in the life cycle of minute virus of mice, an autonomous parvovirus, can facilitate understanding the essential cellular processes of mammalian cells such as DNA replication and gene expression. Furthermore, these studies on MVM can contribute to the understanding of the molecular mechanisms of other related parvoviruses, for example, B19 parvovirus, a known human pathogen. Finally, it has been proposed that MVM can be used as a vector for tumor cell-targeted gene therapy (Dupont *et al.*, 1994 and references therein). This is because it has been shown that the prototype strain of MVM, MVMp, has a strong tropism for tumor cells and can inhibit induced tumorigenesis in laboratory animals, MVMp can grow in a variety of transformed human cells, human transformed cells are significantly more sensitive to the killing effect of MVMp than their untransformed precursors, and MVMp infection of the native host (mouse) is apathogenic as is the closely related parvovirus H 1 which can infect humans without apparent clinical consequences.

1.2. Selected model systems for the study of DNA replication: the replicators and associated proteins in eukaryotes

1.2.1. Replication of the Simian virus 40 (SV40) genome

1.2.1.1.   DNA sequences required for replication initiation

Replicators are the cis-acting elements required for the replication of genomes.   The replicator of SV40 (reviewed by Borowiec *et al.*, 1990; Depamphilis, 1993; Fanning and Knippers, 1992) consists of a 64 bp core origin from nt 5211 to nt 31 and two auxiliary elements, aux 1 and aux 2 (aux 1 extends 16 bp from nt 5208 to nt 5193 and aux 2 extends 41 bp from nt 32 to 72) (Fig. 1).

The core origin is both necessary and sufficient for the initiation of SV40 DNA replication. It has three essential domains: a 17 bp A/T rich domain (from nt 15 to nt 31) referred to as the AT-tract, a 27 bp central domain (from nt 5230 to 13) that is a perfect inverted repeat containing two GAGGC sequences in each arm of the palindrome, and a 10 bp domain (from nt 5211 to 5220) which is strongly biased toward purines on one strand and partially overlaps an imperfect inverted repeat (ie., early palindrome), hence it is referred to as the EP element or EP domain.   The function for each domain in the initation of SV40 DNA replication has been elucidated.   The central domain serves as the binding site of the SV40-encoded large T antigen (T Ag) through its 4 T Ag recognition sequences (GAGGC).   The EP element is the initial site for melting of the core origin and is essential for this opening of the DNA helix.   The AT-tract is required for further unwinding of the core origin since a mutant core origin with the AT-tract deleted cannot be unwound beyond the EP element (Parsons *et al.*, 1990).

Aux 1 has two GAGGC sequences. Aux 2 has 3 SP1 binding sites (GGGCGG) overlapping with 3 weak T Ag binding sites (GGGGC) and binding sites for other proteins.   These two auxiliary elements augment the

A :

| aux 2 | A / T | ← ← → → | | EP | | aux 1 |

core origin

B :

```
30              20              10         1    5240        5230        5220
|               |               |          |    |           |           |
TAATTTTTTTTTATTTATGCAGAGGCCGAGGCCGCCTCGGCCTCTGAGCTATTCCAGAAGTAGTG
ATTAAAAAAAATAAATACGTCTCCGGCTCCGGCGGAGCCGGAGACTCGATAAGGTCTTCATCAC
```

A/T rich domain   central domain   early palindrome

EP domain
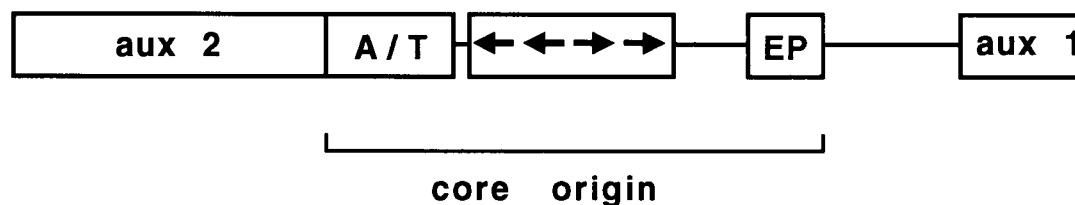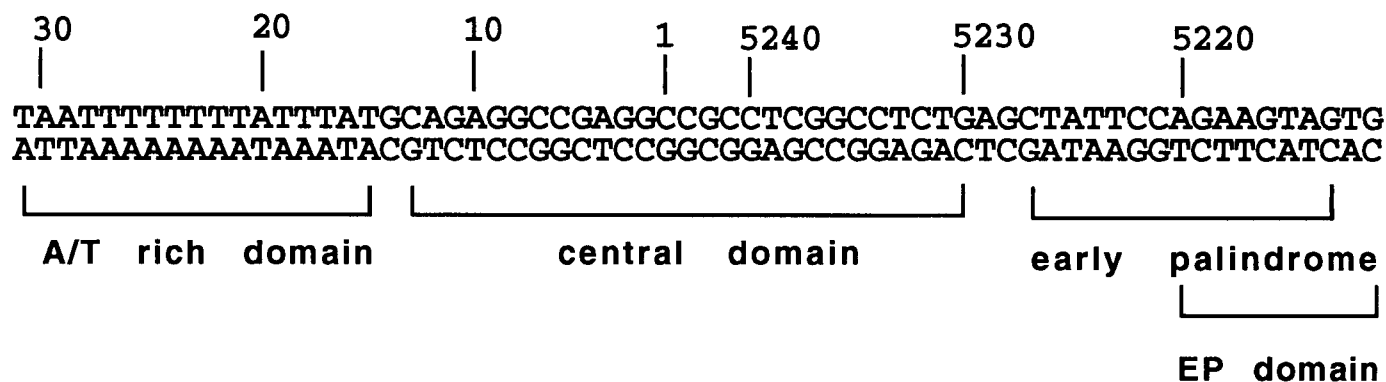
Fig. 1 A. **Organization of SV40 origin.** The origin for DNA replication of SV40 contains the 64 bp core origin from nt 5211 to nt 31 and two auxiliary elements, aux 1 and aux 2. Aux 1 extends 16 bp from nt 5208 to nt 5193 and aux 2 extends 41 bp from nt 32 to 72. The core origin contains three separate domains. The EP domain is 10 bp long (nt 5211-5220), the central domain is 27 bp (nt 5230-13) and the A/T rich domain is 17 bp long (nt 15 to 31). The four arrows in the central domain of the core origin represent the 4 T Ag binding sites (GAGGC) arranged in an inverted orientation as illustrated. The lines between boxes indicate sequences which are not specifically required for the DNA replication of SV40. **Fig. 1B. Nucleotide sequence of the SV40 core origin region** (see text for details).

replication efficiency of the ori core (Guo *et al.*, 1989; Gutierrez *et al.*, 1990). Aux 2 also constitutes part of the promoter for early gene expression.

1.2.1.2. Viral and host cell proteins required for the initiation of SV40 DNA replication

As mentioned above, the core origin binding protein is T Ag which recognizes the GAGGC sequences in the central domain (reviewed by Borowiec *et al.*, 1990). At physiological temperature, the binding of T Ag depends on the presence of ATP. DNAase I protection analysis indicates that in the presence of ATP, T Ag surrounds and spans the entire core ori (Deb and Tegtmeyer, 1987; Boroweic and Hurwitz, 1988a). Moreover, electron micrographs have shown that the bound T Ag is a bi-lobed structure (Dean *et al.*, 1987). In addition, by using scanning transmission electron microscopy it was observed that each lobe is a hexamer of T Ag molecules (Mastrangelo *et al.*, 1989). Dimethyl sulfate and potassium permanganate modification assays indicate that the bound T Ag causes untwisting of the AT-tract and melting of approximately 8 bp of DNA within the EP element (Boroweic and Hurwitz, 1988b; Boroweic *et al.*, 1991; Dean and Hurwitz, 1991).

In the presence of human single-stranded DNA binding protein (hRPA) and topoisomerase I or II, the double-hexamer complex of T Ag bound to the core origin undergoes a conformational change (Sengupta and Hurwitz, 1994) to form two T Ag hexamers (Wessel *et al.*, 1992; Sengupta and Boroweic, 1992) each of which acts as a helicase and unwinds the DNA outward from the core ori (Dodson *et al.*, 1987). As mentioned above, the AT-tract is required for further unwinding of the origin region (Dean *et al.*, 1987a; Brill and Stillman, 1989; Kenny *et al.*, 1989). This unwinding reaction appears

to be a required step in the replication of SV40 DNA based on DNA mutational analysis and pulse-chase experiments (Dean *et al.*, 1987a; Bullock *et al.*, 1989). Since some but not all non-cognate single-stranded binding proteins can substitute for hRPA, it has been suggested that the binding of hRPA to the unwound ssDNA is required for the unwinding of SV40 DNA, and that hRPA also interacts with T Ag and this interaction is important for the unwinding (Dean *et al.*, 1987b; Wold *et al.*, 1987; Kenny *et al.*, 1989). hRPA was later proven to physically interact with T Ag in the absence of DNA (Dornreiter *et al.*, 1992). The observation that a hRPA mutant can bind to the ssDNA but is limited in its ability to unwind DNA or interact with T Ag provides further evidence that T Ag may interact with hRPA during unwinding and this interaction is necessary (Lee and Kim, 1995). However, it has also been shown that RPA from *Saccharomyces cerevisiae* can support the unwinding (Brill and Stillman, 1989) but cannot bind to T Ag (Melendy and Stillman, 1993).

DNA polymerase α-primase is responsible for initiating primer synthesis in the unwound region (Ishimi *et al.*, 1988; Tsurimoto *et al.*, 1990; Weinberg *et al.*, 1990). The complex of T Ag, hRPA, DNA polymerase α-primase and the unwound origin region, which is ready for primer synthesis, is called the preinitiation complex. In the absence of DNA, it was shown that T Ag, hRPA and DNA polymerase α-primase can physically interact with one another (Dornreiter *et al.*, 1992 and references therein; Nasheuer *et al.*, 1992; Collins *et al.*, 1993; Dornreiter *et al.*, 1993) suggesting that in the preinitation complex these three proteins have complicated and delicate physical interactions which may be required for the initation of RNA primer synthesis and subsequently DNA synthesis. The following observations support this proposal:

some heterologous SSB proteins which can support the T Ag-catalyzed unwinding of DNA containing SV40 origin cannot substitute for human RPA for the initiation of primer synthesis (Matsumoto *et al.*, 1990); polymerase α−primase can inhibit the rate of the T Ag-dependent DNA unwinding from the SV40 origin in the presence of hRPA (Murakami and Hurwitz, 1993b); a cloned and expressed domain of human DNA polymerase α-primase, which physically interacts with T Ag, inhibits initiation of SV 40 DNA replication (Dornreiter *et al.*, 1993); primer synthesis at the SV40 ori region specifically requires human DNA polymerase α-primase and mouse DNA polymerase α-primase is not functional (Schneider *et al.*, 1994; Stadlbauer *et al.*, 1996); T Ag appears to facilitate the loading of DNA polymerase α-primase on human (but not *Saccharomyces cerevisiae* and *E. coli*) SSB-coated single-stranded DNA template through interaction with human RPA bound to the ssDNA (Melendy and Stillman, 1993); *Drosophila* DNA polymerase α-primase synthesizes DNA in a SV40 T Ag- and origin-dependent fashion in the presence of *Drosophila* RPA but not human RPA (Kamakaka *et al.*, 1994); T Ag stimulates the synthesis of primer by DNA polymerase α-primase on single-stranded DNA template and the stimulation can be eliminated by monoclonal antibodies that are directed against T Ag and block the binding of T Ag to the polymerase (Collins and Kelly, 1991); several monoclonal antibodies against DNA polymerase α-primase, which disturb the physical interaction of DNA polymerase α-primase with RPA or T Ag but do not inhibit the activity of DNA polymerase α-primase, abolish SV40 DNA replication *in vitro* (Dornreiter *et al.*, unpublished data). DNA polymerase α-primase can stimulate ATP-

dependent T Ag binding to the SV40 ori (Murakami and Hurwitz, 1993a).

Although these multiple protein:protein interactions have been elucidated, it is still poorly understood how the preinitiation complex is assembled and what its structure is. It has been shown that under *in vitro* conditions the synthesized primers are exclusively hybridized to the templates for lagging strand DNA synthesis, suggesting that lagging strand synthesis precedes leading strand synthesis (Bullock *et al.*, 1991; Murakami *et al.*, 1992; Denis and Bullock, 1993). The initiation sites for primer synthesis mapped *in vitro* are found to be located at several specific sites outside of the ori core rather than inside of the ori core (Bullock and Denis, 1995; Bullock *et al.*, 1991; Denis and Bullock, 1993). However, *in vivo* mapping experiments indicate that the earliest initiation event occurs within the core origin in the leading strand (Hay and Depamphilis, 1982). This contradiction suggests that *in vivo* factors such as chromatin structure or other unknown proteins can play a role on the initiation patterns of SV40 DNA replication.

T Ag likely binds to the aux 1 region as a dimer (Ryder *et al.*, 1986; 1985; Deb and Deb, 1989). Mutations in aux 1 that diminish T Ag binding also diminish activity of aux 1, suggesting that bound T Ag is required for the stimulation of ori core by aux 1 (DiMaio and Nathans, 1982; Myers and Tjian, 1980). Furthermore, the orientation and spacing of aux 1 relative to the ori core are critical, hence it is possible that there is direct protein-protein interaction between T Ag bound to aux 1 and T Ag bound to the ori core (Guo *et al.*, 1991). Sp1 and T Ag have been shown to bind to aux 2 (Kadonaga *et al.*, 1986; Delucia *et al.*, 1983). A synthetic oligonucleotide that contains 3 Sp1 sites can provide 75% of aux 2 activity while a synthetic oligonucleotide that contains 3 T Ag binding sites can provide 20% of the aux 2 activity. Therefore,

the combined effects of these two proteins can account for the activity of the intact aux 2 sequence (Guo and Depamphilis, 1992).

How do the bound proteins at the auxiliary sequences stimulate the ori core activity? Aux 2 is one part of the early gene promoter and initiation sites of the early gene transcripts are located within the ori core. However, α-amanitin, a specific inhibitor of RNA polymerase II and III does not have an effect on the initiation of SV40 DNA replication (reviewed by DePamphilis, 1993). Thus, stimulating transcription does not appear to be the reason aux 2 facilitates ori core activity. Moreover, the activity of auxiliary sequences does not depend on the presence of nucleosomes on the SV40 DNA (Guo *et al.*, 1989) suggesting the function of the bound proteins at aux sequences is not to impede the formation of nucleosomes at the ori core and make it more accessible to T Ag. Since saturating amounts of T Ag do not reduce the activity of aux 1 and aux 2, it seems that the bound proteins at auxiliary sequences do not facilitate the assembly of T Ag at ori core. Since deletion of the two auxiliary sequences reduces the efficiency of ori unwinding to the same extent that it reduces DNA replication (Gutierrez *et al.*, 1990), it seems probable that the two aux elements facilitate the unwinding of the ori core and that the proteins bound at aux 1 and aux 2 probably interact with T Ag bound at ori core, stimulating the activity of the ori core.

1.2.1.3.   The complete SV40 DNA replication system

The complete SV40 DNA replication system has been reconstituted with purified proteins: SV40 large T Ag, replication protein A (RPA), DNA topoisomerases I and II, DNA polymerase α-primase, replication factor C (RFC), the proliferating cell nuclear antigen (PCNA), DNA polymerase δ, maturation factor 1 (MF1), and DNA ligase I (Waga *et al.*, 1994). Although RNAase H was not included in this reconstitution system, the DNA ligase I used contained trace amount of RNAase H activity. RNAase H as well as MF1 have been demonstrated to be required for the removal of RNA on a synthetic lagging strand (Turchi and Bambara, 1993). Therefore, it is likely that RNase H is required for SV40 DNA replication.

The primers for both leading strand and lagging strand synthesized by DNA polymerase α-primase are ~24 nt long DNA chains covalently linked to oligoribonucleotides ~10 nt long (Bullock *et al.*, 1991; Nethanel *et al.*, 1988; Denis and Bullock, 1993; Bullock *et al.*, 1994; Nethanel and Kaufmann, 1990; Eki *et al.*, 1992). Following synthesis of the primers, RFC, PCNA and DNA polymerase δ are loaded onto the template-primer junction, replacing DNA polymerase α-primase (Lee *et al.*, 1991; Tsurimoto and Stillman, 1991a and b; Tsurimoto *et al.*, 1990; Weinberg *et al.*, 1990; Eki *et al.*, 1992). The processive RFC/PCNA/pol δ complex then extends the hybrid RNA-DNA primer to yield the continuously synthesized leading strand (Lee *et al.*, 1991; Tsurimoto and Stillman, 1991b; Tsurimoto and Stillman, 1989) and the discontinuously synthesized lagging strand (Okazaki fragments)(Waga and Stillman, 1994; Nethanel and Kaufmann, 1990). Of note is that the synthesis of both leading and lagging strands requires a switch from pol α to pol δ. It is also proposed that a dimer of DNA polymerase δ couples the DNA synthesis of both the leading strand and lagging strand (Waga and Stillman, 1994). MF1, a 5' to 3' exonuclease involved in the removal of the oligoribonucleotide primers, is

found to interact with PCNA and be stimulated by PCNA suggesting that the removal of the RNA primer by MF1 and the gap-filling DNA synthesis by DNA polymerase δ holoenzyme including PCNA and RFC is coupled through MF1 binding to PCNA (Li *et al.*, 1995). After the RNA primer is removed and gap-filling completed, DNA ligase I can seal the two juxtaposed Okazaki fragments (Waga et al., 1994)

1.2.2. Replication initiation in S. *cerevisiae*

1.2.2.1. Autonomous replicating sequences (ARSs)

In 1979, short genomic DNA sequences of *Saccharomyces cerevisiae* were identified as autonomously replicating sequences (ARSs) which confer on plasmids the ability to replicate extrachromosomally (Stinchcomb *et al.*, 1979; Hsiao and Carbon, 1979). In 1987, 2-dimensional gel techniques to examine replicative intermediates demonstrated that the ARS from the endogenous 2 micron plasmid as well as a chromosomal ARS1 colocalize with replication origins on plasmids (Brewer and Fangman, 1987; Huberman *et al.*, 1987). Using similar techniques, it has subsequently been shown that a number of other ARSs as well as ARS1 act as replication origins in their normal chromosomal contexts. However, only a subset of the sequences identified as ARSs act as replication origins in the chromosome, suggesting that chromosomal context can play a crucial role in origin function (Umek *et al.*, 1989). Since ARS1 is the ARS studied most extensively, a detailed description of ARS1 will be given below.

Through deletion analysis, it was found that the 130-bp ARS1 has 2 important functional domains, A and B (Celniker *et al.*, 1984)(Fig. 2A).

A:
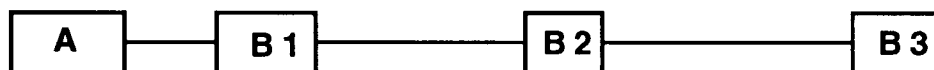
B:

Fig. 2A. The modular structure of ARS1. The 130 bp ARS1 includes the ACS-containing 15 bp domain A, the 13 bp subdomain B1, the 10 bp subdomain B2 and the 12 bp subdomain B3. **Fig. 2B. The modular structure of ARS121.** ARS121 contains the 35 bp domain A which contains the ACS, 72 bp AT-rich domain that is 8 bp away from domain A and is at the 3 '-end of the T-rich strand of ACS. In addition, there are two ABF1 (ARS binding factor 1) binding sites with the proximal one 169 bp from domain A . The space between the two ABF1 sites is 45 bp. ARS121 does not contain ARS1 B1- or B2-like sequences. The domains and subdomains described in **A** and **B** are indicated by labelled boxes. The thin lines represent the DNA sequences between the different domains, which are not specifically required for ARS activity.

Domain A is essential for ARS1 activity and contains one perfect match (11/11) to the ARS consensus sequence (ACS), 5'-(A/T)TTTA(T/C)(A/G)TTT(A/T)-3'. However, this 11 bp ACS can not substitute for the ~15 bp domain A for origin function (Marahrens and Stillman, 1992). Domain A is the major part of the recognition site of a protein complex called ORC (see below). Domain B, located on the 3' side of the T-rich strand of the ACS is essential for ARS1 function. It cannot be inverted or moved relative to the ACS (Diffley and Stillman, 1988) and is shown to be divided into 3 subdomains, B1, B2 and B3, using linker scanning analysis (Marahrens and Stillman, 1992; 1994)(Fig. 2). B1 (~13 bp) is immediately adjacent to and ~12 bp from domain A (Note, the sizes of the A domain and B subdomains have not been accurately determined yet so that the distances described here between different elements are estimations). The efficient binding of ORC to ARS1 required the presence of B1 (although B1 is not essential for low level of binding) *in vitro* and *in vivo* (Rowley *et al.*, 1995; Rao and Stillman, 1995). Point mutations in the 6 bp core of the B1 subdomain identify two important adjacent A nucleotides while the other 4 nucleotides seem to be mutable. Furthermore, mutation of the A nucleotide proximal to the ACS in the B1 subdomain decreases both ORC binding affinity and ARS1 origin function. In contrast, mutation of the A nucleotide distal to the ACS decreases the ARS1 origin function but has no effect on ORC binding (Rao and Stillman, 1995). Therefore, it is proposed that B1 may have two functions: stabilizing ORC and providing the binding site for another unknown factor involved in the initiation of DNA replication (Rao and Stillman, 1995).

B2 (~10bp) is a 9/11 match to the ACS in domain A and is ~28bp from B1. It was proposed that ORC might bind to B2 (Bell and Stillman, 1992;

Diffley and Cocker, 1992). However, single-point mutations at B2 do not affect ARS function (Rao *et al.*, 1994). Thus B2 probably does not provide a specific binding site for a protein but plays a structural role, such as a DNA unwinding element. Alternatively, B2 may bind a protein with low level of sequence specificity.

B3 (~12 bp) which is ~33 bp from B2 is the recognition site for the transcription factor ABF1. B3 can be replaced by the binding sites for other transcription factors (Marahrens and Stillman, 1992). Although domain B as a whole is essential, linker substitutes in any one of the three B subdomains only reduce origin function as detected by plasmid stability assays and do not completely inactivate ARS1 activity (Marahrens and Stillman, 1992; 1994).

Analysis of a large number of ARSs has revealed a common underlying architecture, ie., domain A flanked by stimulatory sequences (reviewed by Newlon, 1988; Campbell and Newlon, 1991; Rowley *et al.*, 1994)(Rao *et al.*, 1994; Rashid *et al.*, 1994; Theis and Newlon, 1994). Domain A which is essential for origin function and present in all of the ARSs contains a close or exact match to an 11 bp ARS consensus sequence (ACS). By itself, domain A is usually not sufficient for ARS function and the flanking sequences of domain A are required. The flanking sequences can be located on either the 5'- or 3'- side of the T-rich strand of the ACS. The ARS binding factor 1 (ABF1) binding site is found to be part of the flanking sequences in some but not all of the ARSs and it functions in an orientation- and distance-independent manner to enhance ARS activity (Walker *et al.*, 1990; 1991). Except for the ABF1 binding site, the other stimulatory sequences of ARSs tend to be AT rich but show little or no resemblance in sequence, size and relative location to the ACS. It will be interesting to learn why different ARSs of *S. cerevisiae* have different stimulatory sequences and how these sequences

help the ACS to achieve efficient ARS activity on the chromosomes. The modular structure of ARS121 is shown in Fig. 2B for comparision with ARS1 (Fig. 2A) (Walker *et al.*, 1990; 1991).

1.2.2.2. Proteins which bind to the ARS1 sequence

1.2.2.2.1. The origin recognition complex (ORC)

ORC was purified in 1992 (Bell and Stillman, 1992). It consists of six polypeptides of 120, 72, 62, 56, 53 and 50 kDa. The genes for these proteins have now been cloned (Bell *et al.*, 1995; Li and Herskowitz, 1993; Foss *et al.*, 1993; Loo *et al.*, 1995). Footprinting experiments both *in vitro* and *in vivo* indicate that ORC can bind to ARS1 and the protection extends across the A and B1 elements with the DNase I cleavage sites within B1 exhibiting a 10 bp periodicity. These data suggest that ORC binds ARS DNA in a bipartite manner with DNA in domain A embedded in ORC (and hence fully protected) and DNA in B1 contacting the protein surface leaving one side of the DNA helix exposed (Bell and Stillman, 1992; Diffley and Cocker, 1992). It has also been shown that the efficient binding of ORC with ARS1 requires the presence of B1 as well as domain A, *in vitro* and *in vivo* (Rowley *et al.*, 1995; Rao and Stillman, 1995). ORC is believed to play a role in replication initiation on the basis of several observations. Firstly, ORC binds *in vitro* to all the ARSs tested, generating similar footprints (Bell *et al.*, 1993). Secondly, mutations in the ACS that disrupt ORC binding *in vitro* also disrupt origin function *in vivo* (Bell and Stillman, 1992). Thirdly, *in vitro* patterns of DNase I protection and hypersensitivity on ARSs are very similar to the genomic footprints (Diffley and Cocker, 1992). Fourthly, mutations in ORC2

and ORC5 cause defects in S-phase entry and/or origin function (Bell *et al.*, 1993; Foss *et al.*, 1993; Fox *et al.*, 1995). Finally, 2D gel analysis has been used to demonstrate that orc2 and orc5 temperature-sensitive mutants are defective for the initiation of chromosomal DNA replication (Liang *et al.*, 1995).

Another important characteristic of ORC is that its specific DNA binding is dependent upon the addition of ATP (Bell and Stillman, 1992). From the cloned genes of ORC, it is known that two of the ORC subunits, Orc1 and Orc5, contain nucleotide-binding motifs (Bell *et al.*, 1995). ORC is also involved in transcription silencing at the silent loci, HMLa and HMRa, however the relationship between this role and its role in replication is not yet understood (Fox *et al.*, 1995; Kelly *et al.*, 1994; Dillin and Rine, 1995).

1.2.2.2.2.   ARS binding factor 1 (ABF1)

ABF1 binds to the B3 element of ARS1 and the related elements of some other ARSs. As discussed above, not all of the ARSs have an ABF1 binding site. There are two major reasons to suggest that ABF1 is involved in the intiation of DNA replication, *in vivo*. Firstly, the genomic footprint over the B3 element of ARS1 is very similar to the *in vitro* footprint generated with purified ABF1. Secondly, temperature-sensitive mutants of ABF1 exhibit elevated instability of plasmids containing ARS sequence (reviewed by Rowley *et al.*, 1994).

How does ABF1 function at the replication origins? Although this question is not answerable at this time, it is known that the ABF1 binding site at ARS121 can function in a distance- and orientation- independent manner (Walker *et al.*, 1990; 1991), the binding sites of other transcription factors can functionally substitute for the B3 element of ARS1 (Marahrens and Stillman,

1992), and B3 of ARS1 is not required for ORC binding *in vitro* and *in vivo* (Rao *et al.*, 1994; Bell and Stillman, 1992; Rowley *et al.*, 1995). DNA recognition events by ORC and ABF1 are most likely independent of each other and ORC and ABF1 probably do not interact directly (Rao and Stillman, 1995). It has been suggested that ABF1 may interact with RPA and contribute to the stabilization of the single-stranded DNA in the early stages of DNA replication (Rowley *et al.*, 1994).

In addition to their presence at some yeast replication origins, ABF1 binding sites have been identified in silencing elements and in the promoters of many genes where they function as upstream activating sequences. Hence ABF1 is a multifunctional protein (Diffley, 1992; Rowley *et al.*, 1994).

1.2.2.2.3.   Other ARS binding proteins

Several other proteins as well as ABF1 and ORC have also been shown to bind to ARSs. One of these is termed Core Binding Factor (CBF) (Estes *et al.*, 1992). The relationship between ORC and CBF is not yet clear, but it has been suggested that CBF is the same as ORC (Rao and Stillman, 1995). Another ARS binding factor is the general transcription factor, TATA binding protein (TBP), which can bind to the B2 element of ARS1 and is possibly involved in the ARS origin function (Lue and Kornberg, 1993). Furthermore, several ACS single-strand binding proteins have been identified, which bind *in vitro* to the T-rich strand of th ACS, but it is not known whether they play a role in yeast DNA replication (Rowley *et al.*, 1994).

1.2.2.2.4.   Proteins which bind to ORC

Although ORC can bind to ARS and is believed to be the initiator protein for DNA replication, no biochemical activities expected of an initiator protein besides origin binding have been detected, suggesting that the purified ORC is not sufficient for initiation and must cooperate with additional proteins and/or be modified posttranslationally to be fully active. This is supported by the observation that *in vivo*, there are two different states for the origins of DNA replication (Diffley *et al.*, 1994). At the end of M phase and throughout the G1 phase of the cell cycle, the origins of DNA replication are in a so-called prereplicative state in which the protein footprint at ARS is markedly different from the one generated with purified ORC. In S, G2 and most of the M phases, origins are in the so-called postreplicative state in which the protein footprint at ARS is very similar to the one with purified ORC.

Over the past three years, many proteins have been identified genetically to be involved in the initiation of DNA replication (Toyn *et al.*, 1995), but only two of them, Dbf4 and Cdc6, besides ORC, are found to physically interact with the origins or ORC (Dowell *et al.*, 1994; Liang *et al.*, 1995) and they are probably components of the prereplicative complex at ARS. Dbf4 was shown to bind to ARS1 *in vivo* using a one-hybrid assay. Efficient interaction required ORC binding at ARS1 and the presence of the B2 element. Whether Dbf4 interaction with B2 is direct or indirect is unknown (Dowell *et al.*, 1994). Dbf4 is a positive regulatory protein of a protein kinase, Cdc7, which is required for the initiation of DNA replication (Sclafani and Jackson, 1994). Thus, Cdc7 could be targeted by Dbf4 to phosphorylate and activate the ORC. Preliminary studies indicate that the Cdc7-Dbf4 complex phosphorylates ORC, *in vitro*, on Orc2 (Wang and Li, 1995).

Another protein, Cdc6, has been shown to be important for the initiaton of DNA replication and physically bind to ORC by co-immunoprecipitation (Liang *et al.*, 1995). Some time ago, Cdc6 was implicated in DNA replication (Hartwell, 1976) and in 1994, genetic evidence was provided showing Cdc6 was needed for formation of the prereplicative complex (Diffley *et al.*, 1994).

Other candidates bound to ORC or ARS sequence are some of members from the MCM (minichromosome maintenance) family (Maine *et al.*, 1984). These proteins have been genetically proven to interact with ORC (Wang and Li, 1995) although no physical interactions between the MCM proteins and ORC proteins are shown. These MCM proteins are located inside yeast nuclei immediately after mitosis, but are lost from nuclei once DNA synthesis begins (Huberman, 1995a). It is proposed that MCM proteins are the yeast licensing factors which explain why DNA replication only happens once in S phase (Toyn *et al.*, 1995).

1.2.3. Replication initiation in metazoan cells

Over the past 10 to 15 years, a considerable number of studies have been carried out to find out whether there are replicators for the initiation of chromosomal DNA replication in the metazoan cells, and if yes, what they are and how they function. It is clear that in differentiated cells there are cis-acting sequences (ie, replicators) which are needed for the site-specific initiations of DNA replication on the chromosomes. The key experimental evidence is the following: approximately 20 different systems have been exploited in the search for DNA replication origins on the chromosomes in different cell lines and species; putative initiation sites have been mapped to

either broad initiation zones or small loci (Huberman, 1995b; Gilbert *et al.*, 1995); that there is a nonrandom distribution of initiation sites on the chromosomes indicates indirectly the existence of replicators; direct evidence for the specific origin sequences are three systems in which the replicators have been identified: 1.), a chromosomal 8 kb deletion which contains the 2 kb initiation region (IR) or a 30 kb deletion about 50 kb 5' to IR in the human beta globin locus eliminates the initiation activity of this IR (Kitsberg *et al.*, 1993; Aladjem *et al.*, 1995); 2.), five short, partially redundant, cis-acting sequences (several hundred base pairs each) located within 8 kb of DNA have been shown to be essential for the amplification of the chorion gene cluster in the third chromosome of *Drosophila melanogaster* and the preferential 1 kb initiation region encompasses AER-d, one of the five cis-acting sequences; furthermore, one of these five elements, ACE (amplification control element), when placed at the other locations in the *Drosophila* genome, caused amplification of the adjacent DNA (DePamphilis, 1993; Carminati *et al.*, 1992); 3.), the 16 kb region including ori beta of the dihydrofolate reductase (DHFR) locus can be transplaced to other locations in the CHO genome where it functions as a DNA replication origin (Handeli *et al.*, 1989).

In contrast, DNA replication within the chromosomes of rapidly dividing cells in *Xenopus* and *Drosophila* early embryos appears to begin at randomly chosen sites (Hyrien and Mechali, 1993; Shinomiya and Ina, 1991). This may suggest that in the early embryos of any species initiation of DNA replication is random and that replicators are not functional despite their existence.

What constitutes a replicator in differentiated cells? From computer analysis (Dobbs *et al.*, 1994), it was shown that the 16 kb replicator of the DHFR locus, the 8 kb replicator of the chorion gene cluster and four other initiation

regions (which were not identified as replicators until now) from different gene loci all have DNA unwinding elements (DUE), and clusters of scaffold attachment regions (SARs) and ARS consensus sequences, a degenerate 21 bp consensus sequence, and pyrimidine tracts (PYR). Although the replicator of the human beta globin locus was not included in this analysis, it does contain the 21 bp consensus sequence (Aladjem *et al.*, 1995). However, it remains to be determined whether DUE, ACS, SAR, PYR and the 21 bp consensus sequence are functionally important. It is also very important that more replicators be identified and characterized to see whether they contain these consensus sequences or not.

How do the replicators function? One hypothesis is that the replicators in higher eukaryotes function as binding sites of unknown initiator proteins which unwind the DNA double helix. Subsequently, the initiation of DNA replication begins as has been shown to occur at the origin sequences in SV40 (Huberman, 1995b). The presence of DUE in the replicators described above and the identification of homologs of yeast ORC subunits in higher eukaryotes (Gavin *et al.*, 1995; Ehrenhofer-Murray *et al.*, 1995; Gossen *et al.*, 1995) support this hypothesis. Other evidence is that some DNA sequences can preferentially promote the autonomous replication of plasmids over others and these sequences have been shown to correspond to the initiation sites in chromosomes (Berberich *et al.*, 1995; Taira *et al.*, 1994; Virta-Pearlman *et al.*, 1993; Wu *et al.*, 1993; Todd *et al.*, 1995; McWhinney *et al.*, 1995). Furthermore, in many of the mapped initiation zones, preferred initiation sites have been found indicating that in these initiation zones, the initiation frequencies at different sites are different (Gilbert *et al.*, 1995). This hypothesis also suggests that random initiation of DNA replication in early embryos may be due to the high concentration of maternally derived initiator proteins.

However, there are conflicting reports that plasmid replication is virtually sequence-independent in transfected human or *Drosophila* cells, as is the DNA introduced into *Xenopus* eggs or egg extracts (Coverley and Laskey, 1994; Krysan *et al.*, 1993; Masukata *et al.*, 1993; Smith and Calos, 1995). These conflicting reports and the observations of broad initiation zones in which the initiation of DNA replication seems to occur throughout a large (several kilobasepairs) region (Huberman, 1995b) argue that in higher eukaryotes an initiation site does not need to have a specific sequence and hence replicators function differently than the replicators of simpler organisms. Hence, an alternate hypothesis has been proposed.

In this alternate hypothesis, it is suggested that in differentiated cells the replicators somehow play a role in determining chromatin structure which specifies which sites are active and which sites are inactive for initiation of DNA replication, and that the initiation sites of DNA replication have no sequence specificity (Coverley and Laskey, 1994). In early embryos the replicators are not necessary for the initiation of DNA replication because the chromatin structure is less compact than in differentiated cells (Montag *et al.*, 1988; Benavante *et al.*, 1985; Stick and Hauseu, 1985; Gilbert *et al.*, 1995). It has been shown that the human beta globin locus control region (LCR) affects chromatin structure (Grosveld *et al.*, 1987; Forrestor *et al.*, 1987; 1989) and a 30 kb deletion which includes the LCR eliminates initiation at IR (see above). It remains to be proven that the elimination of initiation activity at IR by the deletion of LCR is due to a change in chromatin structure determined by the LCR. Also it is believed that in yeast, chromatin structure can determine origin accessibility since nucleosome positioning affects the activity of ARS in plasmids (Simpson, 1990).

Both of the hypotheses described above cannot explain all of the available data. In order to learn how the replicators function, the precise identification and characterization of cis-acting sequences in the replicators and the interacting proteins will be required. Until now no proteins have been identified which bind to the replicators and have been shown to be functionally important for the initiation of DNA replication in metazoan cells.

1.3.   Introduction to Minute Virus of Mice (MVM), an autonomous parvovirus

MVM is a helper-independent virus which belongs to the genus parvovirus of the family Parvoviridae. A typical MVM virion contains a linear single-stranded DNA molecule encapsidated in a nonenveloped icosahedral capsid ~25 nm in diameter. MVM exists as two closely related strains, MVMp and MVMi, which share more than 96% of their genomes (Sahli *et al.*, 1985; Astell *et al.*, 1986). MVMp is the prototypical strain first isolated as a contaminant virus in mouse adenovirus stocks (Crawford, 1966). MVMi is an immunosuppressive strain discovered as a factor in the mouse lymphocyte culture fluids which strongly inhibited cell growth (Bonnard *et al.*, 1976). An important difference between these two strains is in their ability to infect cultured cells: MVMp infects only fibroblasts, while MVMi is restricted to T-lymphocytes (McMaster *et al.*, 1981; Tattersall and Bratton, 1983). MVMp does not cause apparent pathology when injected into its normal host, mouse, but it does cause dwarfing and death when injected into newborn hamsters (Kilham and Margolis, 1970; Brownstein *et al.*, 1992). In contrast, MVMi infection can be lethal in mice (Brownstein *et al.*, 1992;

Segovia *et al.*, 1995; Kapil, 1995). Since MVMp was studied in my thesis research, a detailed introduction to MVMp is given below.

1.3.1. Molecular biology of MVMp

1.3.1.1. The genome of MVMp

By using both physical and enzymatic techniques the MVMp genome was shown to be a single-stranded DNA molecule with hairpin structures at both ends (Bourguignon *et al.*, 1976). The complete sequence of the MVMp genome has been determined (Astell *et al.*, 1979; 1983a and b). From the DNA sequence it is known that the genome is 5149 nt long, and the 115 nt 3'-end and the 206 nt 5'-end have the potential to form hairpin structures. Furthermore, the 206 nt 5'-end region of the genome is not unique and exists as two different sequences (called flip and flop sequences, respectively). This results in two forms of the genome (Fig. 3). However, these two 5'-end sequences are related in that one is the inverted complement of another. In a population of MVM virions, the number of virions with a flip genome is approximately equal to the number of virions with a flop genome (Astell *et al.*, 1983b). For historic reason, the first nucleotide of the 3'-end of the viral genome is numbered as the first nucleotide (nt 1) and the first nucleotide of the 5'-end of the viral genome is numbered as the last nt (nt 5149), the genome is written 3' to 5' (Fig. 3), and the left and right ends of the genome refer to the 3'- and 5'-ends, respectively.

1.3.1.2. Structures of MVMp terminal hairpins

Flip:
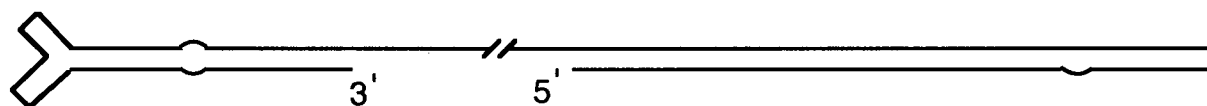
Flop:
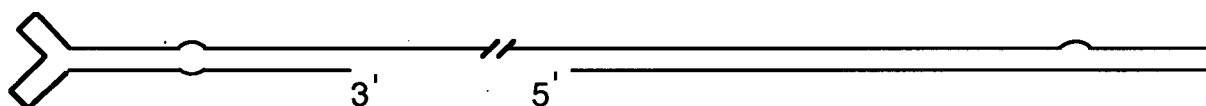
Fig. 3. The genome of the MVMp. The genome of MVMp is a linear single-stranded DNA molecule of 5149 nucleotides with hairpin structures at the two ends. Since the 5'-terminal hairpin can be as either a flip or flop sequence, there are two forms of genomic DNA (Flip or Flop) for MVMp (see text for additional details).

```
        A
        A G
        G   C
          G   C T
          G   G ─── 70
          C   C
60 ─── G   AGT   GTGCAGTGAATGCA  A A G
        C   G TCA  T CACGTCACTTACGT A G ACATGGTTGGTCAGTTCTAAAAAT 3'
        C   G                                          
        C   C         40        30        20        10
        G   G
        C   C
        G   C ─── 50
        C   G
        A
```

                                        90
                    80 | 100   110
                    | | | |

                                    TGTACCAACCAGTCAAGATTTTTACTA

Fig. 4. The structure of 3'-terminal hairpin of MVMp genome. The 115 nt
3'-terminal hairpin has a Y-like configuration with one long stem and two short
arms of different sizes. In the stem there is a bubble formed by the unpaired
nucleotides 25, 26, 89, 90 and 91.

The 3'-terminal hairpin is a stem plus arms or Y-shaped configuration of 115 nt (Fig. 4). Nucleotides 46 to 70 form the two arms with different sizes. In the stem there is a bubble formed by five unpaired nucleotides (nt 25, 26, 89, 90 and 91). This bubble was predicted to play an essential role for the asymmetric resolution of the dimer bridge during DNA replication of MVMp (see below) (Astell et al., 1985). The 3'-end hairpin is not related to the 5'-end hairpin in sequence. Moreover, the DNA sequence of the 3'-hairpin is unique in contrast to the sequence heterogeneity (flip and flop) of the 5'-end hairpin.

Although the DNA sequences of the flip and flop forms of the 5'-terminal hairpins are different, both of them can assume a very similar hairpin structure since the flip sequence (also called flip orientatation) is the inverted complement of the flop sequence (also called flop orientation). The 206 nt 5'-terminal hairpin arranged with the maximum number of base pairs is an extended stem with a bubble (Fig. 5). Recently, the mismatched nucleotides in this bubble were shown to be required for efficient viral DNA replication (Costello et al., 1995). It is also possible that the 5'-hairpin can form a stem structure with two major arms plus a smaller one because of the presence of an internal palindrome within the 206 nt sequence. Deletion mutants with the potential "stem plus arms" structure eliminated but the simple hairpin retained are not able to replicate in vivo, indicating the apparent requirement for the formation of the "stem plus arms" hairpin structure (Salvino et al., 1991). However, in a in vitro replication system, it has been suggested that it is the extended stem structure not the "stem plus arms" structure which can prime the initiation of DNA replication for the complementary strand of viral DNA (Cossons et al., 1996).

Fig. 5A:

```
              4944                                              4993
              |                                                |
       3' TTGGTAATCATAATGATACAAAAATCCCACCCTCCCACCCTCTATGTACACAAG
         5' ATTAGTATTACTATGTTTTTAGGGTGGGAGGGTGGGAGATACATGTGTTC
            |                                                |
          5149                                             5100
```

B:

```
   4994
   |
                                               A G A
   CGATACTCGCTTGACCATGACCAACCAACG                 CGAGTTGGTTGGTCTGGCCG T      FLIP
   GCTATGAGCGAACTGGTACTGGTTGGTTGC ——— GCTCAACCAACCAGACCGGC T T
   |
   5099
```

C:

```
   4994
   |
   CGATACTCGCTTGACCATGACCAACCAACG ——— CGAGTTGGTTGGTCTGGCCG A
                                                              A    FLOP
   GCTATGAGCGAACTGGTACTGGTTGGTTGC T   GCTCAACCAACCAGACCGGC A
                                   T C T                      A
   |
   5099
```

D:

```
        G
      A   A
      G C
      C G
          A
      |
      A T  G
      A T
      C G
      C G
      A T
      A T
      C G
4994  C G
|     A T
CGATACTCGCTTGACCATG  CTGGCCG T
GCTATGAGCGAACTGGTAC  GACCGGC  T
|          T A          T
5099       G C
           G C
           T A
           T A
           G C
           G C
           T A
           T A
            G C
          C     T
            G C
```
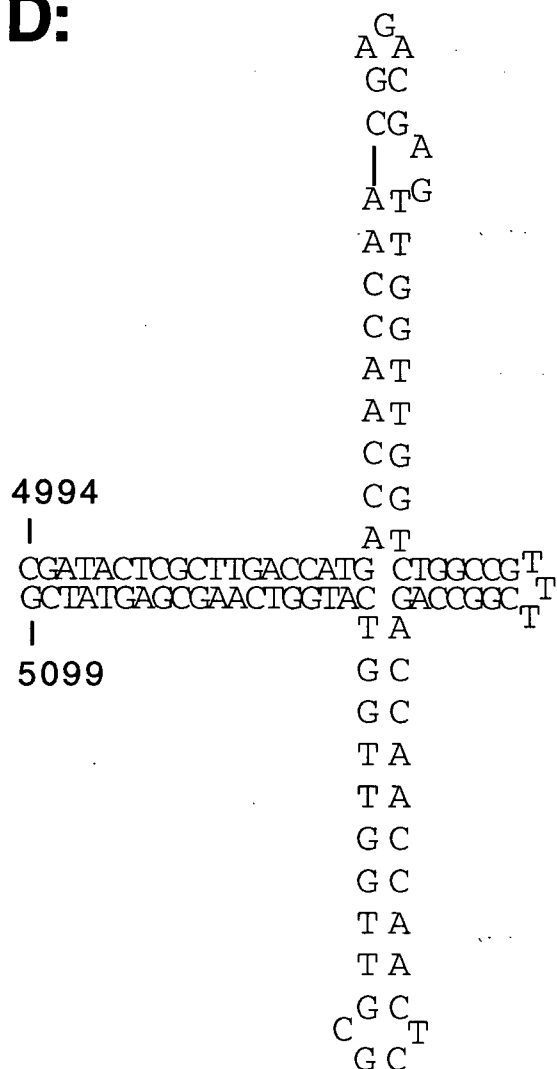
STEMS PLUS ARMS(FLIP)

Fig. 5. The nucleotide sequence and configurations of 5'-terminal hairpin of the MVMp genome. There are two kinds of sequences (flip and flop) for the 206 nt 5'-terminal hairpin. The flip is the inverted complement of the flop. Both flip or flop sequence can assume two kinds of configurations: extended stem or "stems plus arms". The flip form with extended stem configuration is the double-stranded sequence shown in A connected to the double-stranded sequence shown in B. The flop form with the extended stem configuration is the double-stranded sequence shown in A connected to the double-stranded sequence shown in C. The double-stranded sequence in A plus the double-stranded sequence in D is the "stems plus arms" configuration of the flip form. The "stems plus arms" configuration of the flop form is not shown here.

1.3.1.3.   Transcripts and primary translation products of MVMp

All of the transcripts of MVMp are complementary to the MVMp virion strand, hence its definition as a minus strand. Presumably a double-stranded replicative form is the actual template for transcription. MVMp has two promoters, P4 (at map unit 4) and P38 (at map unit 38) driving synthesis of two overlapping transcripts (Fig. 6)(Pintel et al., 1983; Cotmore and Tattersall, 1987). The P4 transripts and P38 transcripts start, respectively, at nucleotides 201 and 2005 (Ben-Asher and Aloni, 1984). Both of them are polyadenlylated and the polyadenylation signal is at nt 4885 (Clemens and Pintel, 1987). Based on the different sizes of spliced transcripts, the transcripts driven by P4 are divided into two major classes, R1 (4.8 kb) and R2 (3.3 kb), and the transcripts from P38 are designated as R3 (3.0 kb).

Between map units 46 and 48, there are two potential splicing donor sites (nt 2280 and 2316 in the MVMp genome) and two potential splicing acceptor sites (nt 2377 and 2399). However, sequence analysis of MVM cDNAs indicated that only three splice combinations are found in the viral transcripts and the splice combination, 2316 to 2377, is not detected (Morgan and Ward, 1986; Jongeneel et al., 1986). All of the three splice combinations can be found in R1, R2 and R3.

Using an in vitro translation system, R1 was shown to encode the nonstructural protein, NS-1 (Cotmore et al., 1983; Cotmore and Tattersall, 1986). Since the start and termination codons for NS-1 are at nt 261 and 2277, all three spliced forms of the R1 transcript should generate an identical protein. All of the spliced R2 transcripts have an large intron between nt 514 and nt 1990 removed (Jongeneel et al., 1986). R2 encodes the nonstructural protein NS-2 (Cotmore and Tattersall, 1986). The start codon is at nt 261 as is
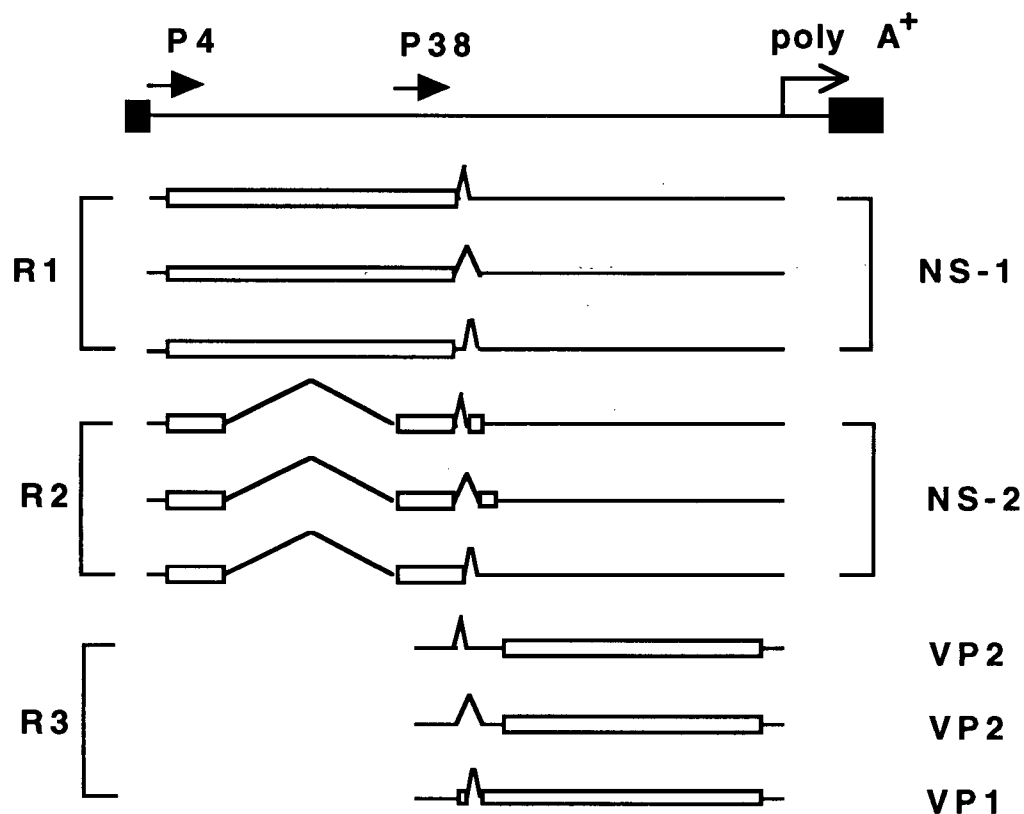
Fig. 6. The gene expression pattern of MVMp. The top line indicates the MVMp genome with the hairpin sequences (black boxes) at the two ends. There are two promoters (P4 and P38) at map units 4 and 38, respectively, of the genome. All of the transcripts share the same polyadenylation signal at nt 4885 and three combinations of splicing between map units 46 and 48. R2 transcripts encoding NS-2 all have a large intron between nt 514 and nt 1990 removed. Open boxes represent the coding region. R1 transcripts encode the same NS-1 protein molecule. R3 transcripts encode VP1 or VP2, depending on the splicing pattern.

the case for NS-1, thus NS-1 and NS-2 share the same 84 aa N-terminal sequence. The three splice forms of the R2 transcripts between map units 46 and 48 result in three NS-2 proteins with different C-terminal aa sequences (Cotmore, 1990). One of the three spliced R3 transcripts encodes the minor capsid protein VP1, the start codon for which is at nt 2286 (Labieniec-Pintel and Pintel, 1986). The other two R3 transcripts in which the start codon for VP1 is spliced out encode the major capsid protein VP2. The start codon for VP2 is at nt 2794 (Labieniec-Pintel and Pintel, 1986). VP1 contains the entire aa sequence of VP2 and both of them share the same termination codon at nt 4555 (Labieniec-Pintel and Pintel, 1986). From the above description, it is obvious that differential splicing can determine the proportions between NS-1 and NS-2 molecules and between VP1 and VP2 synthesized in the infected cells.

1.3.1.4. Viral proteins:

1.3.1.4.1. The nonstructural proteins, NS-1 and NS-2.

NS-1 is the major nonstructural protein of MVMp. This protein has been shown to be essential for the replication of the MVMp genome since a frameshift mutation in the NS-1 coding region blocked replication (Merchlinsky and Ward, personal communication). It has also been shown that NS-1 can enhance transcription from both the P4 and P38 promoter (Doerig et al., 1988; 1990). Thus, like many nonstructural proteins from other viruses, NS-1 is a multifunctional protein.

From the open reading frame of R1 transcripts, it is known that NS-1 consists of 672 aa (Astell et al., 1983b; Cotmore et al, 1983). NS-1 is a nuclear

phosphoprotein (Cotmore and Tattersall, 1986). The phosphorylation of the MVMp NS-1 is exclusively on serine residues. Trypsin digestion and peptide analysis of NS-1 from infected mouse cells indicate there are at least 18 phosphopeptides (Jindal and Astell, unpublished results). However, the role of the phosphorylation of NS-1 is unknown.

The nuclear localization signal of NS-1 is a bipartite lysine-rich motif from aa 194-216 (KK(X)$_{18}$KKK) (Nuesch and Tattersall, 1993). Furthermore, NS-1 is found to form oligomers as mutant NS-1 without the nuclear localization signal can be cotransported into the nucleus with wildtype NS-1 or a C-terminal deletion mutant of NS-1 (aa 1-605) (Nuesch and Tattersall, 1993).

Computer analysis of parvovirus proteins identified a 135 aa sequence (aa 389-524) in NS-1 of MVMp, which is conserved among the large nonstructural proteins of all vertebrate parvoviruses (Astell et al., 1987). Within this conserved sequence, there is a purine nucleotide binding motif. It was shown that purified NS-1 expressed in insect Sf9 cells is an ATP binding protein, ATPase and an ATP-dependent DNA helicase (Wilson et al., 1991; Jindal et al., 1994).

In the modified rolling hairpin model for the MVM genome replication (Astell et al., 1985 and also see below), NS-1 was proposed to nick at specific sites on the DNA replication intermediates and then covalently bind to the resulting phosphate group at the 5'-end of the DNA. Comparison of the sequences of proteins involved in a rolling circle type DNA replication (eg., the gene A protein of phage ϕx 174) revealed that they share two motifs, YuxK and HuHuuu (x=any aa, u=hydrophobic residues). Furthermore, the Y residue in the YuxK motif is predicted to be the aa residue covalently bound to the 5'-end of the nicked DNA and the two H residues are predicted to be

involved in metal binding (Ilyina and Koonin, 1992). In NS-1 of MVMp, the conserved Y residue is predicted to be Y188 and the conserved H residues, H129 and H131, respectively.

Prior to the studies reported in this thesis, it was known that the protein bound to the 5'-end of MVM DNA (replication intermediates and single-stranded viral DNA) was NS-1 (Gunther and Tattersall, 1988; Cotmore and Tattersall, 1989; Cotmore and Tattersall, 1988). However, whether Y188 of NS-1 was involved in the covalent linkage and whether the two H residues are important for the NS-1 function were unknown. Analysis of the chemical stability of the bond between the protein and DNA suggested that NS-1 is linked via a phosphotyrosine bond and not a phosphothreonine or phosphoserine bond (Chow *et al.*, 1986; Cotmore and Tattersall, 1988). Moreover, mutations of the tyrosine residues 188, 197, 210, 310 or 422 to phenylalanine in NS-1 resulted in mutant proteins which were unable to support replication, suggesting one (or more) of these residues is the candidate tyrosine involved in the covalent linkage (Skiadopoulos and Faust, 1993).

As mentioned above, NS-1 is also a transcriptional activator. Analysis of the ability of various Gal4-NS-1 or Lex-NS-1 fusion proteins to stimulate various target promoters in which multiple Gal4 binding sites or LexA operator sequences have been introduced within the promoter sequences has shown that the transactivation domain is the C-terminal 88 residues (Krady and Ward, 1995; Legendre and Rommelaere, 1994; Harris and Astell, 1993). This is supported by the observations that most mutations in the NTP-binding domain of NS-1 yield transcriptionally active NS-1 mutants, although they are inactive for replication (Jindal *et al.*, 1994). Previously, the efforts by different labs to determine whether NS-1 can bind to the double-

stranded DNA from MVMp failed to detect specific binding. However, recently, using an immunoprecipitation procedure, NS-1 was shown to be a sequence-specific DNA binding protein which can bind to the ACCAACCA sequence of the duplex 3'-palindrome of MVMp (Cotmore *et al.*, 1995) and to the P38 promoter (Christensen *et al.*, 1995). Binding of NS-1 to the P38 promoter is required for NS-1 transactivation (Lorson *et al.*, 1996).

NS-2 proteins are a family of proteins with different C-terminal sequences. The NS-2 proteins seem to be involved in many processes in the MVMp life cycle. However, relatively little is known about how these proteins function. NS-2 is not essential for the life cycle of MVMp in rat, hamster and human cell lines, but seems to be required for efficient DNA replication and virus production in murine cells (Cater and Pintel, 1992; Naeger *et al.*, 1990) in which NS-2 appears to be involved in the folding of capsid proteins and progeny ssDNA synthesis (Naeger *et al.*, 1990; 1993; Cotmore *et al.*, 1995b). NS-2 is also believed to be involved in the translation of viral proteins because it was found that although the levels for both viral proteins and viral mRNA were significantly reduced in the mouse LA9 cells infected with MVMp containing a NS-2 mutation compared with wt MVMp infected LA9 cells, the viral protein levels were reduced more than viral mRNA levels (Naeger *et al.*, 1993).

NS-2 of MVMi is also involved in pathogenesis since mice infected with wildtype MVMi die while mice infected with mutant MVMi in which the NS-2 cannot be synthesized are asymptomatic (Brownstein *et al.*, 1992). NS-2 can be phosphorylated and phosphorylated NS-2 is found exclusively in the cytoplasm. Whereas nonphosphorylated NS-2 can be found in both the cytoplasm and nucleus (Cotmore and Tattersall, 1990). The half life of NS-2 is ~1 hr which is significantly shorter than that of NS-1 (>6 hr). All three NS-2

proteins have the same stability, phosphorylation and distribution patterns so that there is as yet no indication that different NS-2 proteins have different functions (Cotmore and Tattersall, 1990).

1.3.1.4.2. The structural proteins, VP1, VP2 and VP3

There are three capsid proteins, VP1 (83 KDa), VP2 (64 KDa) and VP3 (61 KDa). In full MVMp virus particles VP1 constitutes ~15-18% of the protein mass. The amounts of VP2 and VP3 vary inversely in different preparations of full particles (Tattersall *et al.*, 1976). VP3 is absent in empty particles in which again VP1 is 15-18% of the protein mass (Tattersall *et al.*, 1976). *In vitro* translation of mRNA isolated from MVMp infected cells yields VP1 and VP2 in addition to NS-1 and NS-2, suggesting that VP1 and VP2 are primary translation products (Cotmore *et al.*, 1983). Pulse-chase experiments suggest that VP3 is the proteolytic product of VP2 following encapsidation (Tattersall *et al.*, 1976; Clinton and Hayashi, 1975). Peptide map analysis of the capsid proteins supports this notion and also indicates that the cleavage site is approximately 30 aa from the N-terminus of VP2 (Tattersall *et al.*, 1977).

MVMp productively infects fibroblasts but not T cells while MVMi shows the converse tropism (McMaster *et al.*, 1981; Tattersall and Bratton, 1983). However, transfected fibroblasts yield similar numbers of infectious virus particles regardless of which MVM infectious clone is introduced, suggesting that permissiveness or restriction is mediated by the infecting virus particles (Gardiner and Tattersall, 1988a). The observation that virions of the two strains (p and i) compete for the binding to either cell type indicates that the restriction is not at the level of a cell surface receptor (Spalholz and

Tattersall, 1983). Through studies with interstrain recombinant viruses, the host range-specific determinant has been mapped to a small sequence within the capsid coding region shared by VP1 and VP2 (Antonietti *et al.*, 1988; Gardiner and Tattersall, 1988a; 1988b), and it has also been shown that two aa substitutions of MVMi are sufficient to confer fibrotropism (Ball-Goodrich and Tattersall, 1992). Recently, by using recombinant virions consisting of various combinations of VP1 and VP2 from MVMp and MVMi to infect fibroblasts, it was shown that the presence of VP2 but not VP1 from MVMp is necessary to enable infection of fibroblasts (Maxwell *et al.*, 1995). Based on these observations, it is concluded that the tropism of MVM strains is determined by the interaction of intracellular factors with a VP2 domain. However, it is not known what the intracellular factor is and at which stage of the viral replication cycle it acts.

Empty capsids can bind to the 3'-end hairpin structure of MVM viral replicative form DNA (Willwand and Hirt, 1991). Similar observations have been made for the autonomous parvoviruses, Aleutian mink disease virus and bovine parvovirus (Metcalf *et al.*, 1990; Willwand and Kaaden, 1990). It has been suggested that the binding of the parvovirus RF DNA 3'-end to the empty capsid serves for both synthesis of progeny strands and their concomitant encapsidation, and a model for this process has been proposed (Willwand and Kaaden, 1990).

Mutation studies with an infectious clone indicate that VP2, by itself, is sufficient and necessary to form capsid structures which can bind to the 3'-end hairpin structure, and accumulate and encapsidate viral ss DNA (Willwand and Hirt, 1993; Tullis *et al.*, 1993). However, the resulting virus particles are not infectious suggesting VP1 is required for infection. Since the VP2 virion can bind to the cell surface as efficiently as wildtype (VP2 and VP1) capsid, no

initiation of DNA replication is detected in the cells infected with VP2 virions and capsid protein is not required for the initiation of viral DNA replication, it is believed VP1 plays a role during virus entry, nuclear transport or uncoating subsequent to cell binding and prior to the initiation of DNA replication (Tullis *et al.*, 1993). VP1 contains an additional N-terminal sequence rich in basic residues as well as the entire VP2 protein sequence (Tattersall *et al.*, 1977; Labieniec-Pintel and Pintel, 1986). Since VP1 in the virus particles is resistant to proteolytic digestion, it has been suggested that the N-terminus remains on the interior of the capsid and interacts with the ss genomic DNA in the capsid (Tattersall *et al.*, 1977).

As mentioned above, VP3 is derived from the cleavage of VP2 once the particle is assembled. The ratio of VP2 to VP3 depends on the postinfection time: at early times VP2 is predominant, but late in the infection VP3 is the major form (Tattersall *et al.*, 1976). 2-D gel analysis of protein species from empty capsids, the premature full particles and mature particles strongly suggests that posttranslational modification (especially, phosphorylation) of VP2 plays a role in the formation of VP3 (Santaren *et al.*, 1993). From studies with parvovirus H1, it is known that particles are equally infectious regardless of their VP2/VP3 protein content (Paradiso, 1981). Conversion of VP2 to VP3 for MVMp can also take place during virion internalization (Santaren *et al.*, 1993). The function of VP3 in the virus particle remains to be investigated

1.3.2. A model for MVMp DNA replication: the modified rolling hairpin model.

Until recently, the most widely accepted model for MVMp replication was the modified rolling hairpin model (MRHM) proposed in 1985 (Astell *et al.*, 1985) (Fig. 7). This model proposed that the initial step for replication is for the 3'-terminal hairpin to initiate synthesis of a monomeric duplex replicative form (mRF). This mRF is amplified by subsequent round of DNA strand displacement synthesis primed by the 3'-end of the viral complementary strand, resulting in the formation of a dimeric RF intermediate. The dimer RF is resolved at the junction fragment (called the dimer bridge) resulting in two momomers. This process requires site-specific nicking, strand displacement DNA synthesis and nicking and ligation. Synthesis of progeny genomes with two alternate sequence orientations at the 5'-terminal and a unique sequence at the 3'-terminal occurs by strand displacement synthesis and hairpin transfer (originating at the 5'-end).

As mentioned above, this model contains two important mechanisms: hairpin transfer and resolution of the dimer bridge. The hairpin transfer mechanism can explain the heterogeneity of the 5'-end hairpin of MVMp genomes and was first proposed to explain how double-stranded linear DNA molecule with terminal palindromes can replicate their 5'-ends (Cavalier-Smith, 1974). It was an integral mechanism in the original rolling hairpin model for the DNA replication of parvoviruses (Tattersalland Ward, 1976). The resolution mechanism of the dimer bridge as proposed in the MRHM can explain the unique sequence at the 3'-end hairpin.

1.3.2.1. The hairpin transfer mechanism

The hairpin transfer mechanism as proposed in the MRHM is illustrated in Fig. 8. The DNA molecule in line 1 corresponds to the right end
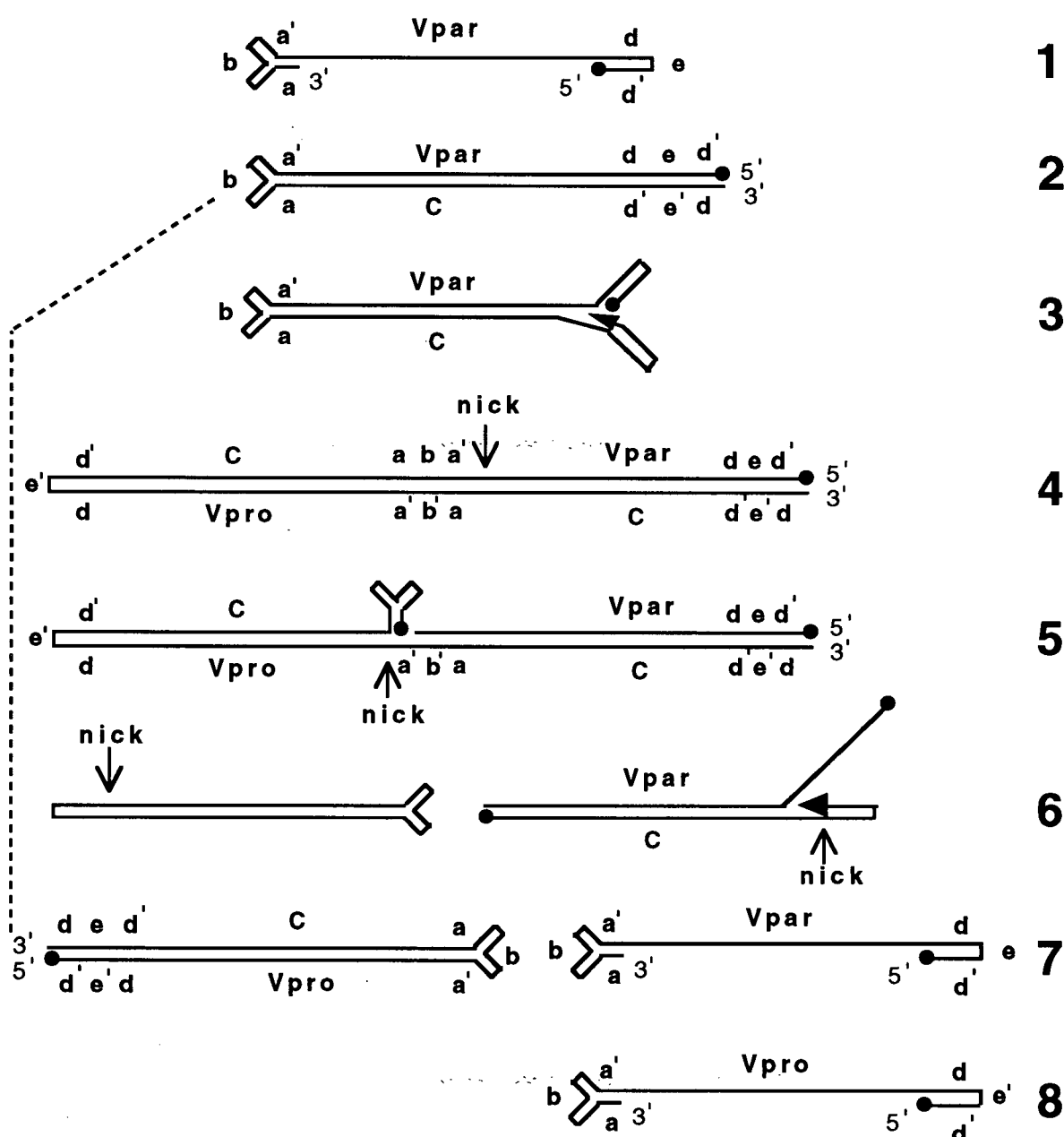
Fig. 7. The modified rolling hairpin model for the DNA replication of MVMp. a b a' and d e d' indicate the 3'- and 5'- terminal hairpin sequences, respectively. Vpar and Vpro indicate the parental and progeny viral strands, respectively. The black circles represent the viral protein NS-1. C indicates the complementary strand. The vertical arrows point to the nick sites and the horizontal arrows indicate the direction of 3'-end priming of DNA synthesis. The dashed lines indicate that the monomer replicative form in line 7 can re-enter into the DNA replication cycles.
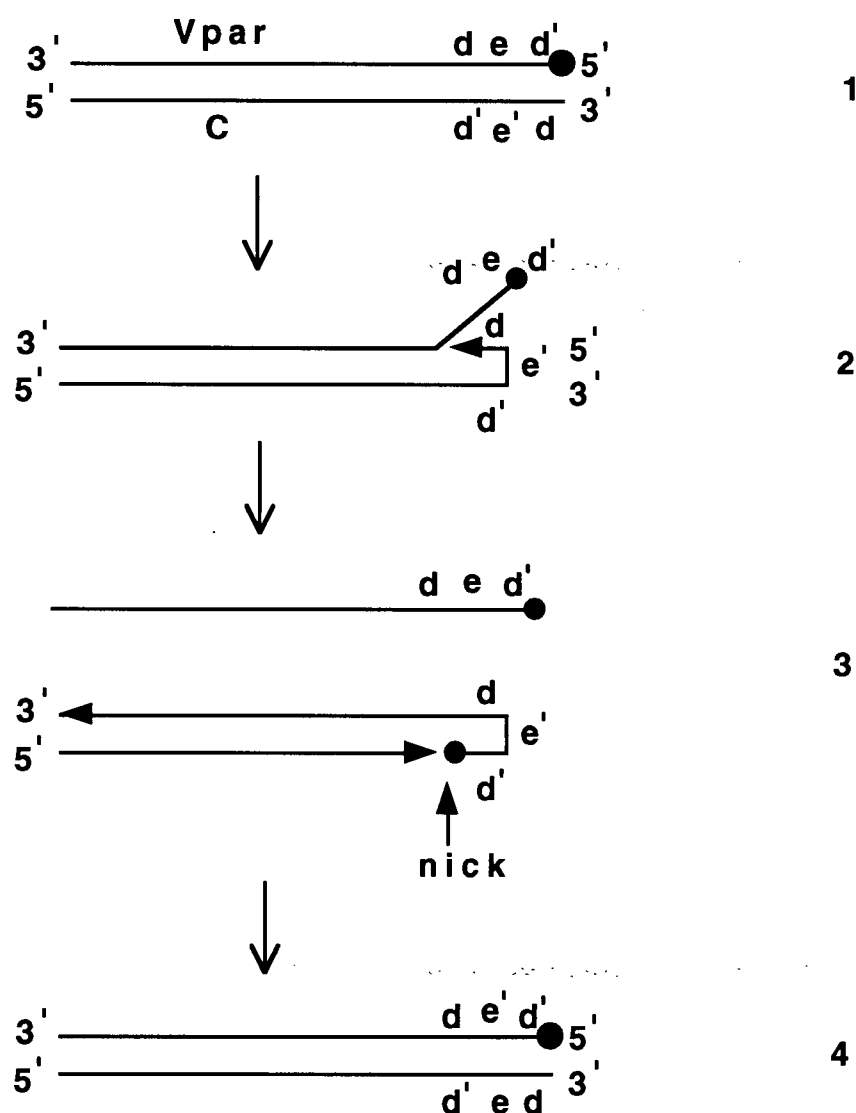
Fig. 8. The hairpin transfer mechanism. The black circles attached to the 5'-ends were proposed to be NS-1. The arrows indicate the 3'-ends to prime DNA synthesis. Vpar denotes the parental viral strand and C indicates the complementary strand.

of the dimer replicative form in Fig. 7 (lines 4 and 5). The 5'-terminal hairpin sequence of the MVMp parental genome is represented by d e d' (d and d' are complementary sequences; the presence of e is to indicate that the 5'-terminal inverted repeat sequence is not a perfect palindrome). The MRHM proposes that the 3'-end of the complementary lower strand can fold back to prime DNA displacement synthesis yielding the progeny single-stranded genomes. The viral protein NS-1 is assumed to nick at a specific site on the C strand near d' becoming covalently bound to the resulting 5'-end. The resulting 3'-end can subsequently extend the lower strand to complete a double stranded DNA molecule with extended 5'-end. Of note is that the 5'-terminal palindrome sequence of the upper DNA strand (Fig. 8, line 4) in this DNA molecule is the inverted complement of the corresponding sequence in the starting DNA molecule (Fig. 8, line 1), and another round of DNA strand displacement synthesis by using this DNA molecule as the substrate yields a single-stranded progeny genome with 5'-terminal sequence to be the inverted complement of the one from the parental genome.

The nicking and displacement DNA synthesis at the closed (left) end of the dimer replicative form (Fig. 7, lines 4 and 5) proposed in MRHM is also a hairpin transfer mechanism inverting the 5'-terminal sequence of the genome (Fig. 7, left side of lines 6 and 7). Although the hairpin transfer mechanism for the DNA replication of MVMp remains to be proven, it has been shown that *in vitro*, the duplex extended form of 5'-terminal palindrome can be melted and the resulting 3'-end can fold back to prime the DNA displacement synthesis (Cossons *et al.*, 1996). It is also known that the protein bound to the 5'-end of MVMp DNA (replication intermediates and single stranded viral DNA) is NS-1 (Gunther and Tattersall, 1988; Cotmore and Tattersall, 1989; Cotmore and Tattersall, 1988). Furthermore, it was

shown that the covalently closed hairpins of adeno-associated virus (AAV) can be resolved into a duplex extended form in extracts derived from AAV/adenovirus infected cells (Snyder *et al.*, 1990)

1.3.2.2.   Resolution of the dimer bridge

The dimer replicative form (or more simply called the dimer) is the DNA molecule in line 4 of Fig. 7. It is also shown in Fig. 9A in which the bold lines indicate the position of the 115 bp 3'-terminal palindrome. The DNA fragment in the dashed box of Fig. 9A is the dimer bridge of MVMp, which includes the 3'-terminal palindrome. The structural features of the dimer bridge, an imperfect palindrome, are indicated in Fig. 9B. The 3'-end hairpin of the MVMp genome has a "bubble" formed by nts 25, 26, 89, 90 and

91 (see Fig. 4), resulting in the $\frac{AG}{TC}$ to $\frac{AAG}{TTC}$ sequence asymmetry within the dimer bridge. The GC-rich region [nt 46-71 from the 3'-end hairpin (Fig. 4)] at the center of the dimer bridge and the T nucleotide (nt 41, Fig. 4) are two additional asymmetries within the dimer bridge. The resolution mechanism of the dimer bridge proposed in the MRHM is illustrated in Fig. 7 (lines 4 through 6).

Fig. 10 shows more clearly resolution of the dimer bridge according to the MRHM. Firstly, NS-1 encoded by MVMp is proposed to give the first nick at a specfic nicking site (site 1). After nicking, NS-1 is covalently bound to the 5'-end of the DNA and at the same time DNA displacement synthesis at the 3'-end by the host cellular DNA polymerase takes place. When this displacement DNA synthesis reaches another specific nicking site (site 2) on the lower DNA strand, NS-1 bound at the 5'-end of the displaced DNA strand
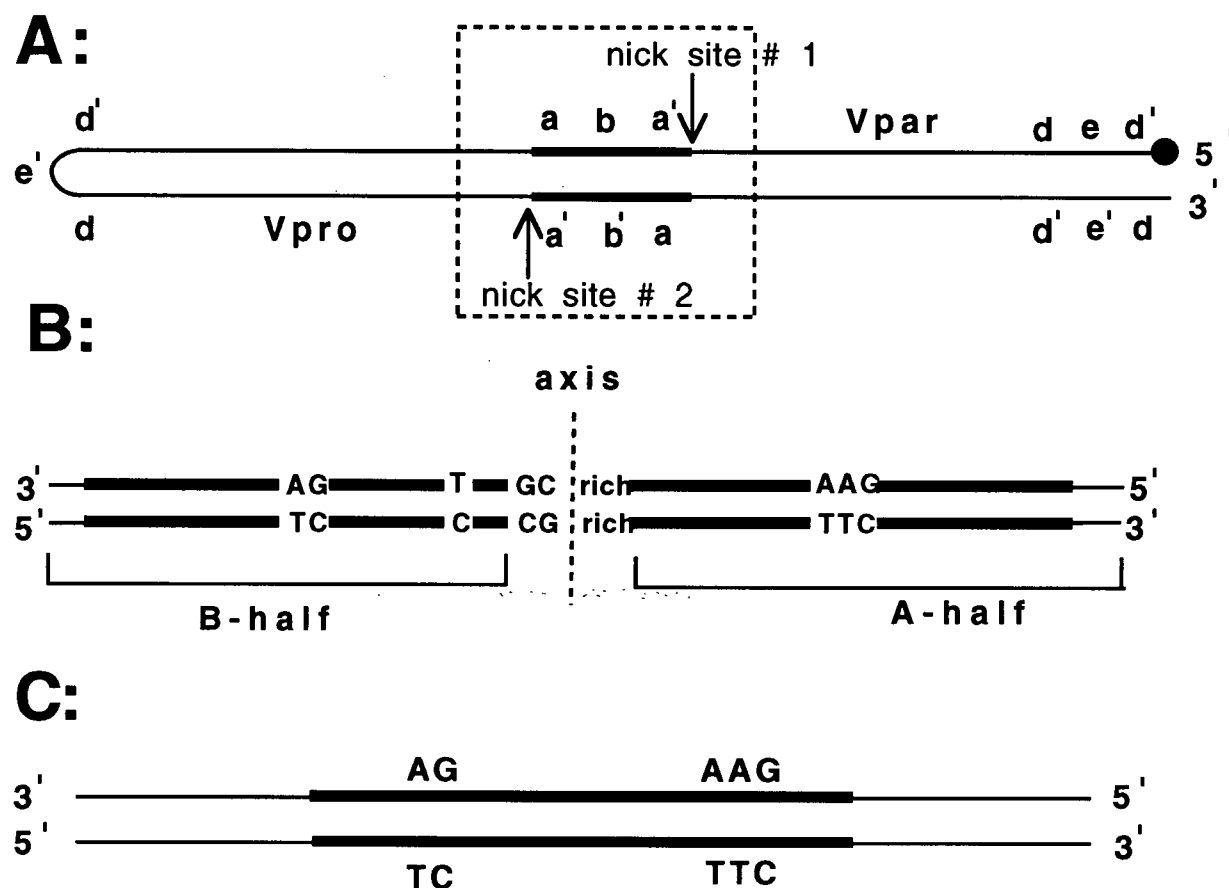
Fig. 9. A. The dimer replicative form of MVMp as shown in line 4 of Fig. 7 is repeated here. The DNA fragment in the dashed box is the dimer bridge. The bold lines indicate the 3' terminal hairpin sequence of the genome and its complementary sequence. **B.** The dimer bridge region of **A** is illustrated with further detail. The axis indicated by the dashed vertical line is drawn to emphasize that the dimer bridge is a palindrome sequence. In order to show that the palindrome of the dimer bridge is not perfect, the nucleotides AG and AAG which form the bubble of the stem of the 3'-terminal hairpin of MVMp genome, nucleotide T which forms the bulge, the GC-rich region which forms the two arms, and their complementary nucleotides are indicated. Also the dimer bridge is further demarcated into the B-half dimer bridge, the A-half dimer bridge, and the central GC rich region. In the following figures of this thesis, the dimer bridge is represented by the DNA molecule shown in **C.** (not drawn to scale)
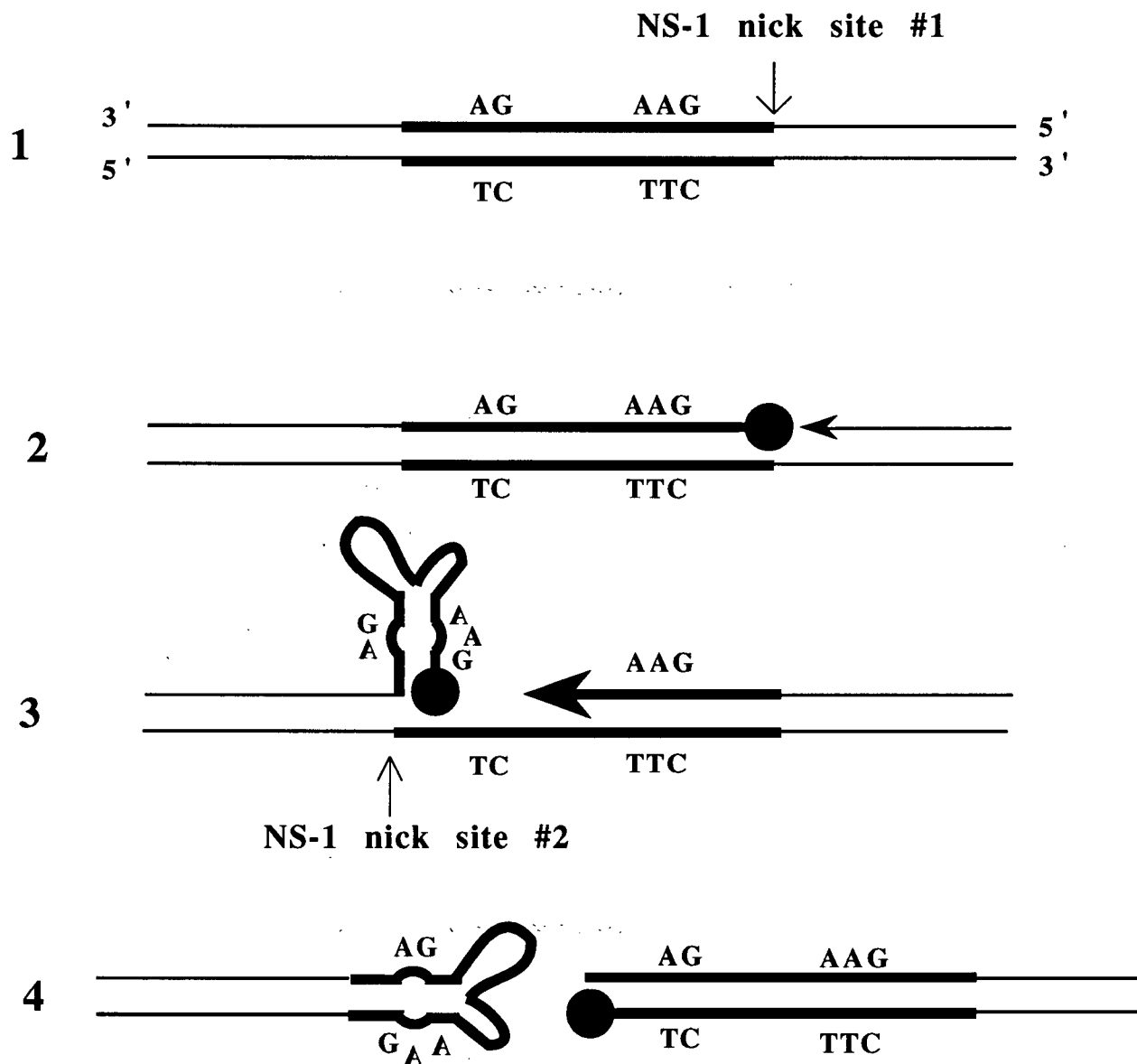
Fig. 10. The resolution of dimer bridge proposed in the modified rolling hairpin model. The DNA molecule in line 1 is the dimer bridge and the two DNA molecules in line 4 are the resolution products of the dimer bridge. The black circles indicate NS-1 protein bound to the 5'-end. The horizontal arrows represent the 3'-end used to prime DNA synthesis. The vertical arrows point to the proposed NS-1 nick sites.

gives the second nick at nick site 2. At the same time this NS-1 molecule is bound to the newly formed 5'-end of the DNA and the 5'-end of the displaced DNA strand ligates with the newly formed 3'-end, resulting in the production of two DNA molecules. One molecule has a closed end or turn-around form end and the end for the the other molecule is an extended form.

One important characteristic of this resolution mechanism of the dimer bridge is its asymmetry. There are two reasons to say this. One reason is that it is proposed that NS-1 can only give the first nick at nick site 1 but not at site 2. The model suggests the reason for NS-1 nicking at site 1 first is that the sequence near site 1, AAG, is different from the sequence near nick site 2, CT. Another reason the resolution mechanism of the dimer bridge is asymmetric is that the two resolution products are asymmetric: the end for the product on the left is closed but not extended whereas the end for the product on the right is extended but not closed.

As mentioned above, this resolution mechanism can explain the unique 3'-end sequence of MVM genome. This is because through such a mechanism the resulting resolution products of the dimer bridge retain the same orientations for the 115 nt 3'-terminal sequences present in the parental genome (see the two resolution products in line 6 and the parental genome in line 1 in Fig. 7 for the comparision). The 3'-terminal hairpin of progeny genomes derived from these two products is unique in sequence (Fig. 7, lines 7 and 8).

In 1985 when the MRHM was proposed, it was unknown how the dimer bridge is resolved, what the resolution products are and whether NS-1 is the enzyme involved in the resolution. In 1992, a report appeared showing that the dimer bridge can be resolved by NS-1 *in vivo* (Cotmore and Tattersall, 1992) although it was unknown whether the resolution products

are as suggested in the MRHM. One part of the research for the my PhD thesis was to answer this question by using an *in vitro* resolution system.

1.3.3. Cis-acting elements for the MVMp genome replication.

Analysis of defective interfering MVMp indicated that the terminal sequences of the genome are preferentially retained, suggesting all of the cis-acting sequence required for DNA replication reside at or near termini (Faust and Ward, 1979). This was confirmed with the observation that a minigenome construct with the terminal 140 and 660 nucleotides from the left and right termini, respectively, is replication competent (Tam and Astell, 1993). Analysis of the terminal deletion mutants of MVMp genome for their replication efficiency has shown that both 3'- and 5'-end hairpins of the genome are required for the replication (Salvino *et al.*, 1991; Tam, 1994) as are the "bubbles" in the stem portions of the 3'- and 5'-end hairpins (Tam, 1994; Costello *et al.*, 1995). The removal of one copy of a tandemly arranged 65-bp repeat found 94 nt inboard of the 5'-terminal hairpin also strongly inhibited viral DNA replication (Salvino *et al.*, 1991), although in a minigenome context, the deletion appeared to have no effect on replication (Tam and Astell, 1993). Although some closely related parvoviruses share these A:T rich tandem direct repeats in their genomes, their function remains to be clarified.

In addition, the deletion of DNA sequence from nt 4489-4695 near the 5'-terminal hairpin was found to eliminate replication of the minigenome (Tam and Astell, 1993). Multiple host cellular proteins have been shown to specifically bind to this region (Tam and Astell, 1994). However, the function of this region is still unknown. One possibility is that it may be involved in

facilitating the folding back of the extended 5'-terminal palindrome during synthesis of the dimer RF (Fig. 7, line 3) and single stranded progeny genomes (Fig. 7, line 6). Currently, linker scanning mutagenesis of this region and the analysis of the replication efficiencies of mutants are ongoing in this laboratory (Brunstein and Astell, unpublished results) and the host proteins which bind to this region will hopefully be identified in order to elucidate the function of this cis-acting sequence.

1.3.4. Focus of the present study: resolution of the dimer bridge

The focus of my research has been towards clarifying the resolution products and resolution procedure of the dimer bridge of MVMp. I have shown that the resolution products predicted by the MRHM are observed, *in vitro*, using a cloned dimer bridge plasmid, LA9 cellular replication extract and recombinant NS-1 (expressed in insect cells). However, when a series of mutant dimer bridge clones which I constructed in order to prevent resolution, were resolved, I concluded that the resolution procedure proposed in the MRHM is likely incorrect (Liu *et al.*, 1994). A report from another lab

indicated that the half dimer bridge containing the $\frac{AG}{TC}$ (but not $\frac{AAG}{TTC}$)

sequence, which is the right half of the dimer bridge shown in Fig. 10B, was nicked by extracts containing NS-1 (Cotmore and Tattersall, 1994). This laboratory also suggested the signal for nicking the half dimer bridge

containing the $\frac{AG}{TC}$ sequence was the spacing between $\frac{AG}{TC}$ sequence and a

putative ATF binding site and implicated the host cell ATF played a role in nicking.

I used highly purified recombinant NS-1 and established that nicking is dependent on the presence of a murine host cell factor or factors. I constructed a series of mutations within the host factor binding region (HFBR) and identified two CG motifs displaced by 10 bp which are required for nicking. Evidence for binding of mouse protein(s) to HFBR was also obtained (Liu and Astell, 1996).

Further studies with mutant NS-1 proteins (tyrosine residues (188, 197 and 210) that were candidates for covalent linkage to the 5' phosphoryl group at the nick site were changed to phenylalanine) indicated that the tyrosine at 197 does not appear to be involved in the covalent linkage whereas tyrosines at 188 and 210 may be involved(Liu et al., unpublished results).

II.   Materials and Methods

2.1.   Materials

Chemicals were purchased from Fisher Scientific, Sigma Chemical Co. BDH, GIBCO/Bethesda Research Laboratories (BRL) or Bio-Rad laboratories unless otherwise specified.

All restriction and DNA modification enzymes were purchased from either GIBCO/BRL or New England Biolabs. DNA sequencing kits using Sequenase were from United States Biochemical Company (USB).

Tissue culture media and supplies were purchased from GIBCO/BRL. Bacteria medium were supplied by Difco Laboratories. Ampicillin was from Ayerst Laboratories.

2.2.   Bacteria

The recombination deficient strain of *E. coli*, SURE (Stratagene), was used to clone plasmids which contain palindrome sequences. DH5α strain was used for routine cloning.

2.3.   Mammalian cell line, LA9.

Mouse LA9 cells (Littlefield, 1964) used in this study are an ouabain resistant isolate of the HGPRT⁻ cell line A9 and were originally obtained from Peter Tattersall (Yale University). LA9 cells have been shown to be permissive to infection by MVMp (Tattersall, 1972).

2.4. Insect cell line, Sf9.

Insect *S. frugiperda* 9 (Sf9) cells were obtained from Dr. F. L Graham (McMaster University).

2.5. Standard cloning techniques

Detailed protocols for many of the molecular cloning procedures have been described in Sambrook *et al.* (1989).

2.6. DNA sequencing

Sequencing of plasmid DNA was carried out using reagents and Sequenase from DNA sequencing kits supplied by United States Biochemical Company (USB). Samples were analyzed on 7" X 14" standard 7 M urea-polyacrylamide gels. The gels were dried and bands detected by autoradiography.

2.7. Plasmid Constructions

2.7.1. Construction of a molecular clone of the wildtype MVMp dimer bridge

Plasmid pCA408F was constructed by P. Tam in this lab (Tam and Astell, 1993) by inserting the left end (ie., the 3'-end) of MVMp genome from a SmaI linker to the AluI site (nt 408 of the MVM genome) [Note, nucleotide sequence numbers refer to the published sequence (Astell *et al.*, 1983b)] into

the SmaI site of pUC19 (Fig. 11A). In order to clone the dimer bridge, pCA408F was digested with XbaI and PstI. The linearized plasmid was treated with exonuclease III and nuclease S1 to delete about 100 bps (ie., nt 1-100 of the left end of MVMp genome) at the XbaI end. The two ends of the linearized, deleted plasmid were ligated and transformed into E. coli DH5α. After selecting a plasmid with the appropriately sized deletion, the plasmid was digested with HindIII, blunt ended by filling in using T4 DNA polymerase, and digested with EcoRI. The shorter DNA fragment (MVMp DNA) was purified by electrophoresis in an agarose gel, recovered using Geneclean (Bio 101), and ligated to pUC19 (digested with SmaI and EcoRI) to generate plasmid pQL1 (Fig. 11B).

The BamHI/PstI fragment (nt 1-410) of MVMp genome from pMM984 (Fig. 11C), an infectious clone of MVMp (Merchlinsky et al, 1983), was cloned into BamHI/PstI digested pUC19. The unique NcoI site [nt 259 within the MVMp sequence (Astell et al, 1983b)] was destroyed by digestion with NcoI, filling-in with T4 DNA polymerase and re-ligating. This BamHI/PstI fragment was then cloned into the BamHI/PstI site of pQL1. The unique NcoI site in this construct was destroyed as described above and this plasmid, designated pQL2 (Fig. 11D), was digested with StyI to isolate the longer DNA fragment which was used later as a vector.

Four synthetic oligonucleotides (oligonucleotides QL1 to QL4 which are two sets of complementary oligos, Table 1) were prepared. The complementary pairs were annealed and ligated to the vector from StyI digestion (see above). The ligation mixture was transformed into E. coli SURE cells by electroporation. The resulting plasmid is the wildtype dimer bridge clone, pQLDB1 (Fig. 12). The restriction endonuclease sites used to release the dimer bridge structure in the resolution assay (see below) are the

A: pCA408F

EcoRI [Smal] [Alul](408) Ncol(259) Styl(144) Smal BamHI Xbal Pstl HindIII

B: pQL1

EcoRI [Smal] [Alul](408) Ncol(259) Styl(144) [Pstl] [HindIII] [Smal] BamHI Xbal Pstl HindIII

C: pMM984

BamHI Styl(144) Ncol(259) Pstl(411) BamHI

D: pQL2

EcoRI [Smal] [Alul](408) Ncol(259) Styl(144) [Pstl] [HindIII] [Smal] BamHI Styl(144) [Ncol](259) Pstl(411) HindIII
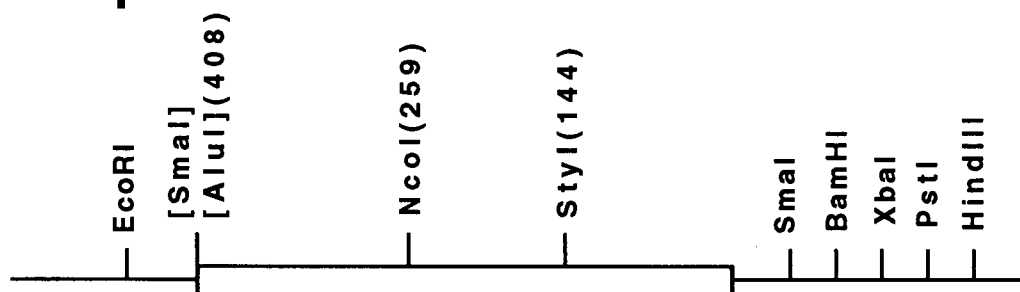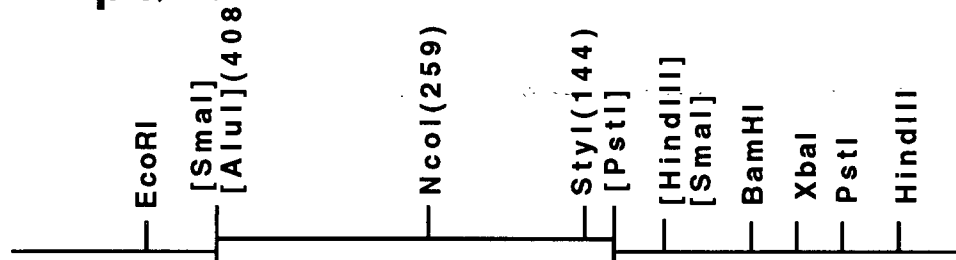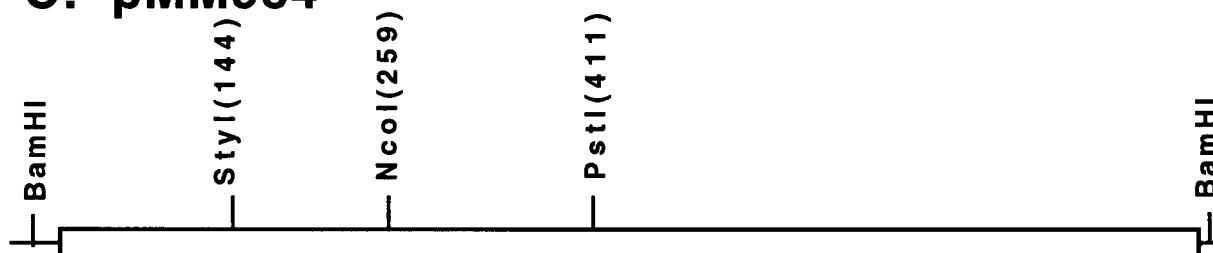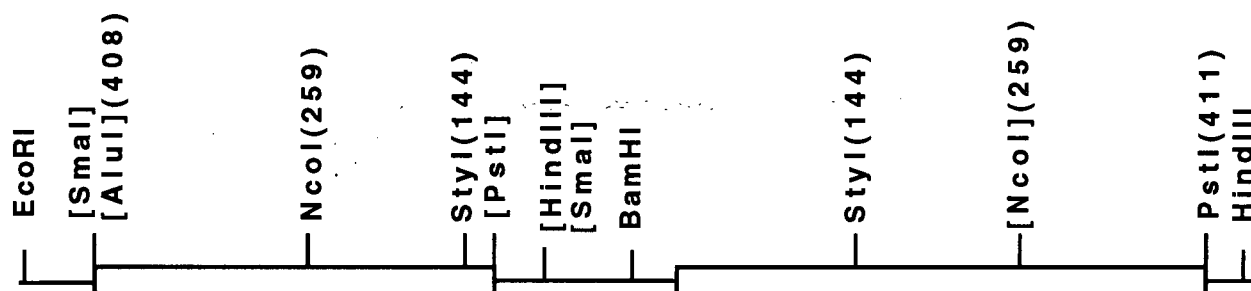
Fig. 11. Schematic diagram of plasmids used for the cloning of the dimer bridge. The open boxes represent MVM DNA. The thin lines represent the vector sequences. The bracketed restriction sites indicate sites destroyed during cloning procedures. **A, B, C** and **D** illustrate pCA408F, pQL1, pMM984 and pQL2, respectively. (Not drawn to scale)

Table 1:   Sequence of oligonucleotides used to construct the wildtype and mutant dimer bridge molecules. The mutant sequences are presented in lower case.

oligo QL1   p TGCCGAAGGCGCGCGCGCAGCGCGCGTCATCACGTCACTTACGTG
95 mer   AACATGGTTGGTCAGTTCTAAAAATGATAAGCGGTTCAGGGAGT
                  TTAAAC

oligo QL2   p CTTGGTTTAAACTCCCTGAACCGCTTATCATTTTTAGAACTGACC
103 mer   AACCATGTTCACGTAAGTGACGTGTGACGCGCGCTGCGCGCGCGC
                  CTTCGAGCGTCA

oligo QL3   p CACGTCACTTACGTTTCACATGGTTGGTCAGTTCTAAAAATGATA
66 mer   AGCGGTTCAGGGAGTTTAAAC

oligo QL4   p CTTGGTTTAAACTCCCTGAACCGCTTATCATTTTTAGAACTGACC
74 mer   AACCATGTGAAACGTAAGTGACGTGTGAC

oligo QL5   p CACGTCACTTACGTgaACATGGTTGGTCAGTTCTAAAAATGATAA
65 mer   GCGGTTCAGGGAGTTTAAAC

oligo QL6   p CTTGGTTTAAACTCCCTGAACCGCTTATCATTTTTAGAACTGACC
73 mer   AACCATGTtcACGTAAGTGACGTGTGAC

oligo QL7   p CACGTCACTTACGTTTCACATGGTTGGTCAGTTCTAActtatcattt
66 mer   CGGTTCAGGGAGTTTAAAC

oligo QL8   p CTTGGTTTAAACTCCCTGAACCGaaatgataagTTAGAACTGACCA
74 mer   ACCATGTGAAACGTAAGTGACGTGTGAC
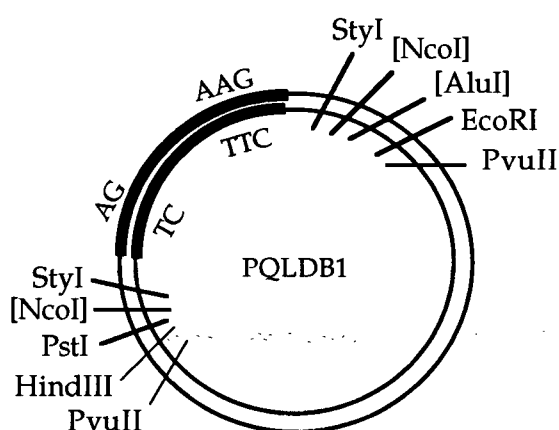
Fig. 12. The wildtype dimer bridge clone, pQLDB1. The bold lines represent the 3'-terminal palindrome sequence. AG and AAG are the bubble nucleotides. Short bars indicate the positions of the restriction sites. Square brackets around restriction sites indicate that these were destroyed during the cloning procedure.

PstI site on the left and PvuII site on the right. Both NcoI sites and the AluI site are surrounded by square brackets indicating these sites were destroyed during the construction. The four synthetic oligonucleotides were used to generate the dimer bridge sequence between the two StyI sites.

2.7.2. Construction of mutant dimer bridge clones

Oligonucleotides QL1, 2, 5 and 6 (Table 1) were used to clone a mutant dimer bridge in which nts 89-91, $\frac{AAG}{TTC}$, in the wildtype dimer bridge were altered to $\frac{CT}{GA}$ (Fig. 13B). The rationale for this construct was that we predicted that the bubble within the stem of the left hairpin may contribute to the asymmetric resolution process (Astell *et al.*, 1985) and this mutant dimer bridge would make each stem of the dimer bridge identical in sequence. This clone is referred to as pQLDB2.

Oligonucleotides QL1, 2, 7 and 8 (Table 1) were used to clone another mutant dimer bridge (pQLDB3) in which the 10 bp sequence spanning the putative nick site #1 (Fig. 10) is inverted (Fig. 13C).

During construction of pQLDB2, an unexpected mutant dimer bridge clone, pQLDB4 (Fig. 13D), was also isolated. pQLDB4 is the same in sequence as pQLDB2 except that nts 102 and 103 of MVMp are deleted. In addition, the dimer bridge in pQLDB4 is inserted in the plasmid in the opposite orientation to that of pQLDB1, 2 and 3. All constructed plasmids containing the mutant dimer bridges were isolated and propagated in *E. coli* SURE cells.

Fig. 13. Schematic diagrams of wildtype and mutant dimer bridge clones. The PvuII to PvuII DNA fragment containing the dimer bridge (wildtype or mutant) is illustrated for each clone. **A** is the wildtype dimer bridge clone, pQLDB1. **B** is the mutant dimer bridge clone, pQLDB2 in which the AAG sequence is mutated into CT. **C** is the mutant dimer bridge clone, pQLDB3 in which the 10 bp sequence containing the predicted nick site #1 is inverted. **D** is the mutant dimer bridge clone, pQLDB4 in which AAG is mutated into CT, and nt 102 and nt 103 are deleted. Of note is that the orientation of the StyI fragment in pQLDB4 is opposite to that in pQLDB1, pQLDB2 and pQLDB4. Bold lines represent the 3'-terminal palindrome. The long open box from PstI to [AluI] indicates the wild type or mutant dimer bridge sequences. The vertical bars indicate restriction sites. [AluI] indicates this site was damaged. Arrows point to the specific nick sites # 1 and 2, dotted small boxes indicate the mutated sites and the dotted triangle indicates a deletion. The horizontal thin lines are the vector sequence from pUC19.

Fig. 13A:
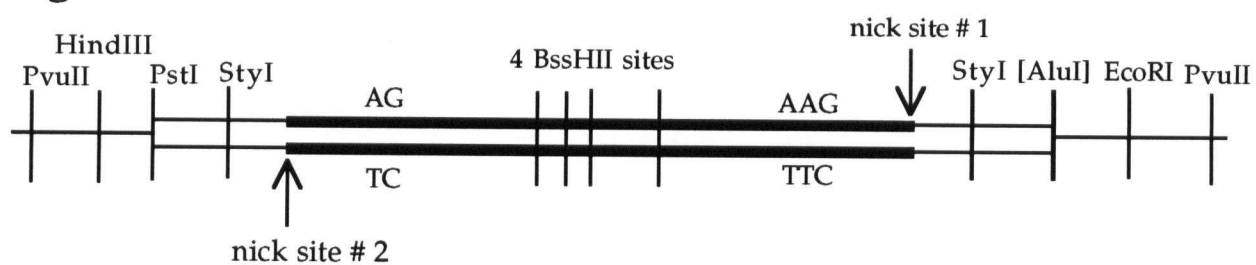
B:
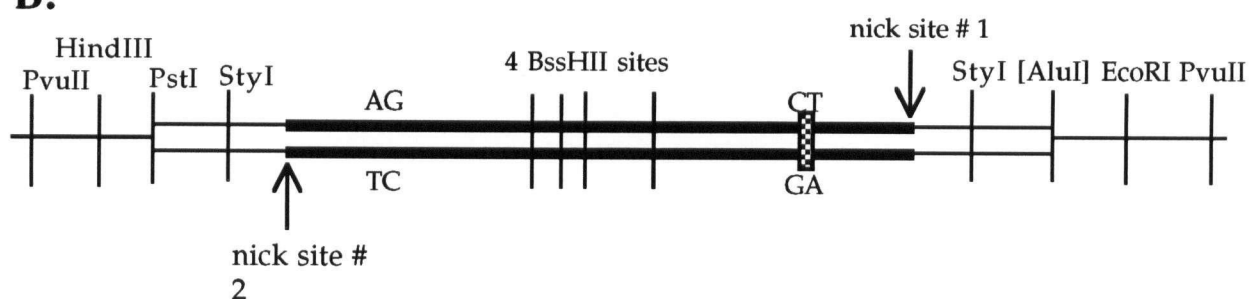
C:
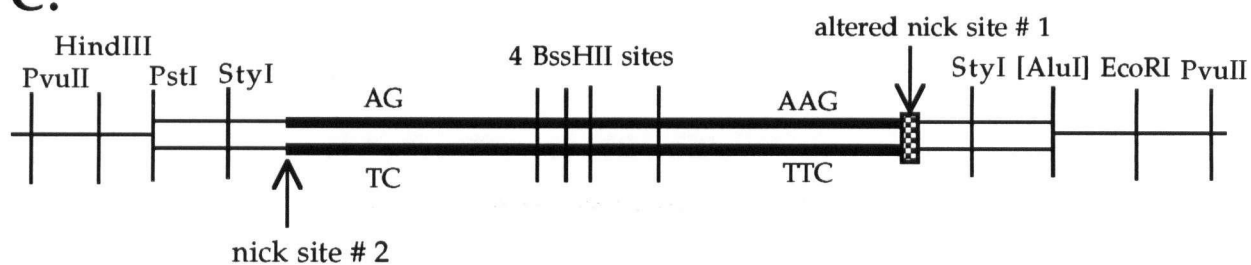
D:
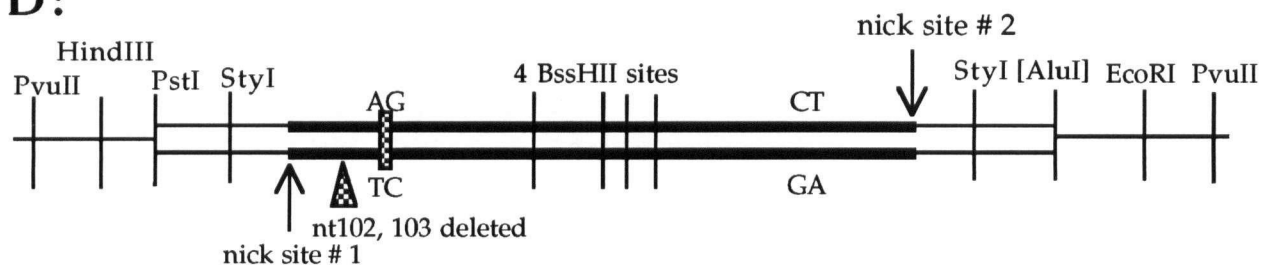
2.7.3. DNA sequencing of the wildtype and mutant dimer bridge clones

Because of the size (~700 bp) of the wildtype dimer bridge in pQLDB1 and its inverted repeat nucleotide sequence, a nested set of deleted dimer bridge clones was generated for sequencing. For mutant dimer bridge clones, pQLDB2, pQLDB3 and pQLDB4, each was digested with StyI, and subsequently the shorter StyI fragment blunt ended, inserted into the SmaI site of pUC19 and sequenced using the universal primer for pUC19. In order to determine the orientation of the mutant dimer bridge in pQLDB2, 3 and 4 (because the four annealed synthetic DNA oligonucleotides can be inserted in either orientation), each plasmid was digested with EcoRI and BssHII. The longer DNA fragment was blunt ended and religated to generate a plasmid which was then sequenced using the M13 forward primer.

2.7.4. Cloning of each half (the A-half and B-half) of the dimer bridge

The wild type dimer bridge sequence (Fig. 13A) can be divided into an A-half dimer bridge, B-half dimer bridge and the central GC rich region containing multiple BssHII sites (Fig. 14). The B-half dimer bridge contains the $\frac{AG}{TC}$ sequence and the A-half dimer bridge contains the $\frac{AAG}{TTC}$ sequence.

In order to clone the B-half dimer bridge, plasmid pQLDB1 which contains the wildtype dimer bridge sequence was digested with BssHII and HindIII, blunt ended, and the shorter fragment containing the B-half dimer bridge was inserted into the SmaI site of pUC19. The resulting plasmid pQLB contains the B-half dimer bridge oriented with the BssHII end proximal to the
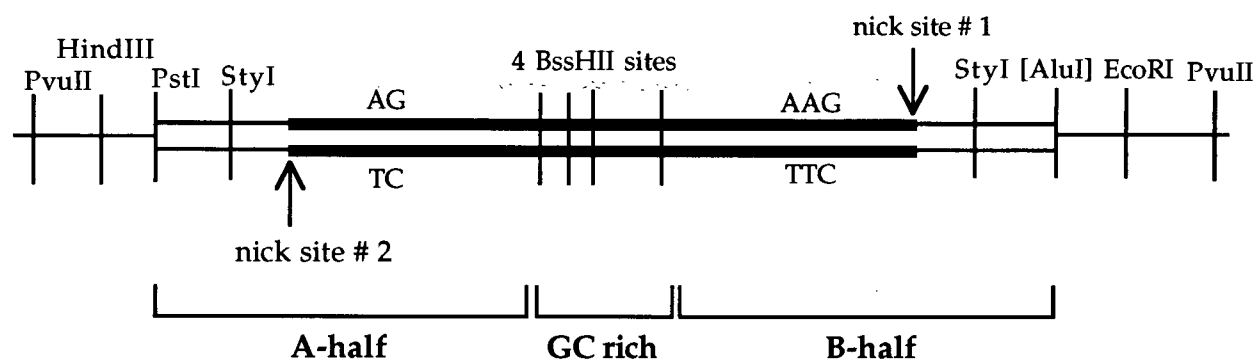
Fig. 14. The illustration of the A-half, B-half and the GC rich region of the wild type dimer bridge in pQLDB1. See the legend of Fig. 13 for the definitions of the symbols.

EcoRI site of pUC19. In a similar procedure, pQLDB1 was digested with BssHII and EcoRI, blunt-ended, and the shorter fragment containing the A-half dimer bridge was cloned into the SmaI site of pUC19. The resulting plasmid pQLA contains the A-half dimer bridge with the BssHII site proximal to the EcoRI site of pUC19.

### 2.7.5.	Construction of B-half clones with mutations in the putative host factor binding region (HFBR)

### 2.7.5.1.	Structure and sequence of pQLB, the B-half dimer bridge clone

The shorter EcoRI/HindIII fragment of the B-half dimer bridge clone, pQLB, and relevant restriction endonuclease sites are illustrated in Fig. 15A. Fig. 15B shows the sequence of part of the B-half dimer bridge. The putative HFBR is the DNA sequence from the BssHII site (destroyed during the construction of the plasmid) to the nucleotide adjacent to the NS-1 binding site.

### 2.7.5.2.	Construction of pQLBDEL (both ATF motifs deleted)

pQLB was digested with BsaAI and Ecl136II, and the larger fragment ligated, deleting the sequences between these two restriction sites. This plasmid, pQLBDEL, has both activating transcription factor (ATF) motifs deleted.

A:

EcoRI Ecl136II [BssHII] BsaAI StyI PstI [HindIII] BamHI HindIII

2 ATF
Binding
Sites

NS-1
Binding
Site

B:

[BssHII] BsaAI

```
5' CGCG | CGTCA | TCA | CGTCA | CTTACGTGAACA | TGGTTGGT | 3'
3' GCGC | GCAGT | AGT | GCAGT | GAATGCACTTGT | ACCAACCA | 5'
```

ATF
Binding
Site 1

ATF
Binding
Site 2

NS-1
Binding
Site
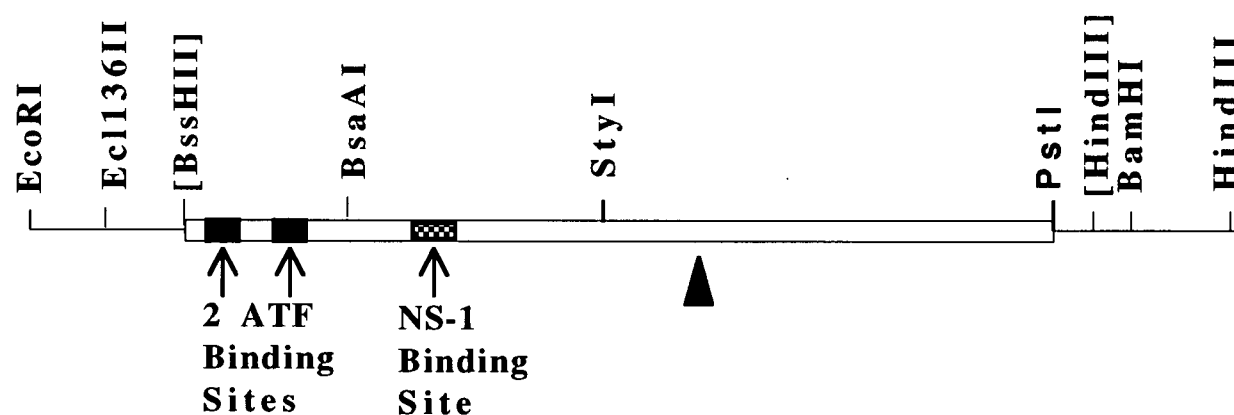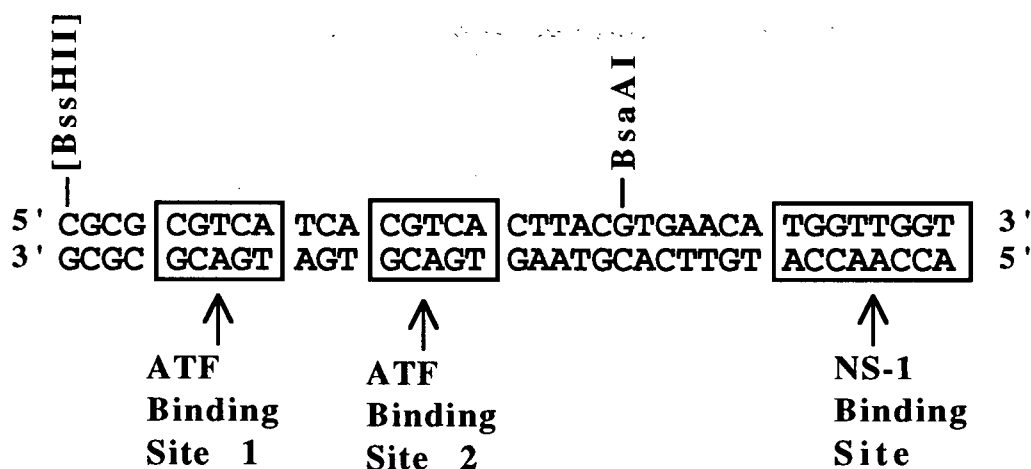
Fig. 15. The schematic diagram and partial sequence of the cloned B-half dimer bridge in pQLB. A. The EcoRI/HindIII fragment of pQLB is shown. The long box represents the B-half. Within this sequence, there are two ATF binding motifs (black boxes) and the NS-1 binding site (dotted box) (Cotmore et al., 1995). The thin lines are vector DNA sequences. Restriction sites used in cloning, [BssHII] and [HindIII], or subsequent construction of mutants are indicated. The filled triangle indicates the NS-1 nicking site reported in this thesis (see section 3.4.1.) **B.** The nucleotide sequence from the [BssHII] site to the distal nucleotide of the NS-1 binding site [Cotmore et al., (1995)] is shown. The sequences for the two ATF motifs and the NS-1 binding site are boxed.

2.7.5.3.   Construction of pQLBWT13 (one ATF motif deleted)

pQLB was digested with BsaAI and Ecl136II, and the larger fragment was ligated with a 13 bp DNA fragment obtained by annealing two synthetic oligonucleotides [oligo 1 and oligo 1c (Table 2)]. The clone with the correct sequence orientation (pQLBWT13) has the ATF motif (site 1) deleted (Fig. 16A). The nucleotide composition of part of this plasmid is shown (Fig. 16B). For reference, each nucleotide is numbered consecutively. (*NB*, this numbering system is arbitrary and does not correspond with nucleotide numbers in the MVMp genome)

2.7.5.4.   Construction of single nucleotide mutations (Positions 3 through 13) in pQLBWT13

In order to change each nucleotide from 3 to 13 in pQLBWT13, pQLB was digested with BsaAI and Ecl136II, and the larger DNA fragment was ligated, respectively, with eleven 13 bp DNA fragments derived from eleven annealed oligo pairs (oligos 2-12 and oligos 2c-12c, Table 2). The eleven clones are referred to, respectively, as pQLBA3G, pQLBC4A, pQLBG5A, pQLBT6C, pQL13C7T, pQLBA8G, pQLBC9T, pQLBT10C, pQLBT11C, pQLBA12G, and pQLBC13T. The nucleotide change is indicated by the wildtype nucleotide, its numerical designation (Fig. 16B), and the mutant nucleotide (e.g., A3G).

2.7.5.5.   Construction of single nucleotide mutations (positions 14 through 20) in pQLBWT13

Table 2: List of synthetic oligodeoxynucleotides for the cloning of B-half dimer bridge mutants and HFBR

name	sequence	name	sequence
oligo 1	TCACGTCACTTAC	oligo 10	TCACGTCACTcAC
oligo1c	GTAAGTGACGTGA	oligo 10c	GTgAGTGACGTGA
oligo 2	TCgCGTCACTTAC	oligo 11	TCACGTCACTTgC
oligo 2c	GTAAGTGACGcGA	oligo 11c	GcAAGTGACGTGA
oligo 3	TCAaGTCACTTAC	oligo 12	TCACGTCACTTAt
oligo3c	GTAAGTGACtTGA	oligo 12c	aTAAGTGACGTGA
oligo 4	TCACaTCACTTAC	primer1	aTGAACATGGTTGGTCAGTT
oligo4c	GTAAGTGAtGTGA	primer2	GcGAACATGGTTGGTCAGTTC
oligo5	TCACGcCACTTAC	primer3	GTaAACATGGTTGGTCAGTTCT
oligo 5c	GTAAGTGgCGTGA	primer4	GTGgACATGGTTGGTCAGTTCTA
oligo 6	TCACGTtACTTAC	primer5	GTGAgCATGGTTGGTCAGTTCTAA
oligo 6c	GTAAGTaACGTGA	primer6	GTGAAtATGGTTGGTCAGTTCTAAA
oligo 7	TCACGTCgCTTAC	primer7	GTGAACgTGGTTGGTCAGTTCTAAAA
oligo7c	GTAAGcGACGTGA	QL18mer	CGCCCACTTCCTTTTCGC
oligo 8	TCACGTCAtTTAC	HFS	GTGAACAT
oligo 8c	GTAAaTGACGTGA	HFSc	GATCATGTTCAC
oligo 9	TCACGTCACcTAC	HFSG14A	aTGAACAT
oligo 9c	GTAgGTGACGTGA	HFSG14Ac	GATCATGTTCAt

Note: The letters in lower case are the mutant nucleotides.

A

B:
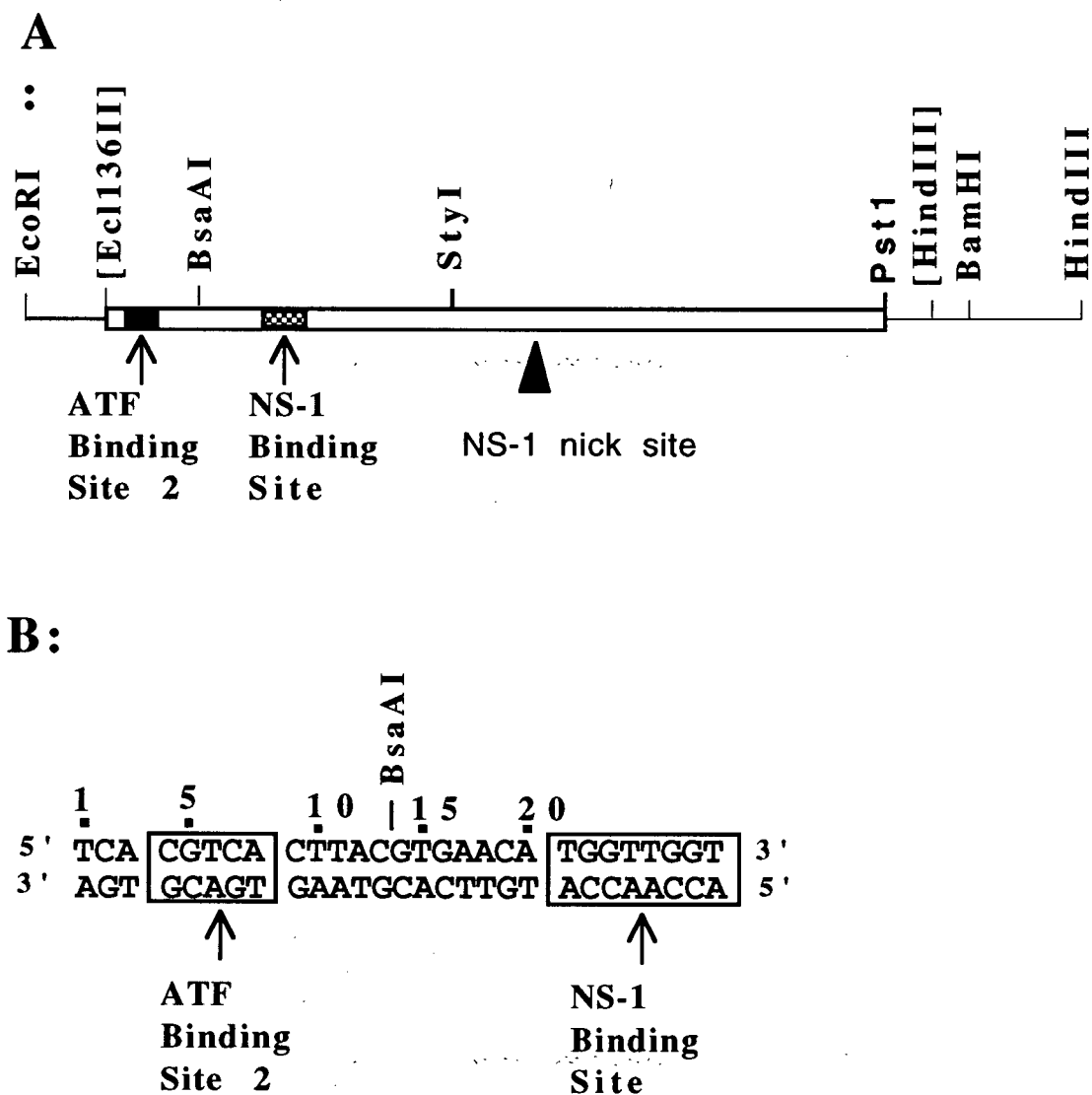
Fig. 16. The schematic diagram and partial sequence of the cloned B-half dimer bridge with ATF binding site 1 deleted in pQLBWT13. **A.** The EcoRI/HindIII fragment of pQLBWT13 is shown. The filled triangle indicates the NS-1 nick site. **B.** Nucleotide sequence of the fragment from the [Ecl136II] site to the distal nucleotide of the NS-1 binding site. For ease of reference, the nucleotides are numbered (arbitrarily) from the left.

In order to change nucleotides 14 to 20 in pQLBWT13, PCR mutagenesis was used. Seven oligonucleotides in which one of the seven nucleotides (14-20) was changed were synthesized and used to prime a PCR reaction on pQLBWT13. The second primer in each case was oligo QL18 mer (Table 2, Fig. 17). The seven amplified fragments were digested with StyI and ligated to the larger DNA fragment from a StyI/BsaAI digestion of pQLBWT13. These clones are referred to as pQLBG14A, pQLBT15C, pQLBG16A, pQLBA17G, pQLBA18G, pQLBC19T, and pQLBA20G.

2.7.6. Construction of plasmids containing a wildtype or mutated host factor binding region (HFBR)

pQLBWT13 was digested with BsaAI and BamHI. The larger DNA fragment was ligated with either annealed oligo HFS and oligo HFSc or annealed oligo HFSG14A and oligo HFSG14Ac (Table 2). The clones are referred to as pUCWT which contains the wild-type binding site for host factor(s), and pUCG14A which contains a G→A mutation at position 14 of the host factor binding site. The NS-1 binding site and nicking site present in pQLBWT13 (Fig. 16A) are not present in these plasmids.

Plasmid pQLBC4A was also digested with BsaAI and BamHI, and the larger fragment ligated with annealed oligo HFS and oligo HFSc or annealed oligo HFSG14A and oligo HFSG14Ac. The clones obtained are referred to as pUCC4A which is mutated in the host factor(s) binding site at position 4 (C→A), and pUCC4AG14A which contains two mutations in the host factor(s) binding site at positions 4 and 14 (C→A and G→A, respectively).
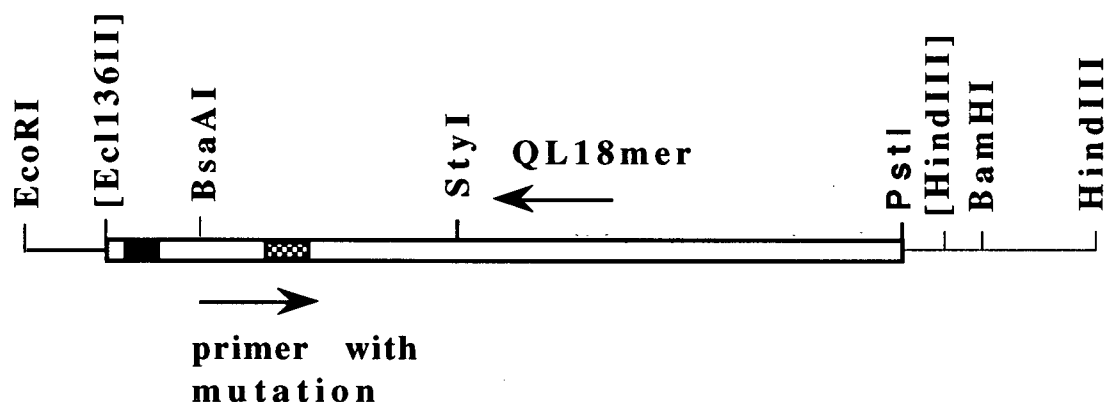
Fig. 17. PCR mutagenesis scheme to mutate nucleotides 14 to 20 of pQLBWT13. The small black box and the small dotted box represent ATF binding site 2 and the NS-1 binding site, respectively. The two horizontal arrows indicate the two primers. A series of PCR products were generated using QL18 mer as a primer and seven different mutation primers (Table 2). Each PCR product was digested with StyI and ligated into the parent plasmid digested with BsaAI and StyI.

2.8.   **Preparation of mouse LA 9 replication extracts**

LA9 replication extracts were prepared using a procedure adapted from Stillman and Gluzman (1985). Mouse LA9 cells were grown in suspension culture in Joklik's MEM supplemented with 5% FBS (GIBCO). Cells (1L) grown to a density of 5-6 x 10^5 cells/ml were harvested by centrifugation (1, 200 rpm, Beckman JA14 rotor), and washed once with PBS. The cell pellet was resuspended in 10 ml ice-cold hypotonic buffer (20 mM HEPES, pH 7.5, 5 mM KCl, 1.5 mM MgCl$_2$, 0.1 mM dTT), centrifuged and resuspended in 5 ml of hypotonic buffer. After 10 min on ice, the swollen cells were disrupted using a Dounce homogenizer. The cells were left on ice for a further 30 min and centrifuged at 11 K (Beckman JA17 rotor) for 10 min. The supernatant was removed, aliquoted and stored at -70°.

2.9.   **Preparation of Sf9 cell extracts containing NS-1**

Insect cell extracts containing recombinant NS-1 were prepared by a procedure adapted from Wilson et al.. (1991). A recombinant baculovirus containing the MVM NS-1 gene was used to infect a spinner culture of Sf9 cells (Wilson et al., 1991). Approximately 1.2 x 10^8 Sf9 cells (100 ml) were infected with recombinant virus (AcNS-1) at a m.o.i. of 5. Cells were harvested at 72 hr p.i. by centrifugation (300 xg, 5 min, 4°C), washed three times with cold PBS, resuspended in 2.5 ml of hypotonic buffer (see section 2.8.), and incubated for 15 min on ice. Cells were lysed using a Sonic Dismembrator (Quigley-Rochester, Inc.) until >95% of the cells were disrupted. Nuclear and cellular debris were pelleted by centrifugation (300 xg,

10 min, 4°C) and the supernatant transferred to a fresh tube, aliquoted and stored at -70°C.

2.10.   Purification of NS-1 from Sf9 cells

The purification of NS-1 was essentially as described previously (Wilson *et al*, 1991) with the following modifications introduced to reduce the time and increase the activity. After centrifugation of sonicated infected Sf9 cells, the supernatant was diluted five-fold using buffer 1 containing NaCl (instead of dialyzing the supernatant against this buffer). The diluted crude extract was loaded directly onto an AC6 coupled sepharose column (AC6 is a monoclonal antibody to NS-1 (Yeung *et al.*, 1991)), and after 30 min unbound protein was washed off the column and NS-1 was eluted with buffer 2 containing peptide 1 (incubation with peptide 1 was for 30 min before elution).

2.11.   The dimer bridge resolution assay

2.11.1.   Analysis of resolution products on one-dimensional non-denaturing agarose gels

A standard reaction (25 µl) contained 30 mM HEPES, pH 7.5, 7 mM $MgCl_2$, 0.5 mM dTT, 100 µM of all four dNTPs, 3 mM ATP, 200 µM each of CTP, UTP, and GTP, 40 mM creatine phosphate, 1 µg creatine phosphokinase, 0.8 µg substrate (plasmid DNA containing dimer bridge), 20 µCi α-^{32}PdATP, 9 µl of LA9 replication extract and 2-6 µl of cytoplasmic extract from Sf9 cells containing NS-1 or 3 ul of purified NS-1 (~300 ng). The reaction mixture was

incubated for 2 hr at 37°C. Following incubation, the mixture was digested with proteinase K (28 μg/ml) in the presence of 0.5% SDS and 5 mM EDTA for 1 hr at 37°C and 3 hr at 60°C. The samples were subsequently extracted with phenol/chloroform/isoamyl alcohol (50:49:1), desalted by centrifugation through 1 ml Sephadex G-50 spin columns to get rid of $\alpha-^{32}PdATP$, and precipitated with ethanol. The DNAs were redissolved, digested with appropriate restriction endonucleases, and separated on 1.4% agarose gels (TAE buffer). The dried gels were exposed to X-ray film (Agfa). This procedure was adapted from that described previously (Stillman and Gluzman, 1985; Cotmore et al, 1992).

2.11.2. Two-dimensional neutral/alkaline agarose gel electrophoresis of the NS-1 resolution products

Two identical DNA samples from the in vitro resolution assay were run on the same neutral 1.4% agarose gel as described above (section 2.11.1.). One lane was excised and immersed in alkaline electrophoresis buffer (50 mM NaOH, 1 mM EDTA) for 45 min. The gel lane equilibrated with alkaline buffer was then inserted into a depression in an alkaline 1.4% agarose gel and electrophoresed at 90° to the original direction of electrophoresis. Both the neutral and alkaline agarose gels were dried and exposed to X-ray film. The procedure for alkaline agarose gel electrophoresis is essentially as that described in Sambrook et al. (1989).

2.11.3. Quantitation of NS-1 resolution products

NS-1 resolution products were separated on a 1.4% agarose gel and transferred to a nylon membrane (Genescreen plus^{TM}, Dupont) using a vacuum blotter (LKB). A ^{32}P-labeled DNA probe was prepared with random DNA primers (Pharmacia). The DNA probe corresponded to the StyI (nt 140) to PstI (nt 411) sites in the dimer bridge. After hybridization, the membrane was washed at high stringency (0.1xSSPE, 0.1% SDS, 70°C) and exposed to X-ray film. Results were quantitated by densitometry. (A phophorimager was not available when this quantitation was done.)

2.11.4.   Immunoprecipitation.

pQLDB1 was incubated with LA9 extract and Sf9 extract containing NS-1 in a 25 μl standard resolution reaction mixture as described in section 2.11.1. Following incubation, 6 μl of 10% SDS and 1 μl of 0.5M EDTA were added. The mixture was then incubated for 30 min at 60°C to disassociate any proteins not covalently bound to DNA. Subsequently, 200 μl of 50 mM Tris HCl (pH 8.0) were added to dilute the mixture followed by 9 μl of rabbit polyclonal antibodies against NS-1 (a gift of Dr. E. Faust, McGill University). The resulting mixtures were incubated at 4°C for 3 hrs. Subsequently, 50 μl of formalin-fixed *Staphylococcus aureus* (10%) (Boehringer-Mannheim, Mannheim, Germany) which had been washed with RIPA buffer (50 mM Tris HCl pH8.0, 0.1% SDS, 0.5% DOC, 1.0% NP-40 and 150 mM NaCl) were added. The mixture was incubated at 4°C for about 12 hrs. The immunoprecipitates were pelleted and washed three times using 500 μl of RIPA buffer each time. The pellet from the RIPA buffer washing was then washed using 500 μl of 1 X Reaction buffer 2 from BRL, resuspended in 10 μl of 1 X Reaction buffer 2 from BRL, digested with PstI/PvuII and centrifuged. The resulting

supernatant which is supposed to contain bands 1, 3, 4, 5 and 6 if NS-1 is covalently bound to bands 2 and 7 was electrophoresed on a 1% neutral agarose gel (Fig. 22, lane 3). The resulting pellet which is supposed to contain bands 2 and 7 if NS-1 is covalently bound to bands 2 and 7 was resuspended in 10 µl of 1 X Reaction buffer 2 from BRL, digested with proteinase K and centrifuged to remove the residual bacteria. The resulting supernatant which is supposed to contain bands 2 and 7 was also electrophoresed (Fig. 22, lane 4). As a control, a mouse monoclonal antibody against bovine rhodopsin (a gift of Dr. Molday, UBC) was also used to do the immunoprecipitation experiment described above. However, only the supernatant after proteinase K digestion and centrifugation was electrophoresed in lane 1 of Fig. 22 and the supernatant after restriction enzyme digestion and centrifugation is not shown.

2.12. Nicking assay of A-half or B-half clones of the dimer bridge

2.12.1. Analysis of nicked products on alkaline agarose gels

Two µg of plasmid DNA containing wildtype or mutant half dimer bridge molecules was linearized by digestion with SspI (one site present in the pUC sequences) and 3'-end labelled by an exchange reaction using $\alpha\text{-}^{32}PdATP$ and T4 DNA polymerase. The linearized and labelled plasmid was incubated for one hour with 9 µl of LA9 cellular extract and 2 µl of purified NS-1(~200 ng) in the same buffer (25 µl) for the resolution assay (section 2.11.1.). The reaction was then digested with proteinase K (28 µg/ml), extracted with phenol/CHCl$_3$ and precipitated with ethanol. The DNA pellet was redissolved in alkaline loading buffer (50 mM NaOH, 1 mM EDTA and 10%

glucose), loaded onto an alkaline agarose gel (1%), and run for 7 hr at 30V (Sambrook *et al.*, 1989). After electrophoresis, the gel was dried and exposed to X-ray film or analyzed using a phosphorimager (Molecular Dynamics).

2.12.2. Determination of the nicking efficiency of B-half dimer bridge mutants

SspI digested plasmid DNA (2 µg, unlabelled) was used in the nicking assay described above. After electrophoresis, the DNA was transferred to a nylon membrane (Genescreen plus™, DuPont) and hybridized with the labelled smaller SspI/EcoRI DNA fragment from pUC19. The membrane was washed and the amount of probe hybridized was quantitated using a phosphorimager.

2.13. Binding of a host cell protein(s) to the HFBR: gel mobility shift assays.

The substrate for gel mobility shift assays used to detect binding of a host factor(s) to the B-half dimer bridge was a ~60 bp fragment obtained by digesting plasmid pUCWT with EcoRI/HindIII. The competitor DNA used was obtained by digesting plasmids pUCWT, pUCC4A, pUCG14A or pUCC4AG14A with PvuII. LA9 cellular extract (2 µl) in 25 µl of binding buffer (10 mM Tris HCl, pH 7.5; 50 mM NaCl, 1 mM DTT, 5% glycerol, and 0.2 µg/µl salmon sperm DNA) was incubated at room temperature for 10 min in the presence or absence of competitor DNA followed by the addition of 1 µl (1 ng/µl) end labelled probe. The incubation was continued at room temperature for an additional 30 min, loaded onto a pre-run polyacrylamide

gel (4% in 0.5 x TBE and 0.5% glycerol) and electrophoresed for 2.5 hrs at 150V. The running buffer was the same buffer used to cast the gel. The gel was dried and analyzed using a phosphorimager.

2.14.   Competition nicking assay

The competition nicking assay was performed as described above (section 2.12.1.) except different amounts of competitor DNA fragment were added to the assay tubes before the incubation for nicking.

III.   Results

3.1.   Predicted products from *in vitro* resolution of the cloned
**   wildtype dimer bridge**

The plasmid pQLDB1 contains the dimer bridge which is the junction fragment of MVMp dimer RF. It comprises the Pst I site (nt 411) on the left of the junction to the AluI site (nt 408) on the right of the junction (see Materials and Methods, section 2.7.1.). The total length of the cloned junction in pQLDB1 is ~700 bp. The dimer bridge clone is identical in sequence to the one in the dimer RF except both NcoI sites (nt 259) were destroyed (indicated by square brackets) during construction of the clone. The orientation of the insert in relation to restriction sites used during the cloning is illustrated in Fig. 13A. Resolution of this dimer bridge according to the Modified Rolling Hairpin Model is predicted to result in a DNA molecule illustrated in Fig. 18A. Subsequent restriction with PstI and PvuII should generate four fragments, a 514 bp extended fragment, a 353 bp turn-around fragment, and 193 bp and 2350 bp linear fragments derived from the vector, pUC19 (Fig. 18B).

3.2.   *In vitro* resolution of the wildtype dimer bridge clone, pQLDB1,
**   in the presence or absence of recombinant NS-1**

3.2.1.   Analysis of resolution products on one-dimensional agarose gel

To test for *in vitro* resolution of the wildtype dimer bridge, pQLDB1 was incubated with Sf9 cytoplasmic extracts containing NS-1, LA9 replication extract, $\alpha-^{32}$PdATP and other components as described in Materials &

A:

B:

353 bp
turn-around form

514 bp
extended form

193 bp
vector fragment

2350 bp
vector fragment
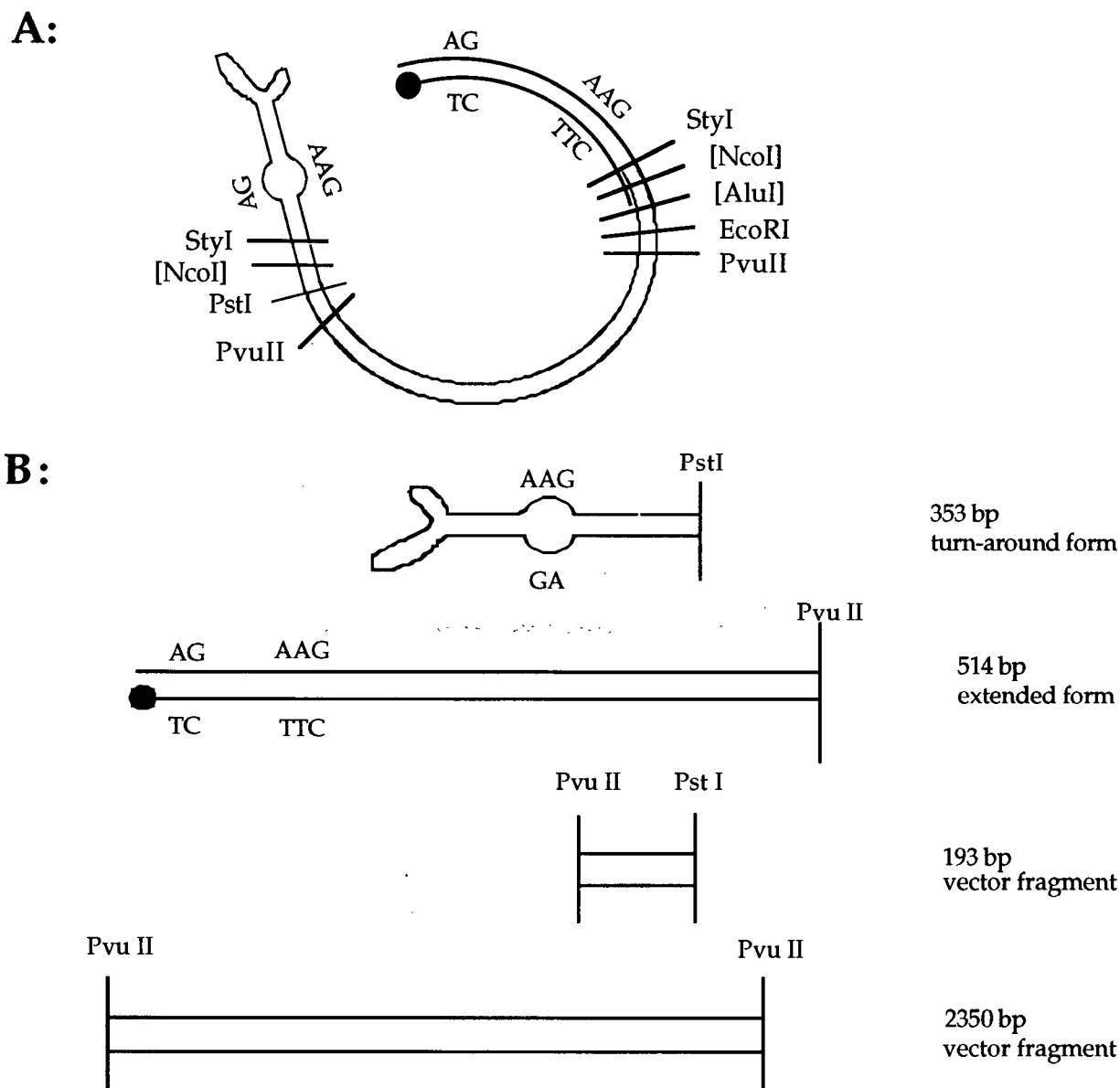
Fig. 18. The predicted resolution products of pQLDB1. Relevant restriction sites are illustrated. Restriction sites in square brackets are sites which were destroyed during construction of pQLDB1. The black circle indicates NS-1 covalently bound to the 5'-end of the extended end of the resolved dimer bridge. **A.** shows the structure of the resolved pQLDB1 after incubation with NS-1 and LA9 extracts. **B.** shows the four DNA fragments from the PstI/PvuII digestion of the resolved pQLDB1 shown in **A.** The sizes of the fragments are indicated. (not drawn to scale)

Methods (section 2.11.). The LA9 replication extract can provide DNA polymerase and some other essential proteins for the resolution of the dimer bridge. It is also believed that pQLDB1 can be labelled through random nick translation in the presence of LA9 extracts and α-^{32}PdATP. As shown in Fig. 19, in the presence of Sf9 cytoplasmic extract containing NS-1, seven labelled fragments were detected (Fig. 19, +NS-1 lane). Fragments 1 to 4 correspond in size to the predicted fragments described in the previous paragraph (Fig. 18B) if resolution is as described in the MRHM (Fig. 10). In order of decreasing size: band 1 corresponds to the 2350 bp vector fragment; band 2 to the 514 bp extended fragment; band 3 to the 353 bp turn-around fragment; and band 4 to the 193 bp fragment from the vector. Fragment 5 is the correct length (810 bp) for the unresolved PstI to PvuII fragment containing the unresolved dimer bridge due to excess input plasmid. However, bands 6 and 7 are not predicted.

Since the dimer bridge is a palindrome sequence, it is believed that a cruciform structure (see text illustrated below) can form and subsequently recombination (indicated in the illustration) occurs due to the presence of recombination enzymes in the LA9 or Sf9 cellular extracts. After recombination, pQLDB1 becomes a linearized DNA molecule with two turn-around form ends (see text illustration below). Subsequent digestion of this DNA molecule could produce four DNA fragments three of which are the same as bands 1 (vector DNA), 3 (turn-around form) and 4 (vector DNA) (Fig. 19) from the resolution of the dimer bridge. The fourth band would be a turn-around fragment corresponding in size to band 6 (455 bp).

Fig. 19. *In vitro* **resolution of the wildtype dimer bridge clone, pQLDB1, in the presence of recombinant NS-1.**

Plasmid pQLDB1 which contains the wildtype dimer bridge sequence was incubated with mouse LA9 extract plus insect cell extract from cells infected with the wildtype baculovirus or recombinant virus, AcNS-1. The products of the resolution assay were digested with proteinase K, then with PstI and PvuII, and analysed on a 1.4% agarose gel as described in the Methods. The outer lanes (+NS-1, duplicate experiments) display the four bands expected from resolution, labelled 1 - 4. (See Fig. 18 an for explanation of these bands.) The additional bands are 5 (810 bp) corresponding to the unresolved junction fragment, and bands 6 (455 bp) and 7 (411 bp) which correspond, respectively, to a turn-around form and extended form if initiation of resolution begins at nick site #2 (Fig. 10). The middle lane (minus NS-1) contains band 3 and 6 which can also arise by recombination (see Text for details).

Fig. 19

recombination
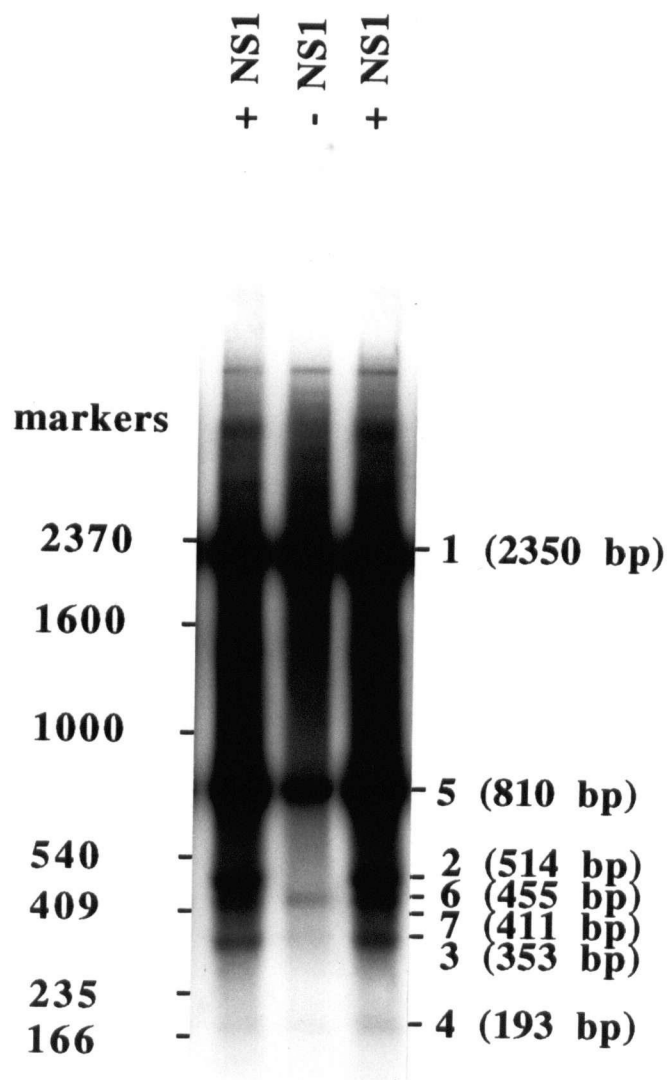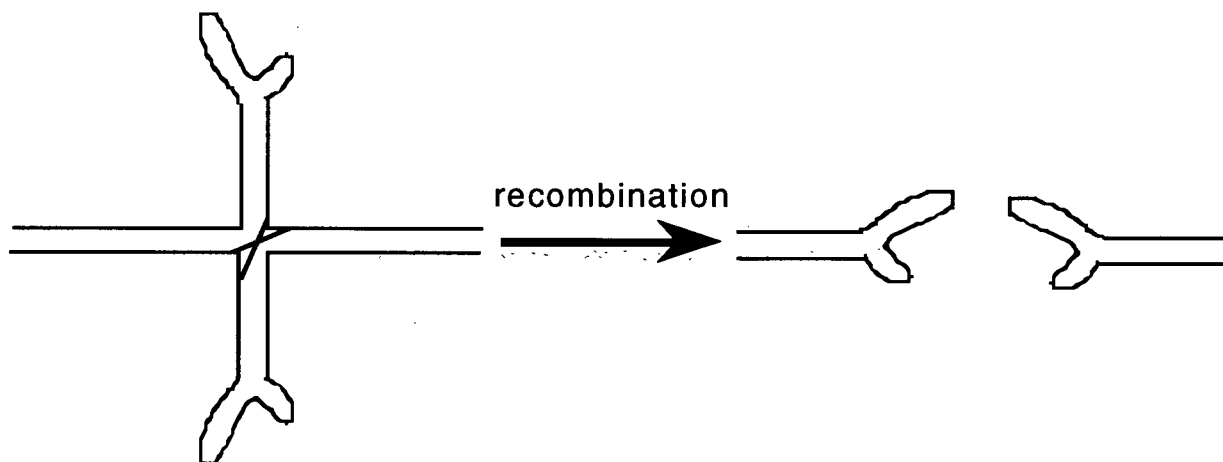
Band 7 (detected at a very low level but seen more clearly in Fig. 20) corresponds to the extended fragment of 411 bp if resolution initiates with NS-1 nicking at nick site #2 (*NB*, I now believe the actual resolution procedure of the dimer bridge is likely not as described in MRHM and the production of band 7 is likely not from NS-1 nicking at nick site # 2; see Discussion part of the thesis), contrary to the procedure described in the MRHM. The corresponding turn-around form is identical to band 6 which also arises from recombination as stated earlier. The relative intensities of the extended forms (Fig. 19, compare bands 2 and 7) is consistent with the hypothesis that resolution of the dimer bridge is asymmetric as predicted by the Modified Rolling Hairpin Model. (*NB*, this autoradiograph was deliberately overexposed in order to determine whether band 7 can be detected.) In the absence of NS-1, bands 2 and 7 were not detected (Fig. 19, middle lane), indicating that resolution of the dimer bridge requires NS-1.

There is a high background in Fig. 19 which appears to include a few discrete weaker bands. This background is likely due to random nicking/cutting of the DNA in the presence of the crude LA9 and Sf9 extracts while the weaker bands may be due to partial restriction enzyme digests as

well as intermediates of the NS-1 resolution process which we have not yet characterized.

Since the dimer replicative form of MVMp is a linear DNA molecule, linearized pQLDB1 was also used in the resolution assay. The same conclusion about the resolution products of the dimer bridge (data not shown) was reached as when the circular pQLDB1 was used as the substrate. In the *in vitro* resolution assays described above and below, crude Sf9 cytoplasmic extracts containing NS-1 instead of purified NS-1 was used. This is because NS-1 purified according to the older lengthier method described by Wilson *et al.* (1991) is not active in the resolution assay although it does have demonstrable helicase and ATPase activities. Later a modified purification method (see Materials and Methods) was used and highly purified NS-1 was obtained. This highly purified NS-1 is active for the resolution of the dimer bridge and the resolution products (data not shown) were the same as when the crude Sf9 cytoplasmic extracts containing NS-1 were used.

3.2.2. Quantitation of resolution products by Southern blotting

When the Sf9 cytoplasmic extract containing no NS-1 is used in the resolution assay, apparent recombination of the dimer bridge occurs (bands 3 and 6 in the middle lane of Fig. 19). As described above, in the +NS-1 lane, band 3 is believed to result from NS-1 resolution as well as from recombination and band 6 is believed to result from a minor NS-1 resolution procedure (initiating nick at site # 2) as well as from recombination. If this is true, the following relationships should be observed: 1) the amount of DNA in band 3 of the +NS-1 lane should be greater than that of band 3 in the -NS-1 lane; 2) the amount of DNA in band 6 subtracted by the amount in band 7

(both in the +NS-1 lane) should be equal to the amount of DNA in band 6 in the -NS1 lane; 3) In the +NS-1 lane, the amount of DNA in band 3 should be equal to band 2 plus band 6 minus the amount of DNA in band 7.

In the experiments illustrated in Fig. 19, these quantative relationships cannot be determined because the intensity of the bands in the + NS-1 lane is greater than the intensity of the corresponding bands in the -NS-1 lane, probably due to the helicase activity of NS-1 and also because the random nick translation labelling used in the resolution assay results in longer DNA molecules incorporating more radiolabel. Therefore, a Southern blot analysis of the resolution products of the dimer bridge was used for quantitation (Fig. 20).

I carried out a resolution assay in the absence of $\alpha-^{32}PdATP$, separated the products by electrophoresis, and probed the gel with a fragment of DNA that detects resolution products (Fig. 20). Quantitation of bands 2, 3, 6 and 7 by densitometry revealed the quantitative relationships described above except that the intensity of band 6 (+NS-1 lane) subtracted by the intensity of band 7 (+NS-1 lane) is significantly greater than that of band 6 in the -NS-1 lane. These observations show that the ratio between the two NS-1 resolution products (the turn-around form and the extended form shown in Fig. 10) is approximately 1 : 1 while the exception noted above suggests that recombination in the presence of Sf9 cytoplasmic extract containing NS-1 is enhanced over that of Sf9 cytoplasmic extract not containing NS-1. It would be interesting if NS-1 does indeed contribute to the recombination event (see the Discussion). Based on the intensity of band 2 relative to the unresolved band 5, the resolution efficiency in this *in vitro* assay is ~5-10%.

In this Southern blotting analysis, the PstI/StyI fragment from the dimer bridge was labelled as the probe. This fragment was not expected to
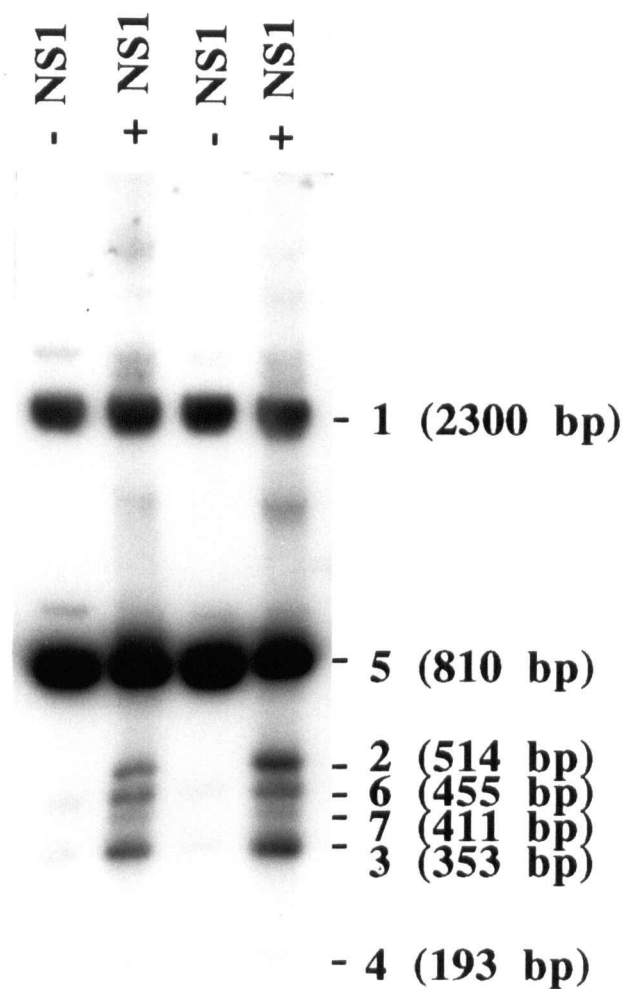
Fig. 20. Southern blot analysis of pQLDB1 resolution products

The resolution assay of pQLDB1 was done in the absence of α-^{32}PdATP. The PstI/PvuII digested resolution products were run on a neutral agarose gel, transferred to a nylon membrane and then probed with the labelled StyI/PstI fragment from the MVMp dimer bridge. The amount of DNA in each lane was quantitated by densitometry.

detect band 1 since band 1 is from the pUC19 vector DNA. Computer analysis indicated that the PstI/StyI fragment from the dimer bridge has no apparent homology to the vector DNA. Since the PstI/StyI fragment for the probe was isolated from an agarose gel after PstI/StyI digestion of pQLDB1, it seems possible that the isolated PstI/StyI fragment may be contaminated with a trace amount of vector DNA. However, even if this is the case, the contamination is likely minor and should not interfere with the quantitation of bands 2, 6, 7 and 3 as band 4 (Vector DNA) is not visible and also in the -NS-1 lane band 6 containing vector sequence has the same intensity as band 3 not containing vector DNA. Also the intensity of the unresolved dimer bridge (band 5) is much greater than the vector sequence (band 1).

In the +NS-1 lanes (Fig. 20), there is a minor band between band 5 and band 1. This band has not been characterized. In the left -NS-1 lane, the minor band above band 1 or band 5 is likely from partial restriction enzyme digestion.

3.2.3. Two-dimensional neutral/alkaline gel electrophoresis to characterize extended and turn-around forms

In order to confirm the structure of the extended and turn-around species, resolution products were separated first under neutral conditions followed by alkaline gel electrophoresis to denature the strands (Fig. 21). The radioactive spots 1, 5 and 2 which are on a diagonal correspond with the 2350 bp band 1, 810 bp band 5 and 514 bp band 2 in Fig. 19. From the sizes of the denatured DNA of these spots on the denaturing gel, it can be concluded that the corresponding bands are extended forms. Spots 3 and 6 which are seen on the lower concave diagonal correspond to the 353 bp band 3 and 455 bp band 6
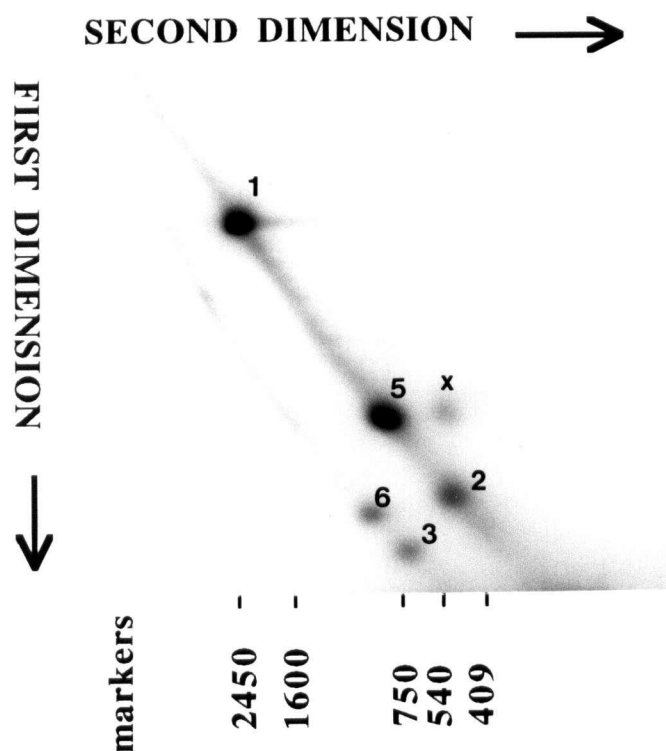
Fig. 21. Two-dimensional neutral/alkaline agarose gel electrophoresis analysis of resolution products from the wildtype dimer bridge plasmid, pQLDB1.

The products of a standard resolution assay were analyzed on a neutral gel in the first dimension and on a denaturing gel in the second dimension as described in the Methods. The spots which correspond with the bands in Fig. 19 are numbered. The two spots 3 and 6 migrate more slowly in the second direction confirming that they are turn-around forms. A possible explanation of spot X is provided in the Discussion.

(Fig. 19) and migrate as ~700 nt and ~910 nt long fragments, respectively. Therefore, bands 3 and 6 are turn-around forms. The continuous line of fragments generated by linear and turnaround forms likely result from random nicking/cutting of the substrate DNA due to nuclease activities in the crude extracts. One spot labelled as " X " migrated faster than expected for a linear single-stranded DNA fragment (see Discussion for possible explanation).

3.2.4. Immunoprecipitation to show that NS-1 is covalently bound to the extended form resolution product of the dimer bridge.

The MRHM predicts that NS-1 is covalently bound to the extended form resolution product of the dimer bridge (Fig. 10). In order to confirm this, an immunoprecipitation experiment was done using polyclonal antibodies against NS-1. (These antibodies are called SDP-2.) Lanes 3 and 4 of Fig. 22 are supernatants after RE digestion and proteinase K digestion, respectively, (see section 2.11.4) when SDP-2 was used. Lane 1 of Fig. 22 is the supernatant after proteinase K digestion when a control monoclonal antibody against bovine rhodopsin was used for the immunoprecipitation (the supernatant after RE digestion is not shown in this figure). Lane 2 shows the resolution products of pQLDB1. The presence of band 2 in lane 4 of Fig. 22 indicates that SDP-2 preferentially binds to the extended form resolution product (band 2). It is further believed that the association of NS-1 and band 2 is covalent because the resolution products of the dimer bridge were treated in relatively high concentration (2%) of SDS at 60°C for 30 min before the addition of antibodies.

Fig. 22. The extended form resolution product is covalently bound to NS-1.

The resolution products of pQLDB1 were incubated in 2% SDS at 60°C for 30 min (see section 2.11.4.) and diluted using 50 mM Tris HCl buffer (pH8.0). Rabbit polyclonal antibody to NS-1, SDP-2, was added. After incubation for 3 hrs, fixed *S. aureus* bacteria were added and incubated for about 12 hrs to precipitate the antibodies. The pellet was washed and redissolved into 1 X Reaction buffer from BRL in order to digest the DNA with PstI/PvuII digestion. After the digestion, the reaction mixture was centrifuged. The supernatant was loaded onto a neutral agarose gel (lane 3). The pellet was digested with proteinase K, and centrifuged to remove the residual bacteria. The resulting supernatant was also loaded on the gel (lane 4). As a control, a mouse monoclonal antibody against bovine rhodopsin was used to do the experiment described above and the resulting supernatant after proteinase K digestion and centrifugation was loaded on the gel (lane 1). Standard resolution products of pQLDB1 were also electrophoresed (lane 2) to serve as markers.

Fig. 22

That band 5 occurs in lane 3 and very weak band 1 and band 5 occur in lane 4 is probably due to nonspecific binding of DNA with fixed *Staphylococcus aureus* or/and SDP-2. That bands 3, 4 and 6 do not occur in lane 3 and band 7 does not occur in lane 4 is believed due to their relatively low intensities. I do not think the presence of band 2 in lane 4 is due to nonspecific binding of DNA with fixed bacteria or/and SDP-2 because the intensity of band 2 in lane 4 is apparently higher than the intensities of band 1 and band 5 in the same lane. In lane 2, it is clear that the intensity of band 2 is lower than that of band 1 and is similar to that of band 5.

It should be mentioned that a pre-immune serum rather than the monoclonal antibody against bovine rhodopsin is the best control for this immunoprecipitation experiment. Unfortunately, when this experiment was done no pre-immune serum was available. It is known that *S. aureus* precipitates mouse IgG2A, 2B, 3 and 1 with lower efficiency than rabbit IgG's.

3.3.   Resolution of mutant dimer bridge clones

We tested the mutant dimer bridge clones, pQLDB2, pQLDB3 and pQLDB4, for *in vitro* resolution in order to determine if sequences within the dimer bridge affect the site of initiation of resolution and hence provide information about the resolution procedure of the dimer bridge. Previously it had been predicted that the "bubble" in the stem of 3'-end hairpin (Fig. 4) may provide the sequence asymmetry that is recognized during resolution of the dimer bridge. This asymmetry was predicted to result in initiation of resolution predominantly at nick site # 1 (Fig. 10) and consequently conservation of the unique sequence at the left end of the viral and RF DNAs (Astell *et al.*, 1985).

To test these predictions, pQLDB2 was designed to comprise a dimer bridge in which $\frac{AAG}{TTC}$ is mutated to $\frac{CT}{GA}$ (Fig. 13B), and assayed for *in vitro* resolution (Fig. 23, lane 4). Although band 2 is slightly reduced and band 7 increased relative to their intensities generated with pQLDB1 (Fig. 23, lane 1), overall pQLDB2 is resolved with approximately the same efficiency as pQLDB1. (This result was unexpected because according to the MRHM, pQLDB2 does not have the recognition motif ($\frac{AAG}{TTC}$) required for nicking to occur at site # 1 and was predicted not to be resolved.)

In the second mutant dimer bridge clone, pQLDB3, the 10 bp sequence surrounding the putative nick site # 1 was altered by inverting the sequence (Fig. 13C). Relative to the wildtype pQLDB1, resolution products of pQLDB3 (Fig. 23, lane 3) reveal that the intensity of band 2 is decreased slightly and band 7 is increased. This is also a surprising result because according to the MRHM, mutation of nick site # 1 was predicted to block resolution of the dimer bridge, assuming there is sequence specificity for nicking to occur.

For the third mutant dimer bridge clone, pQLDB4, which contains the same mutant dimer bridge except a 2 bp deletion as pQLDB2 (Fig. 13D), the orientation of the mutant dimer bridge in the pUC19 vector is reversed from that of pQLDB1, pQLDB2 and pQLDB3. Hence band 7 in lane 2 (Fig. 23) corresponds to the extended form if resolution initiates at nick site #1 and band 2 corresponds to the extended form if resolution initiates at nick site #2. From the results shown in lane 2, it can be concluded that pQLDB4 is also resolved approximately as well as the wildtype dimer bridge clone. Also, comparing lane 2 (pQLDB4) with lane 4 (pQLDB2), it is clear that band 2 of lane 2 is weaker than band 7 of lane 4, suggesting that NS-1 may recognize

Fig. 23. Resolution products of the mutant dimer bridges.

Plasmids pQLDB2 (lane 4), pQLDB3 (lane 3), and pQLDB4 (lane 2) which contain minor sequence changes within the dimer bridge are all resolved approximately as efficiently as the wildtype dimer bridge, pQLDB1 (lane 1). Note that the orientation of dimer bridge in plasmid pQLDB4 is opposite to that of the other plasmids, hence the turn-around and extended form resolution products from resolution initiating at putative nick site #1 of pQLDB4 are, respectively, bands 6 and 7, while the turn-around and extended form products from resolution initiating at nick site #2 are, respectively, bands 3 and 2.
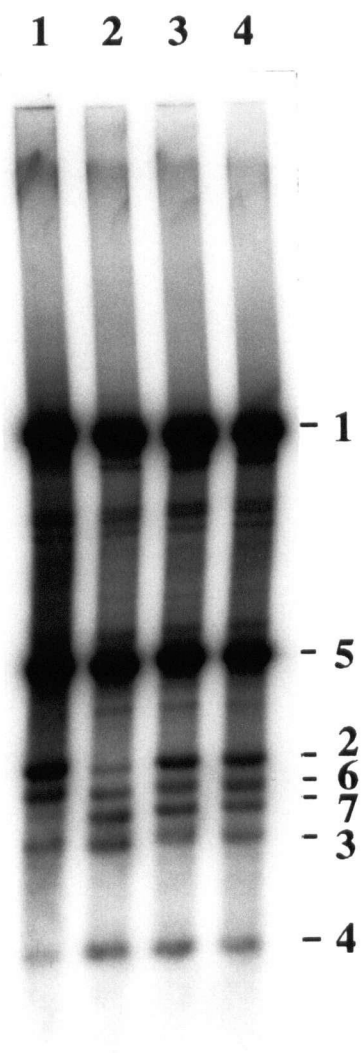
Fig. 23

both the bubble asymmetry and the distance between the bubble and the nick site. According to the MRHM, I predicted that pQLDB4 could not be resolved or at least resolution would be severely impaired.

Two dimensional gel electrophoresis of the resolution products from pQLDB2, pQLDB3 and pQLDB4 revealed that bands 2, 7, 1 and 4 are extended forms, and bands 3 and 6 are turn-around forms (Fig. 24) as was the case for pQLDB1. The resolution results of these three dimer bridge mutants strongly suggest that the resolution procedure of the dimer bridge as described in the MRHM is likely incorrect (see Discussion).

3.4. The B-half of the dimer bridge is nicked with recombinant NS-1 and replication extract from mouse LA9 cells

3.4.1. The B-half (and not the A-half) of the dimer bridge undergoes site-specific nicking in the presence of recombinant NS-1.

It has been reported that NS-1 can nick the B-half but not the A-half (see Fig. 14) of the MVMp dimer bridge (Cotmore and Tattersall, 1994). In order to confirm this observation, I constructed similar half dimer bridge clones and both the B-half and A-half clones were tested in the nicking assay. If the B-half clone, pQLB, is nicked as reported previously, NS-1 should nick the lower strand at a relatively specific site about 50 bp from the [BssHII] site (Fig. 15A) and produce a radioactive fragment corresponding to ~650 nucleotides. In addition, a ~3040 nt labelled fragment should be detected (Fig. 25A). The 3040 nt band consists of the end labelled upper strand (not nicked) and any non-nicked lower strand, while the 650 nt fragment is the labelled fragment from the nicked lower strand. (The ~2390 nt fragment from the

Fig. 24. **Two-dimensional neutral/alkaline agarose gel electrophoresis analysis of resolution products from the mutant dimer bridge plasmids.**

The products of standard resolution assays of mutant dimer bridge plasmids were analyzed, respectively, on a neutral gel in the first dimension and on a denaturing gel in the second dimension as described in the Methods. The spots which correspond with the bands in Fig. 23 are numbered. **A** is pQLDB2. **B** is pQLDB3 and **C** is pQLDB4. In **B**, there are two small arrows which indicate the positions of two weak spots there. These two spots are visible on the X-ray film. See Discussion for a possible explanation of these products.

Fig. 24

A. SspI .... SspI

nick site

B.

1 2 3 4

← x

← 3040 nt

← 650 nt
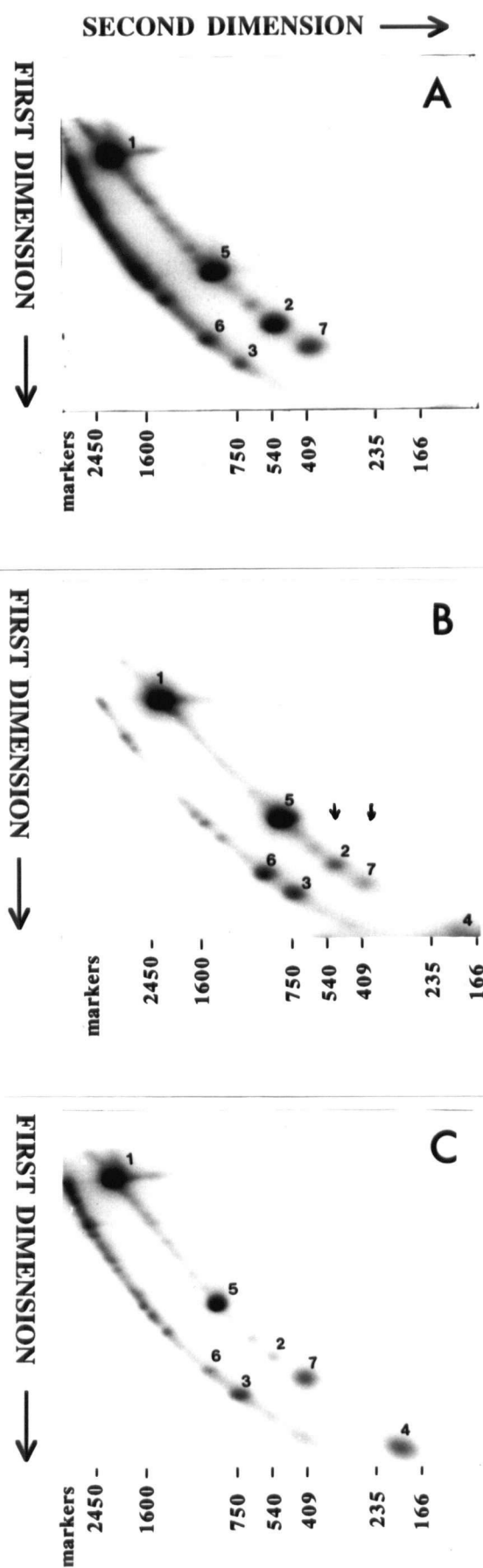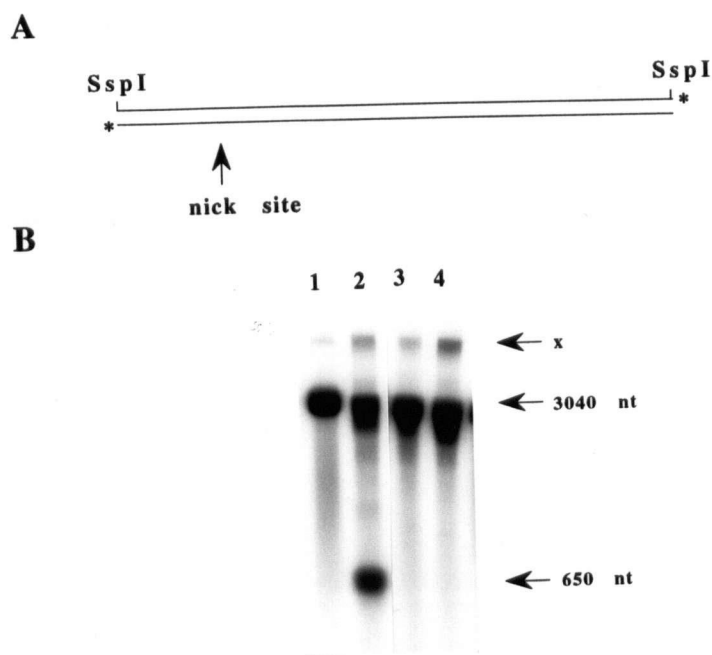
Fig. 25. The B-half of the dimer bridge is nicked by crude recombinant NS-1 but the A-half is not nicked.

A. The schematic diagram of the end-labelled and linearized pQLB which is nicked at a specific site. **B.** Labelled DNA (lanes 1 and 2 for pQLB, lanes 3 and 4 for pQLA) was incubated with LA9 extract in the presence (lanes 2 and 4) or absence (lanes 1 and 3) of crude NS-1 extract. The DNA samples were digested with proteinase K, precipitated, and analyzed on a denaturing agarose gel. The dried gel was exposed to X-ray film to detect the product of the nicking reaction. NB: pQLB and pQLA were analyzed on different gels and the results combined in this figure.

lower strand is not labelled, hence, not detected in the assay.) For the A-half clone, pQLA, one band (~3040 nt) should be seen if it is not nicked. The observed products obtained using the B-half (Fig. 25B, lane 2) and A-half (Fig. 25B, lane 4) dimer bridge clones were as predicted, confirming the previous observations (Cotmore and Tattersall, 1994).

In addition to the predicted fragments, a larger unexpected band X was also observed in all 4 lanes. This band is not present in input labelled DNA (data not shown) nor is it due to the presence of the NS-1-containing Sf9 extract as it is also seen with just LA9 cellular extract (Fig. 25B, lanes 1 and 3). When LA9 extract is incubated in the nicking reaction mixture in the presence of $\alpha-{}^{32}PdATP$ but in the absence of plasmid DNA, band X did not appear on the gel, suggesting that it is not from the LA9 extract but from the plasmid. When the nicking assay products were detected by Southern blotting using radiolabelled plasmid DNA as the probe, this band was detected only after extensive overexposure of the phosphoimager screen (data not shown). (In Fig. 27 which is a Southern blot result without overexposure, band X is not detected.) When the plasmid was digested with SspI and linearized plasmid DNA isolated from a gel and used as the substrate for nicking assay, band X was still apparent. Based on the experiments described in this paragraph, it seems possible that band X may be the ligation product of the linearized plasmid in the presence of LA9 extract. That band X could not be easily detected by Southern blotting is likely due to the very low levels of this molecule generated in the nicking assay.

3.4.2. Mouse LA9 replication extract is required for nicking of the B -half of the dimer bridge

In order to determine if host factor(s) is required for nicking of the B-half of the dimer bridge by NS-1, the nicking assay was carried out using immunoaffinity purified NS-1 in the presence or absence of LA9 cellular extract (Fig. 26A). In the absence of LA9 extract, the B-half of the dimer bridge is not nicked by purified NS-1 (Fig. 26A, lane 1) indicating that a host cellular factor(s) is required for nicking. When both purified recombinant NS-1 and LA9 extract are present, the 650 nt product of the nicking assay is readily seen (lanes 2 and 3, duplicate experiments). Using the conditions of this assay, based on the radioactivity in the 650 nt band, approximately 50% of the substrate is nicked. The purified NS-1 used in the nicking assays described above was obtained using a modified purification procedure (see Materials and Methods). SDS-PAGE analysis of this immunoaffinity purified NS-1 revealed a major band of ~83 kDa and a minor band of lower molecular weight (Fig. 26B). Western blot analysis using a monoclonal antibody against NS-1 indicated that the major band is NS-1 and the minor band is not a degradation product of NS-1 (Liu and Astell, data not shown). It is ofcourse better to use purer NS-1 to do the nicking assay described above. But it will be a big effort to get purer NS-1 which is active for nicking since lengthier purification procedure seems to inactivate NS-1 as mentioned in section 3.2.1..

3.5. Identification of nucleotides important for site-specific nicking: two CG motifs within the B-half of the dimer bridge.

Since it has been shown that NS-1 can bind to the ACCAACCA sequence of the B-half of the dimer bridge and a mutation in the adjacent

A:

B:
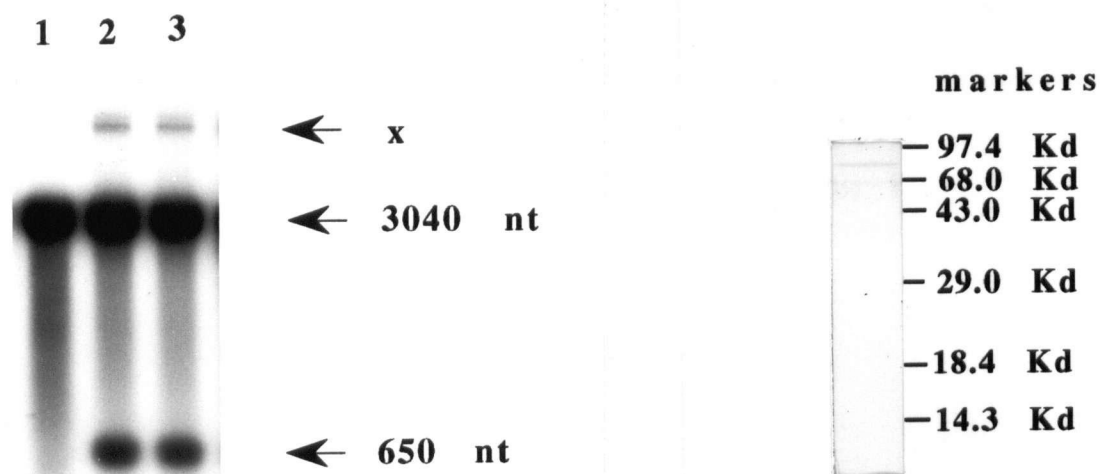
Fig. 26. Nicking of pQLB with purified recombinant NS-1 requires LA9 cellular extract.

A. pQLB was linearized by digestion with SspI and end-labelled with T4 DNA polymerase. The labelled DNA was incubated with immunoaffinity purified recombinant NS-1 in the absence (lane 1) or presence (lanes 2 and 3) of LA9 cellular extract. The samples were analyzed as described in Fig. 25. **B.** SDS-PAGE analysis of the purified NS-1 using immunoaffinity column (see Methods).

region of the CG basepair in position 4 (Fig. 16B) to an AT basepair can significantly decrease the nicking efficiency of the B-half, it was suggested that host cell activating transcription factor (ATF) may be important for nicking (Cotmore *et al.*, 1995a). In order to test this idea, I decided to determine which nucleotides in the region [subsequently referred to as the putative **h**ost **f**actor(s) **b**inding **r**egion (HFBR)] adjacent to the NS-1 binding site are important in the nicking reaction. Thus, a series of B-half mutants were constructed and the nicking efficiency of each was determined. When the ATF binding site 1 (Fig. 15B) was deleted, the nicking efficiency of this mutant, pQLBWT13 (Fig. 16), increased by 25% compared with pQLB (Fig. 27A, lanes 1 and 2). This observation suggests that the ATF binding site 1 is not required for nicking. Gel mobility shift assays using LA9 extract indicated that murine host factor(s) (possibly ATF) can bind to site 1, although the affinity is relatively weak (data not shown). If host cell ATF does bind to site 1, it may partially block access to the B half of the dimer bridge to other host factor(s) and thus inhibit nicking of pQLB.

When both ATF binding sites are deleted from mutant pQLBDEL, the DNA is not nicked (Fig. 27A, lane 10). This observation implies that nucleotides in ATF site 2 are required for nicking. When each of the five nucleotides (CGTCA) of ATF site 2 were mutated, the nicking efficiency was reduced to less than wildtype nicking efficiency: pQLBC4A (5% of wildtype), pQLBG5A (10% of wildtype), pQLBT6C (60% of wildtype), pQLBC7T (80% of wildtype), and pQLBA8G (80% of wild-type). These results suggest that C4 and G5 of ATF site 2 are considerably more important than the other three positions and imply that ATF, which recognizes a CGTCA motif (Nichols *et al.*, 1992), is unlikely the host factor required for nicking.

When nucleotides 9 through 20 of the putative HFBR were mutated
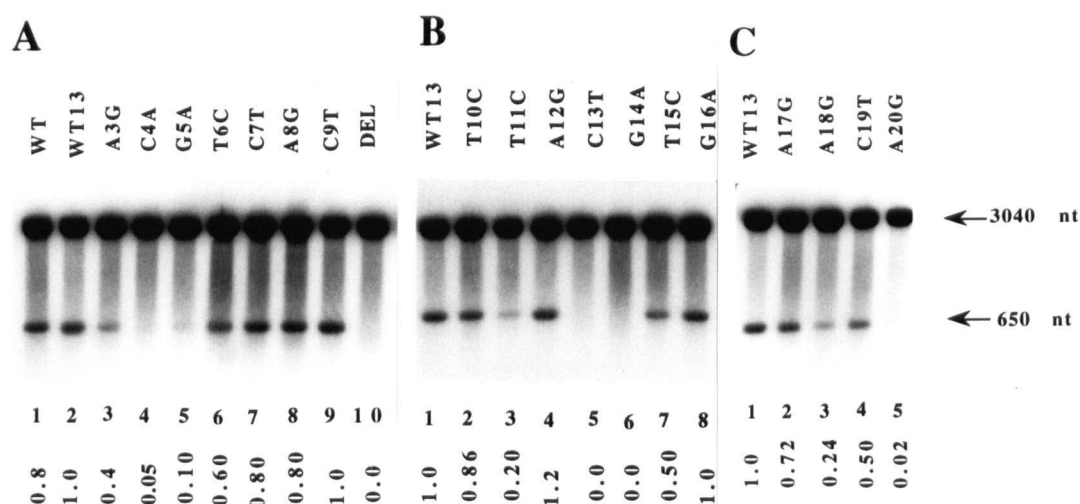
Fig. 27. Determination of the nicking efficiency of mutants of the B-half dimer bridge.

Each B-half clone was digested with SspI (but not labelled with ^{32}P). The linearized DNAs were incubated with LA9 extract and purified recombinant NS-1. After proteinase K digestion, phenol/chloroform extraction and EtOH precipitation, the samples were loaded onto a denaturing agarose gel and electrophoresed. The DNA on the gel was transferred to a nylon membrane and probed with the labelled SspI/EcoRI fragment from pUC19. The ~650 nt fragment was quantitated using a phosphorimager. The data at the bottom of each panel indicate the nicking efficiency for each plasmid relative to pQLBWT13 which is given a value of 1.0. In **A**, the plasmids analyzed were pQLB (wildtype), pQLBWT13, pQLBA3G, pQLBC4A, pQLBG5A, pQLBT6C, pQLBC7T, pQLBA8G, pQLBC9T and pQLBDEL, respectively. In **B**, lanes 1 to 8 are pQLBWT13, pQLBT10C, pQLBT11C, pQLBA12G, pQLBC13T, pQLBG14A, pQLBT15C and pQLBG16A, respectively. In **C**, lanes 1 to 5 are pQLBWT13, pQLBA17G, pQLBA18G, pQLBC19T and pQLBA20G, respectively.

one by one and tested for nicking efficiency, it was found that nucleotides T11, C13, G14, A18 and A20 are also important for nicking. Nucleotides 18, 19, and 20 are protected by binding of NS-1 (Cotmore *et al*, 1995a), hence, the reduction in nicking efficiency due to mutation at nucleotides 18 and 20 is probably not due to impaired binding of host cell factor(s). Also, when nucleotide T11 is changed to C, this creates an E box (CANNTG) (Gu *et al.*, 1995), hence, binding of the E box factor to this region may prevent binding of host cell factor(s) required for nicking. Therefore, only C13 and G14 are important for nicking (and hence binding of host cell factor(s)) within the region of nucleotides 9 through 20.

Based on the nicking efficiencies of all the B-half mutants, it appears that two CG motifs (nt 4, 5 and 13, 14, Fig. 16B) are required for nicking and these sequences likely are important in binding of host factor(s). Also, these results suggest that ATF is not the host protein essential for nicking as it binds to the sequence CGTCA.

3.6. **Gel mobility shift assays show that host cell factor(s) can bind to HFBR from wildtype DNA and binding to mutant DNA sequences is impaired**

The putative HFBR region (nucleotides 1 through 17, Fig. 16B) and three mutant HFBR sequences were cloned into pUC19. These plasmids are referred to as pUCWT (wildtype HFBR sequence), pUCC4A (C4 changed to A), pUCG14A (G14 changed to A), and pUCC4AG14A (C4 and G14 were both changed to A). The ~60 bp EcoRI/HindIII fragment containing the wildtype sequence was the probe used in gel mobility shift assays in which competitor DNA containing the wildtype or mutant HFBR sequences was added at two

different levels (10-fold and 40-fold molar excess). In most lanes, three sequence-specific complexes (one major and two minor) were observed (Fig. 28). It is likely that the fastest migrating complex is formed with a proteolytic product of the factor that forms the major complex. The slowest migrating complex is present at a very low level and could be due to binding of additional protein(s) to the complex. When the wildtype competitor is used (lanes 6 and 7), most of the specific complexes do not form. When the single mutant competitor DNAs are used (G14A and C4A), the specific complexes are partially reduced relative to no competitor, while the double mutant (C4AG14A) has very little effect on formation of the complexes. These data support the earlier suggestion that both CG motifs within the HFBR are required for binding of host factor(s).

3.7. The DNA fragment containing the wildtype HFBR of the B-half of the bridge dimer can inhibit nicking: mutant HFBR sequences are less effective inhibitors.

When the EcoRI/HindIII fragments containing the HFBR sequence with wildtype or mutant CG motifs (from plasmids pUCWT, pUCC4A, pUCG14A, and pUCC4AG14A) as well as the EcoRI/HindIII fragment from pUC19 were added, respectively, to a nicking assay mixture using pQLBWT13, it was observed that the wildtype HFBR strongly inhibits nicking (by 30% to 70%, depending on the concentration of the competitor) (Fig. 29, lanes 7 and 8). The competitor from pUCC4A or pUCG14A reduces nicking efficiency slightly (Fig. 29, lanes 9 to 12); however, the competitor DNA from pUC19 or pUCC4AG14A did not inhibit nicking (Fig. 29, lanes 3 to 6). These results provide further evidence that the unknown host factor(s) which binds to the
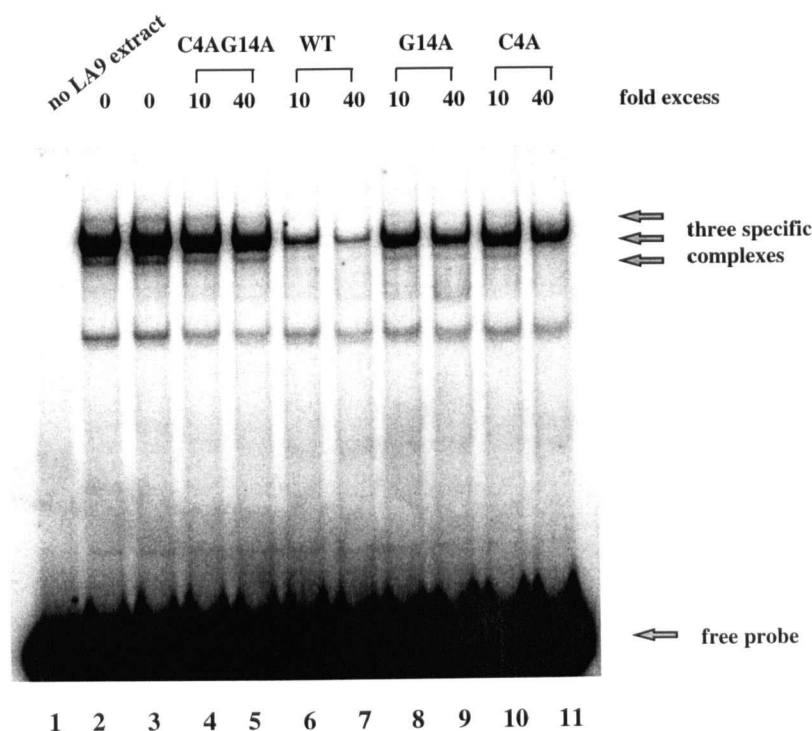
Fig. 28. Gel mobility shift assay of the HFBR fragment.

LA9 cellular extract was incubated at room temperature for 10 min in the absence (lanes 2 and 3) or presence (lanes 4 to 11) of competitor DNAs in 10- and 40-fold molar excess of the probe. The α^{32}P-labelled HFBR probe was then added and after a further 30 min incubation at room temperature, the samples were loaded onto a 4% polyacrylamide gel and electrophoresed. The gel was dried and analyzed using a phosphorimager. The radioactive probe was the EcoRI/HindIII fragment from pUCWT. The competitor DNAs were the short PvuII fragments contained in pUCC4AG14A (lanes 4 and 5), pUCWT (lanes 6 and 7), pUCG14A (lanes 8 and 9) and pUCC4A (lanes 10 and 11). Lane 1 is the probe without LA9 cellular extract.
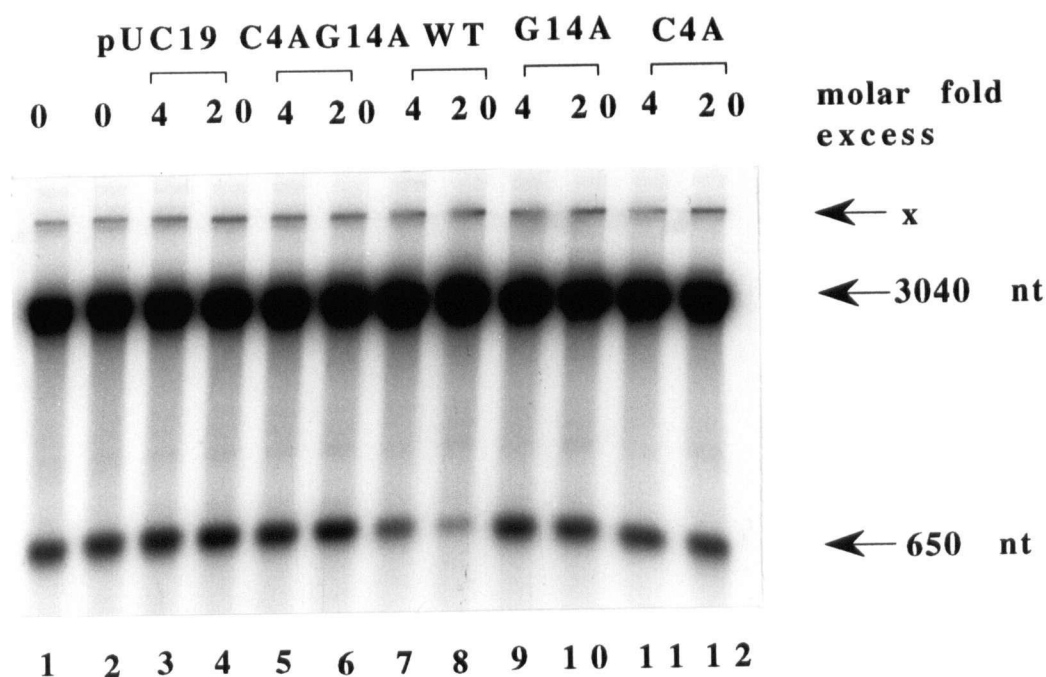
Fig. 29. Competition nicking assay of pQLBWT13.

Plasmid pQLBWT13 was digested with SspI and 3'-end labelled. The labelled DNA was incubated with LA9 cellular extract and purified recombinant NS-1 in the absence (lanes 1 and 2) or presence (lanes 3 to 12) of competitor DNAs. After incubation, the samples were analyzed as described in Fig. 25. The competitor DNAs were the small EcoRI/HindIII fragments from pUC19 (lanes 3 and 4), pUCC4AG14A (lanes 5 and 6), pUCWT (lanes 7 and 8), pUCG14A (lanes 9 and 10) and pUCC4A (lanes 11 and 12).

HFBR of the B-half of the dimer bridge is essential for nicking by NS-1.

3.8.   **The resolution assay of the wildtype dimer bridge clone,**

        pQLDB1, using mutant recombinant NS-1.

The plasmid pQLDB1 was incubated with mouse LA9 replication extract and insect Sf9 cellular extract containing wildtype NS-1 (Fig. 30, lane 1), Tyr188Phe mutant NS-1 (lane 2), Tyr197Phe mutant NS-1 (lane 3), or Tyr210Phe mutant NS-1 (lane 4). Subsequently, DNA samples were treated as described in Methods, digested with Pst1 and PvuII, and loaded onto a neutral agarose gel. After electrophoresis the gel was dried and autoradiographed. From the results shown in Fig. 30, it appears that the Tyr197Phe NS-1 mutant (but not Tyr188Phe NS-1 mutant and Tyr210Phe NS-1 mutant) is active in resolution of the dimer bridge, suggesting that Tyr188 and/or Tyr210 may be the candidate amino acid residue involved in the covalent linkage with DNA. When these three tyrosine NS-1 mutant proteins were used in the nicking assay of either the A-half dimer bridge or B-half dimer bridge, surprisingly, none was active for nicking (data not shown). See Discussion for the possible explanations.

One point which should be mentioned here is that the NS-1 mutant, Tyr197Phe, expressed in HeLa cells using the vaccinia virus vector was found not to be active for the resolution of the dimer bridge (Nuesch *et al.,* 1995). It is not clear whether or not this is due to the His tag fused to the mutant NS-1 expressed in the HeLa cells inactivating the (His)$_6$-NS-1 (Tyr197Phe) mutant protein.

Fig. 30. *In vitro* **resolution of the wildtype dimer bridge clone, pQLDB1, in the presence of mutant NS-1.**

Plasmid pQLDB1 which contains the wildtype dimer bridge was incubated with mouse LA9 extract plus insect cell extracts containing the wildtype NS-1 (lane 1), Tyr188Phe NS-1 mutant (lane 2), Tyr197Phe NS-1 mutant (lane 3), or Tyr210Phe NS-1 mutant (lane 4), respectively. The products of the resolution assay were treated with proteinase K, digested with PstI and PvuII, and analysed on a 1.4% agarose gel as described in the Methods.
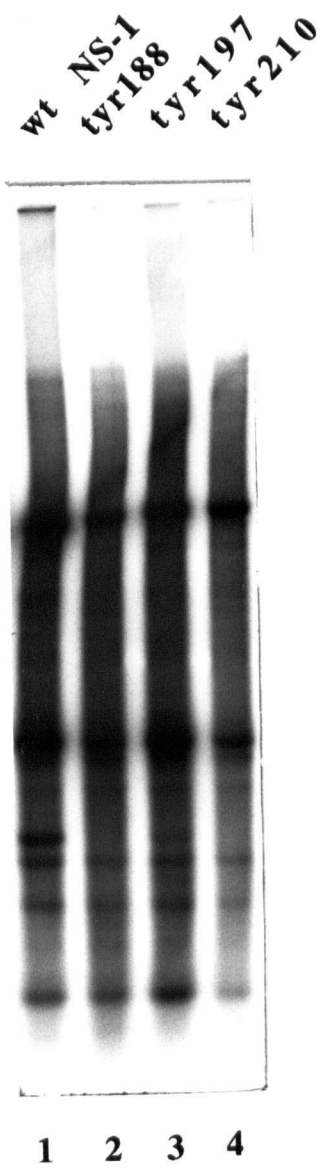
Fig. 30

IV.   Discussion

4.1.   The resolution products of the wildtype dimer bridge

One-dimensional agarose gel electrophoresis of the resolution products of the wildtype dimer bridge has shown that the MVMp dimer bridge can be resolved, *in vitro,* by recombinant NS-1 (Fig. 19). The resolution products contain the predicted ones (bands 1, 2, 3 and 4) according to the modified rolling hairpin model (MRHM) (Astell *et al.,* 1985) and also two bands not predicted (bands 6 and 7). Band 6 is thought to arise from recombination as well as a minor resolution process with the initiating nick occurring in the B-half (at nick site # 2) yielding band 7 and band 6. Hence, the results in Fig. 19 strongly support the dimer bridge resolution products predicted in the MRHM. Furthermore, characterization of extended form and turn-around form bands by 2-D gel electrophoresis (Fig. 21) proved the configuration of the resolution products. Result from the Southern blotting experiment (Fig. 20) confirmed that the ratio between the two NS-1 resolution products (the turn-around form and the extended form) is approximately 1 to 1.

NS-1 has been shown to be covalently bound to the 5'-ends of the replicative form and single-stranded DNA of MVM (Cotmore and Tattersall, 1988). This observation supports the prediction of the MRHM that the extended form resolution product (ie, band 2) is covalently bound to NS-1. Immunoprecipitation with polyclonal antibodies against NS-1 indicated that band 2 can be preferentially precipitated and the interaction of NS-1 with band 2 is likely covalent as the resolution products were treated at 60°C in a relatively high concentration of SDS (2%) prior to immunoprecipitation (Fig. 22). Therefore, all of these experimental results described above support the
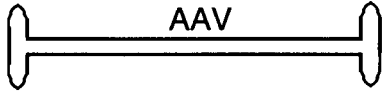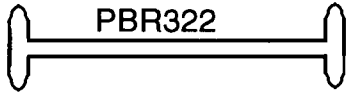
predicted resolution products of the dimer bridge described by the MRHM. The same conclusion was reached by Cotmore *et al.* (1993) from Yale University who used a LA9 or Hela cellular replication extract and LA9 or Hela nuclear extract containing recombinant NS-1 expressed using a Vaccinia Virus expression vector.

However, there are differences between the experimental data from this laboratory and that of the Yale group. The turn-around form described by the Yale laboratory corresponding to band 6 from our laboratory is minor in the presence of NS-1. In addition, they did not observe recombination when the dimer bridge was incubated with a cellular replication extract and nuclear extract without NS-1. Thus, the occurrence of a low level of recombination in the absence of NS-1 in our *in vitro* system is possibly due to enzymatic activities found in Sf9 cells. However, since the incorporation of radiolabel into plasmid DNA in the absence of NS-1 was much lower in the *in vitro* resolution system used by the other group, it is also possible that a low level of recombination actually occurred during the incubation of dimer bridge with cellular replication extract and nuclear extract without NS-1 but was not detected. This possibility is supported by the earlier observation that palindromic sequences do undergo recombination yielding two turn-around forms when incubated with a cellular replication extract and nuclear extract lacking NS-1 (Cotmore *et al.*, 1992). Hence, in the presence of NS-1, band 6 observed more readily in our resolution system than in theirs is probably due to a higher level of recombination in our resolution system.

As illustrated in Fig. 20, the Sf9 cytoplasmic extract containing NS-1 can increase the recombination compared with the Sf9 cytoplasmic extract lacking NS-1. There are two possible reasons for this increase. One is that the expression of NS-1 in Sf9 cells induces the expression of recombination

enzymes in Sf9 cells and another possibility is that NS-1 itself can somehow facilitate recombination.

Ward and Berns (1991) have studied "rescue" of AAV sequences from AAV/pBR322 plasmids. This phenomenon requires the intact AAV terminal repeat sequences (TRS), *in cis*. These workers proposed excision occurs due to formation of a cruciform structure (Holliday recombination intermediate) which is resolved by recombination (see section 3.2.1.). The two products are linear duplex AAV DNA and pBR322 DNA with AAV TRS (covalently closed) at each end (**AAV** and **PBR322**). I presume that a similar event occurs to give our recombinant turn-around products and propose that NS-1 enhances this reaction either directly or indirectly.

The AAV rep protein binds preferentially to AAV ends in the hairpin form (Im and Muzyczka, 1990), hence, the rep protein may promote formation of Holliday junctions. To date, MVMp NS-1 has not been shown to bind to the hairpinned forms of either the left or right terminal regions although recently it has been shown to bind to the linear form of the left end (Cotmore *et al.*, 1995). It seems likely that MVMp NS-1 can also bind preferentially to the hairpin form, as the rep protein does, and hence stimulate recombination. However, so far the conditions for this activity have not been observed. Further resolution assays using LA9 replication extract in the presence and absence of purified NS-1 are required to test whether NS-1 does contributes to the recombination event.

4.2. The resolution procedure of the dimer bridge

As mentioned in section 3.3., mutant dimer bridge clones pQLDB2, pQLDB3 and pQLDB4 were expected not to be resolved according to the resolution procedure of the dimer bridge proposed in the MRHM. However, they are resolved quite well. Furthermore, a major contradiction of the MRHM developed when it was shown that the B-half dimer bridge but not the A-half dimer bridge can be nicked by NS-1 (Cotmore and Tattersall, 1994; this thesis). Cotmore and Tattersall subsequently proposed a resolution procedure (Fig. 31) (Berns, 1996) different from that described by the MRHM. According to this model, NS-1 first nicks the B-half of the dimer bridge (Fig. 31, line 2) followed by the formation of a cruciform structure and displacement DNA synthesis. Unique about the displacement DNA synthesis is the replication complex is required to switch template strands (Fig. 31, line 3). After the displacement DNA synthesis is completed (Fig. 31, line 4), an asymmetric recombination occurs to yield the resolution products of the dimer bridge predicted by the MRHM (Fig. 31, line 5; Fig. 7, line 6).

According to the resolution procedure shown in Fig. 31, the minor band 7 (extended form) observed in Fig. 19 is possibly due to a low level of symmetric recombination of the molecule shown in line 4 of Fig. 31. The DNA of spot " X " that I observed (Fig. 21) comigrates with the DNA of spot 5 in the first dimension (neutral gel) and has the same size as spot 2 in the second dimension (denaturing agarose gel). Hence, spot " X " corresponds in size to the DNA strand from the NS-1 nick site # 2 to the PvuII site if the dimer bridge is nicked at site # 2 but not resolved into the two products. A DNA strand from nick site # 2 to the PstI site is not detected in Fig. 21 probably because the resulting 3'-end after nicking at site # 2 is extended by DNA synthesis to various lengths.

1

AG   AAG

3' ———————————————— 5'
5' ———————————————— 3'

TC   TTC

2

AG   AAG

3' ———————————————— 5'
5' ——————●———————————— 3'

TC   TTC

3

4

5

AG   AAG
AG   AAG
TC   TTC
TC   TTC
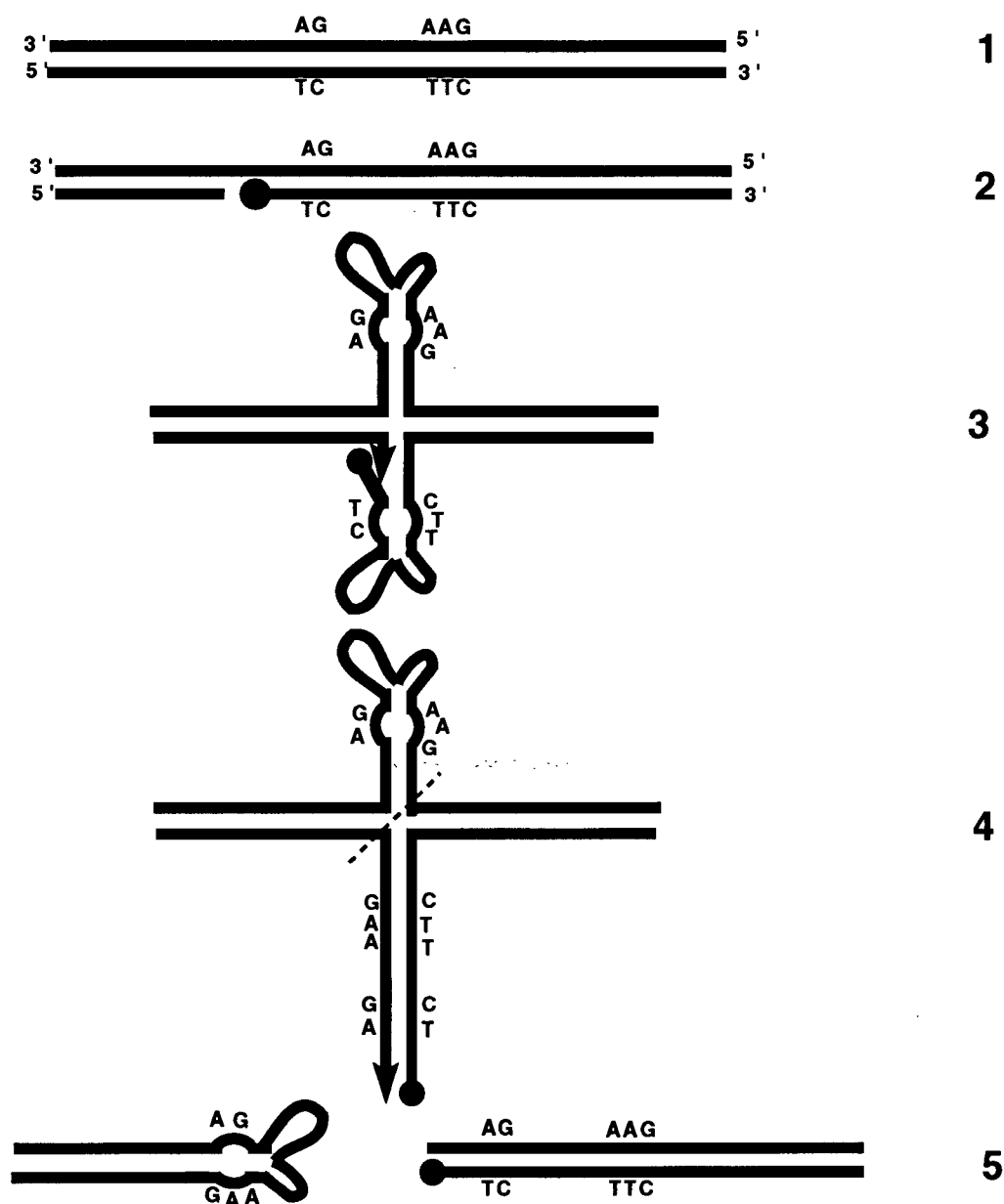
Fig. 31. **The resolution procedure of the dimer bridge proposed by Cotmore and Tattersall.** The DNA molecule in line 1 represents the dimer bridge. In line 2 the dimer bridge is nicked within the B-half by NS-1 as illustrated. The black circle indicates covalently attached NS-1. In line 3 the dimer bridge assumes a cruciform structure and displacement DNA synthesis (indicated by the vertical arrow) occurs. The displacement DNA synthesis requires the polymerase to switch template strands as illustrated (line 3). The slanting dashed thin line indicates asymmetric recombination (line 4). and the two DNA molecules in line 5 are the two resolution products described in the MRHM.

The model shown in Fig. 31 can explain the resolution of pQLDB2, pQLDB3 and pQLDB4. Both pQLDB2 and pQLDB3 are resolved symmetrically

(Fig. 23, lanes 4 and 3). The mutation of $\frac{AAG}{TTC}$ into $\frac{AG}{TC}$ in pQLDB2 likely results in the substrate DNA having two potential nick sites. Both nick site # 2 and the mutated nick site # 1 of pQLDB3 seem to be nicked (This is revealed by the two arrows in panel B of Fig. 24). The symmetric resolution products of these two dimer bridge mutants can be explained by assuming that NS-1 nicks the two sites on the same plasmid, the two resulting 3'-ends are then extended through displacement DNA synthesis to form the two extended form resolution products (bands 2 and 7), and the recombination of the mutant dimer bridge produces the two turn-around form bands (3 and 6). The resolution products of pQLDB2 can also be explained by assuming that NS-1 nicks either one of the two nick sites followed by the formation of the cruciform structure, displacement DNA synthesis as described in Fig. 31 and then a symmetric or asymmetric recombination. The resolution procedure of pQLDB4 is probably the same as described in Fig. 31. NS-1 probably does not efficiently nick the mutant half of the dimer bridge in pQLDB4 because the deletion of nt 102 and 103 in the mutant half mutates the NS-1 binding site (ACCAACCA) (nt 95 -102) (Fig. 4).

However, one very interesting observation is that the NS-1 tyrosine mutant, Tyr197Phe, can resolve the dimer bridge (Fig. 30) but cannot nick both half dimer bridges (data not shown). This result cannot be explained with the resolution procedure shown in Fig. 31 and may suggest that the resolution procedure shown in Fig. 31 is not right. I would like to propose two resolution procedures shown in Fig. 32A and B.

Fig. 32A:
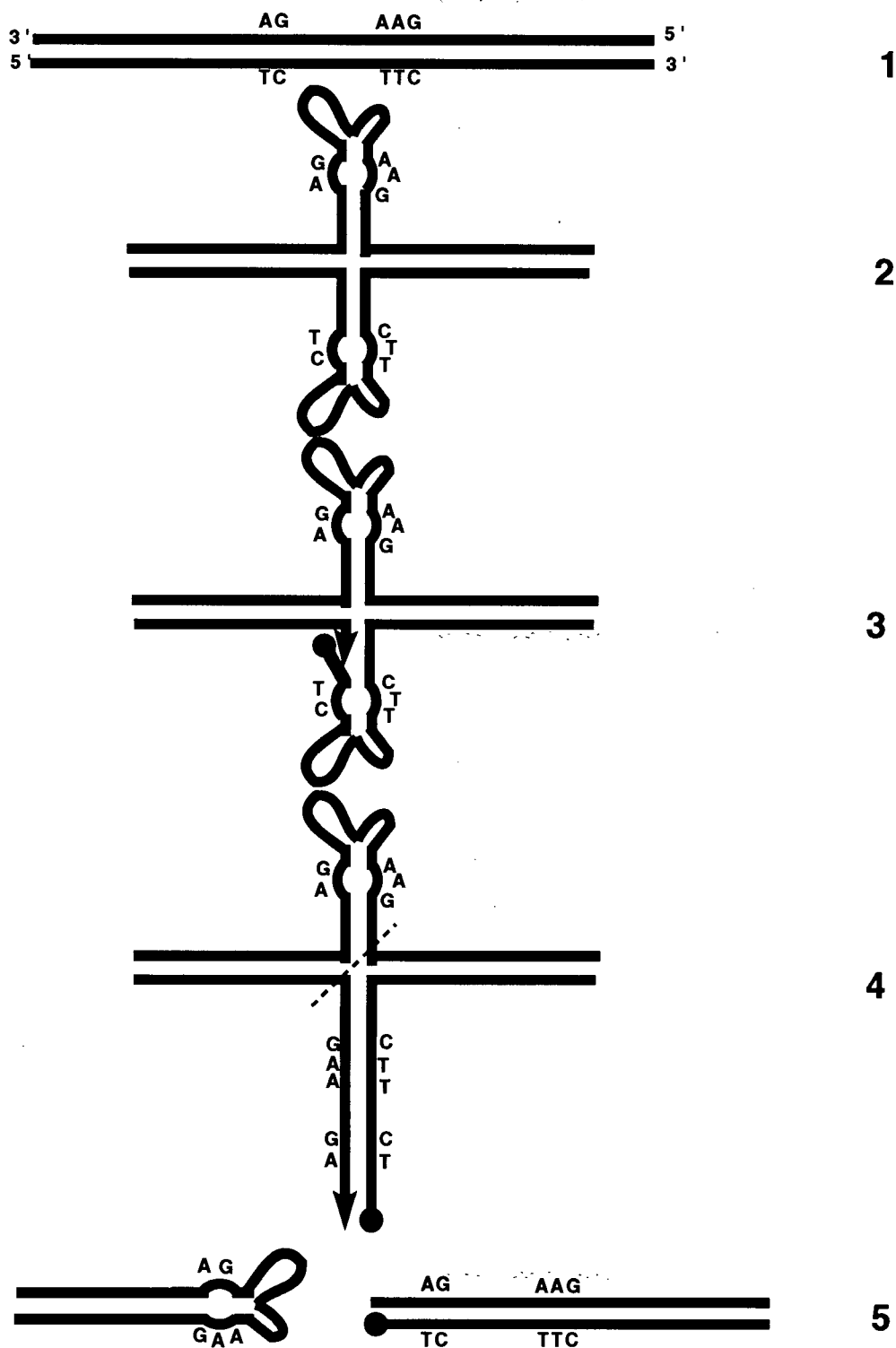
Fig. 32B:
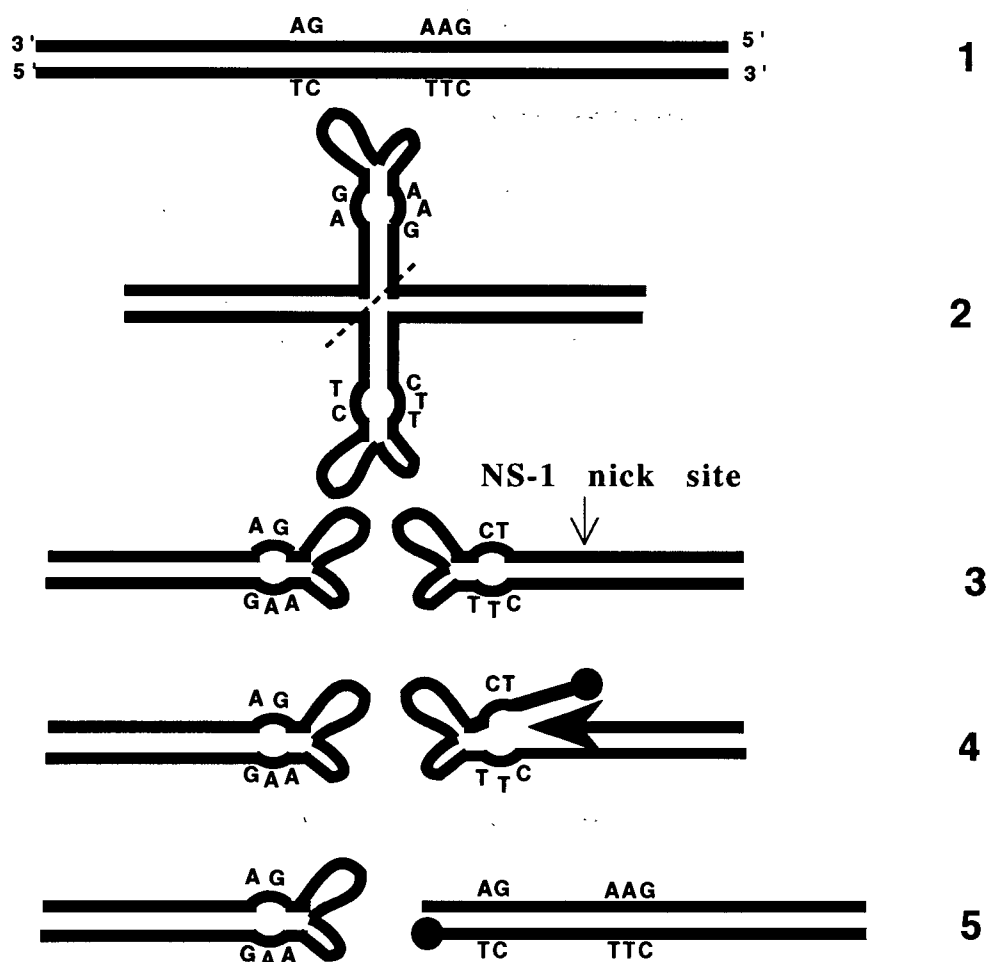
Fig. 32. The possible resolution procedures of the dimer bridge. **A.** A resolution procedure in which nicking occurs before recombination. The vertical arrows indicate displacement DNA synthesis. **B.** A resolution procedure in which recombination occurs before nicking. The vertical arrow points to the NS-1 nick site. The horizontal arrow indicates displacement DNA synthesis. For both **A** and **B**, the DNA molecule in line 1 is the dimer bridge. The two DNA molecules on the bottom line represent the resolution products predicted in MRHM. The slanting dashed line indicates asymmetric recombination. The filled black circle represents NS-1.

In Fig. 32A, the linear form of the dimer bridge (Fig. 32A, line 1) firstly becomes arranged into the cruciform configuration (Fig. 32A, line 2) which can be nicked (Fig. 32A, line 3) followed by displacement DNA synthesis (Fig. 32A, line 3) and asymmetric recombination (Fig. 32A, line 4) to form the two resolution products (Fig. 32A, line 5). In Fig. 32B, the dimer bridge (line 1) can undergo an asymmetric recombination first (Fig. 32B, line 2) to form two turn-around forms (Fig. 32B, line 3) one of which can be nicked by NS-1 followed by displacement DNA synthesis (Fig. 32B, line 4) to yield the extended form resolution product (Fig. 32B, line 5) and another one of which is the turn-around form resolution product. The major difference between the resolution procedures shown in Fig. 32 and Fig. 31 is that in Fig. 32, one hairpin of the cruciform dimer bridge or one turn-around form from the asymmetric recombination instead of the extended form dimer bridge (Fig. 31, line 1) is the substrate for nicking. To test the resolution procedure in Fig. 32, turn-around form DNA substrate needs to be prepared to do the NS-1 nicking assay.

Based on Fig. 32, the reason for NS-1 tyr197 mutant protein to resolve the dimer bridge but not to nick both half dimer bridges may be that NS-1 tyr197 mutant protein nicks hairpins of the cruciform dimer bridge (Fig. 32A, line 2) or turn-around forms from the asymmetric recombination (Fig. 32B, line 3). Furthermore, the resolution procedures proposed in Fig. 32 are not obviously contradictory to the available data from the resolution experiments of the wildtype and mutant dimer bridges. Although the observation that the B-half dimer bridge can be nicked is not included in Fig. 32, it is possible that nicking of the B-half dimer bridge is not involved in the resolution of the dimer bridge.

As mentioned above, the resolution procedure shown in Fig. 31 cannot explain the result that NS-1 tyr197 mutant protein can resolve the dimer bridge but cannot nick both half dimer bridges. This result is repeatable. However, since the resolution efficiency of NS-1 tyr197 mutant protein is low (see Fig. 30), the reason for me not to detect the products in the nicking assays using this NS-1 mutant may not be that the half dimer bridges cannot be nicked but may be that the nicking assay conditions are not sensitive enough to reveal low amount of product from nicking. Furthermore, even if NS-1 tyr197 mutant protein cannot nick both half dimer bridges at all, it does not necessarily mean that the resolution procedure shown in Fig. 31 for wildtype NS-1 is wrong because mutant NS-1 may resolve the dimer bridge through a different resolution procedure from that in Fig. 31.

It is possible that resolution assays and nicking assays using more dimer bridge mutants, half dimer bridge mutants and NS-1 mutants would help the elucidation of the resolution procedure.

4.3. The host factor(s) required for nicking

The results presented in this paper demonstrate that host cell factor (or factors) is (are) required for nicking of the B-half of the Minute Virus of Mice dimer bridge. This host factor binds to the HFBR of the B-half and the efficiency of binding is highly dependent on the presence of two CG motifs. Although the CG motifs have been identified as the most important nucleotides for the binding of the host factor, it is possible the recognition sequence includes other nucleotides as these CG motifs lie within two four

nucleotide repeats,
$$\overset{\overset{4\ 5}{|\ |}}{\text{ACGTNNNNNACGT}}\overset{\overset{13\ 14}{|\ |}}{}$$. I observed that the nicking efficiency

is reduced from that of wild-type when A3, T6 and T15 are mutated, however,

a mutation at A12 appeared to have no effect.

Although A20, C19 and A18 can be protected by NS-1 bound to the region

adjacent to the HFBR, it has been shown by others that they are not required

for NS-1 to bind to the ACCAACCA sequence (Cotmore *et al*, 1995). The fact

that pQLBA20G cannot be nicked, and pQLBA18G and pQLBC19T cannot be

nicked efficiently was unexpected and may suggest that although A20, C19

and A18 are not important for NS-1 binding, they are important for NS-1

nicking, or that the contex for the NS-1 binding site also plays a significant

role for the efficient NS-1 binding.

The mutation at T11 to C decreased the nicking efficiency of the B-half of

the dimer bridge to 20% of that of wildtype (Fig. 27B). We believe this may be

due to the creation of an E-box motif, and cellular E-box binding proteins

within the LA9 extract would be expected to bind and compete with the host

factor required for nicking. However, for the following reasons it is highly

unlikely that the decrease of nicking efficiency of the mutants at the C4, G5,

C13 or G14 is due to the creation of binding motifs for other factors. Firstly,

no known protein binding sites are generated in these mutants. Secondly, if a

new host factor binding site is created, there is likely to be competition for

binding between the nicking factor and the new factor; hence, it is unlikely

that nicking efficiency would be eliminated or almost eliminated. Thirdly,

the deletion of C4 greatly decreases the nicking efficiency (Cotmore and

Tattersall, 1994). It is unlikely that both the deletion and mutation of C4

create an unknown protein binding motif. Fourthly, a mutant in which both

A12 and C13 are mutated was made and this mutant cannot be nicked (Liu and Astell, unpublished results). Additional mutants (eg., G14 to T or C) can be made to confirm the important role of C4, G5, C13, and G14.

It has been suggested that ATF, the recognition sequence of which is TGACG, may be the host factor required for nicking of the B-half of the dimer bridge (Cotmore *et al.*, 1995). From several of my observations, it is highly unlikely that ATF is the host protein required for nicking. Firstly, efficient nicking of the B-half dimer bridge and binding of the host factor requires the

presence of $\underset{\text{|}\,\text{|}}{\overset{4\ 5}{}}\text{ACGTN}\overset{13\ 14}{\underset{\text{|}\,\text{|}}{\text{NNNNACGT}}}$ which is not an ATF binding site. Secondly, *in vitro* translated ATF protein does not facilitate NS-1 nicking (data not shown). This observation has also been made by Cotmore *et al.* (personal communication). Furthermore, the bandshift assay with a DNA fragment containing nt 1 to 13 (Fig. 16) does not detect specific binding with the proteins from the LA9 replication extract. Finally, if only the C4 and G5 from the ATF binding site but not C13 and G14 are required for the binding of the host factor, the only explanation for the competitor DNA from pUCC4AG14A to be a poorer competitor than the competitor DNA from pUCC4A is that the mutation of G14 to A in pUCC4AG14A creates an unknown protein binding motif around A14. However, when the EcoRI/HindIII fragment of pUCC4AG14A was used as a probe to do the bandshift assay, binding of proteins was not detected (data not shown).

In order to further identify and characterize the host factor(s) that is/are required for nicking and binding to the HFBR, several approaches may be taken. Since the binding site of this host factor(s) is known, it should be possible to purify it from LA9 cells through DNA affinity chromatography

and then using partial aa sequence to clone the gene. It may also be possible to clone its gene directly using the yeast one hybrid system, assuming the host factor binding to the HFBR is a monomer or homo-oligomer. Once the protein(s) required for nicking of the B-half dimer bridge is identified, how this protein(s) assists in NS-1 nicking can be studied. It would also be of interest to learn its function(s) within the host cell. Currently, the purification of this LA9 cell factor(s) required for NS-1 nicking using DNA affinity chromatography is in progress.

V. References

Aladjem MI. Groudine M. Brody LL. Dieken ES. Fournier RE. Wahl GM. Epner EM. Participation of the human beta-globin locus control region in initiation of DNA replication. Science. 270(5237):815-9, 1995.

Antonietti JP. Sahli R. Beard P. Hirt B. Characterization of the cell type-specific determinant in the genome of minute virus of mice. Journal of Virology. 62(2):552-7, 1988.

Astell CR. Chow MB. Ward DC. Sequence analysis of the termini of virion and replicative forms of minute virus of mice DNA suggests a modified rolling hairpin model for autonomous parvovirus DNA replication. Journal of Virology. 54(1):171-7, 1985.

Astell CR. Gardiner EM. Tattersall P. DNA sequence of the lymphotropic variant of minute virus of mice, MVM(i), and comparison with the DNA sequence of the fibrotropic prototype strain. Journal of Virology. 57(2):656-69, 1986.

Astell CR. Mol CD. Anderson WF. Structural and functional homology of parvovirus and papovavirus polypeptides. Journal of General Virology. 68 (Pt 3):885-93, 1987.

Astell CR. Smith M. Chow MB. Ward DC. Structure of the 3' hairpin termini of four rodent parvovirus genomes: nucleotide sequence homology at origins of DNA replication. Cell. 17(3):691-703, 1979.

Astell CR. Thomson M. Chow MB. Ward DC. Structure and replication of minute virus of mice DNA. Cold Spring Harbor Symposia on Quantitative Biology. 47 Pt 2:751-62, 1983a.

Astell CR. Thomson M. Merchlinsky M. Ward DC. The complete DNA sequence of minute virus of mice, an autonomous parvovirus. Nucleic Acids Research. 11(4):999-1018, 1983b.

Ball-Goodrich LJ. Tattersall P. Two amino acid substitutions within the capsid are coordinately required for acquisition of fibrotropism by the lymphotropic strain of minute virus of mice. Journal of Virology. 66(6):3415-23, 1992.

Bell SP. Kobayashi R. Stillman B. Yeast origin recognition complex functions in transcription silencing and DNA replication [see comments]. Science. 262(5141):1844-9, 1993.

Bell SP. Mitchell J. Leber J. Kobayashi R. Stillman B. The multidomain structure of Orc1p reveals similarity to regulators of DNA replication and transcriptional silencing. Cell. 83(4):563-8, 1995.

Bell SP. Stillman B. ATP-dependent recognition of eukaryotic origins of DNA replication by a multiprotein complex [see comments]. Nature. 357(6374):128-34, 1992.

Ben-Asher E. Aloni Y. Transcription of minute virus of mice, an autonomous parvovirus, may be regulated by attenuation. Journal of Virology. 52(1):266-76, 1984.

Benavente R. Krohne G. Franke WW. Cell type-specific expression of nuclear lamina proteins during development of Xenopus laevis. Cell. 41(1):177-90, 1985.

Berberich S. Trivedi A. Daniel DC. Johnson EM. Leffak M. In vitro replication of plasmids containing human c-myc DNA. Journal of Molecular Biology. 245(2):92-109, 1995.

Berns KI. Parvoviridae: the viruses and their replication in Fields Virology. 3nd edition. eds. Fields BN. Knipe DM. Harley PM et al.. Lippincott-Raven Publishers, Philaddephia. 2173-2197, 1996.

Bonnard GD. Manders EK. Campbell DA Jr. Herberman RB. Collins MJ Jr. Immunosuppressive activity of a subline of the mouse EL-4 lymphoma. Evidence for minute virus of mice causing the inhibition. Journal of Experimental Medicine. 143(1):187-205, 1976.

Borowiec JA. Dean FB. Bullock PA. Hurwitz J. Binding and unwinding--how T antigen engages the SV40 origin of DNA replication. [Review] Cell. 60(2):181-4, 1990.

Borowiec JA. Dean FB. Hurwitz J. Differential induction of structural changes in the simian virus 40 origin of replication by T antigen. Journal of Virology. 65(3):1228-35, 1991.

Borowiec JA. Hurwitz J. ATP stimulates the binding of simian virus 40 (SV40) large tumor antigen to the SV40 origin of replication. Proceedings of the National Academy of Sciences of the United States of America. 85(1):64-8, 1988.

Borowiec JA. Hurwitz J. Localized melting and structural changes in the SV40 origin of replication induced by T-antigen. EMBO Journal. 7(10):3149-58, 1988.

Bourguignon GJ. Tattersall PJ. Ward DC. DNA of minute virus of mice: self-priming, nonpermuted, single-stranded genome with a 5'-terminal hairpin duplex. Journal of Virology. 20(1):290-306, 1976.

Brewer BJ. Fangman WL. The localization of replication origins on ARS plasmids in S. cerevisiae. Cell. 51(3):463-71, 1987.

Brill SJ. Stillman B. Yeast replication factor-A functions in the unwinding of the SV40 origin of DNA replication. Nature. 342(6245):92-5, 1989.

Brownstein DG. Smith AL. Johnson EA. Pintel DJ. Naeger LK. Tattersall P. The pathogenesis of infection with minute virus of mice depends on expression of the small nonstructural protein NS2 and on the genotype of the allotropic determinants VP1 and VP2. Journal of Virology. 66(5):3118-24, 1992.

Bullock PA. Denis D. DNA synthesis generally initiates outside the simian virus 40 core origin in vitro. Molecular & Cellular Biology. 15(1):173-8, 1995.

Bullock PA. Seo YS. Hurwitz J. Initiation of simian virus 40 DNA replication in vitro: pulse-chase experiments identify the first labeled species as topologically unwound. Proceedings of the National Academy of Sciences of the United States of America. 86(11):3944-8, 1989.

Bullock PA. Seo YS. Hurwitz J. Initiation of simian virus 40 DNA synthesis in vitro. Molecular & Cellular Biology. 11(5):2350-61, 1991.

Bullock PA. Tevosian S. Jones C. Denis D. Mapping initiation sites for simian virus 40 DNA synthesis events in vitro. Molecular & Cellular Biology. 14(8):5043-55, 1994.

Campbell, J.L. and Newlon, C.S. In The Molecular and Cellular Biology of the Yeast Saccharomyces: Genome dynamics, Protein Synthesis and Energetics(Broach, J.R., Pringle, J.R. and Jones, E.R., eds). pp 41-146, Cold Spring Harbor Lab, Cold Spring Harbor, NY. 1991.

Carminati JL. Johnston CG. Orr-Weaver TL. The Drosophila ACE3 chorion element autonomously induces amplification. Molecular & Cellular Biology. 12(5):2444-53, 1992.

Cater JE. Pintel DJ. The small non-structural protein NS2 of the autonomous parvovirus minute virus of mice is required for virus growth in murine cells. Journal of General Virology. 73 (Pt 7):1839-43, 1992.

Cavalier-Smith T. Palindromic base sequences and replication of eukaryote chromosome ends. Nature. 250(5466):467-70, 1974.

Celniker SE. Sweder K. Srienc F. Bailey JE. Campbell JL. Deletion mutations affecting autonomously replicating sequence ARS1 of Saccharomyces cerevisiae. Molecular & Cellular Biology. 4(11):2455-66, 1984.

Chow M. Bodnar JW. Polvino-Bodnar M. Ward DC. Identification and characterization of a protein covalently bound to DNA of minute virus of mice. Journal of Virology. 57(3):1094-104, 1986.

Christensen J. Cotmore SF. Tattersall P. Minute virus of mice transcriptional activator protein NS1 binds directly to the transactivation region of the viral P38 promoter in a strictly ATP-dependent manner. Journal of Virology. 69(9):5422-30, 1995.

Clemens KE. Pintel D. Minute virus of mice (MVM) mRNAs predominantly polyadenylate at a single site. Virology. 160(2):511-4, 1987.

Clinton GM. Hayashi M. The parovivirus MVM: particles with altered structural proteins. Virology. 66(1):261-1, 1975

Collins KL. Kelly TJ. Effects of T antigen and replication protein A on the initiation of DNA synthesis by DNA polymerase alpha-primase. Molecular & Cellular Biology. 11(4):2108-15, 1991.

Collins KL. Russo AA. Tseng BY. Kelly TJ. The role of the 70 kDa subunit of human DNA polymerase alpha in DNA replication. EMBO Journal. 12(12):4555-66, 1993.

Cossons N. Faust EA. Zannis-Hadjopoulos M. DNA polymerase d-dependent formation of a hairpin structure at the 5' terminal palindrome of the minute virus of mice genome. Virology. 216:258-264, 1996.

Costello E. Sahli R. Hirt B. Beard P. The mismatched nucleotides in the 5'-terminal hairpin of minute virus of mice are required for efficient viral DNA replication. Journal of Virology. 69(12):7489-96, 1995.

Cotmore SF. Christensen J. Nuesch JP. Tattersall P. The NS1 polypeptide of the murine parvovirus minute virus of mice binds to DNA sequences containing the motif [ACCA]2-3. Journal of Virology. 69(3):1652-60, 1995a.

Cotmore SF. Gene expression in the autonomous parvoviruses. Handbook of parvoviruses. Edited by Tijssen P. Volume 1:141-154, 1990.

Cotmore SF. Gottlieb R. D'Abramo A. Bratton J. Tattersall P. NS-2 is required for correct folding and/or assembly of the MVM capsid proteins in mouse cells. VIth parvovirus workshop. LeCorum, Montpellier, France. Page 8, Sept. of 1995b.

Cotmore SF. Nuesch JP. Tattersall P. Asymmetric resolution of a parvovirus palindrome in vitro. Journal of Virology. 67(3):1579-89, 1993.

Cotmore SF. Nuesch JP. Tattersall P. In vitro excision and replication of 5' telomeres of minute virus of mice DNA from cloned palindromic concatemer junctions. Virology. 190(1):365-77, 1992.

Cotmore SF. Sturzenbecker LJ. Tattersall P. The autonomous parvovirus MVM encodes two nonstructural proteins in addition to its capsid polypeptides. Virology. 129(2):333-43, 1983.

Cotmore SF. Tattersall P. The autonomously replicating parvoviruses of vertebrates. Adanced Virus Research. 33:91-174, 1987.

Cotmore SF. Tattersall P. A genome-linked copy of the NS-1 polypeptide is located on the outside of infectious parvovirus particles. Journal of Virology. 63(9):3902-11, 1989.

Cotmore SF. Tattersall P. Alternate splicing in a parvoviral nonstructural gene links a common amino-terminal sequence to downstream domains which confer radically different localization and turnover characteristics. Virology. 177(2):477-87, 1990.

Cotmore SF. Tattersall P. An asymmetric nucleotide in the parvoviral 3' hairpin directs segregation of a single active origin of DNA replication. EMBO Journal. 13(17):4145-52, 1994.

Cotmore SF. Tattersall P. In vivo resolution of circular plasmids containing concatemer junction fragments from minute virus of mice DNA and their subsequent replication as linear molecules. Journal of Virology. 66(1):420-31, 1992.

Cotmore SF. Tattersall P. Organization of nonstructural genes of the autonomous parvovirus minute virus of mice. Journal of Virology. 58(3):724-32, 1986.

Cotmore SF. Tattersall P. The NS-1 polypeptide of minute virus of mice is covalently attached to the 5' termini of duplex replicative-form DNA and progeny single strands. Journal of Virology. 62(3):851-60, 1988.

Coverley D. Laskey RA. Regulation of eukaryotic DNA replication. [Review] Annual Review of Biochemistry. 63:745-76, 1994.

Crawford LV. A minute virus of mice. Virology. 29(4):605-12, 1966.

Dean FB. Borowiec JA. Ishimi Y. Deb S. Tegtmeyer P. Hurwitz J. Simian virus 40 large tumor antigen requires three core replication origin domains

for DNA unwinding and replication in vitro. Proceedings of the National Academy of Sciences of the United States of America. 84(23):8267-71, 1987a.

Dean FB. Bullock P. Murakami Y. Wobbe CR. Weissbach L. Hurwitz J. Simian virus 40 (SV40) DNA replication: SV40 large T antigen unwinds DNA containing the SV40 origin of replication. Proceedings of the National Academy of Sciences of the United States of America. 84(1):16-20, 1987b.

Dean FB. Dodson M. Echols H. Hurwitz J. ATP-dependent formation of a specialized nucleoprotein structure by simian virus 40 (SV40) large tumor antigen at the SV40 replication origin. Proceedings of the National Academy of Sciences of the United States of America. 84(24):8981-5, 1987c.

Dean FB. Hurwitz J. Simian virus 40 large T antigen untwists DNA at the origin of DNA replication. Journal of Biological Chemistry. 266(8):5062-71, 1991.

Deb SP. Deb S. Preferential binding of simian virus 40 T-antigen dimers to origin region I. Journal of Virology. 63(7):2901-7, 1989.

Deb SP. Tegtmeyer P. ATP enhances the binding of simian virus 40 large T antigen to the origin of replication. Journal of Virology. 61(12):3649-54, 1987.

DeLucia AL. Lewton BA. Tjian R. Tegtmeyer P. Topography of simian virus 40 A protein-DNA complexes: arrangement of pentanucleotide interaction sites at the origin of replication. Journal of Virology. 46(1):143-50, 1983.

Denis D. Bullock PA. Primer-DNA formation during simian virus 40 DNA replication in vitro. Molecular & Cellular Biology. 13(5):2882-90, 1993.

DePamphilis ML. Eukaryotic DNA replication: anatomy of an origin. [Review] Annual Review of Biochemistry. 62:29-63, 1993.

Diffley JF. Cocker JH. Dowell SJ. Rowley A. Two steps in the assembly of complexes at yeast replication origins in vivo. Cell. 78(2):303-16, 1994.

Diffley JF. Cocker JH. Protein-DNA interactions at a yeast replication origin. Nature. 357(6374):169-72, 1992.

Diffley JF. Eukaryotic DNA replication. [Review] Current Opinion in Cell Biology. 6(3):368-72, 1994.

Diffley JF. Stillman B. Purification of a yeast protein that binds to origins of DNA replication and a transcriptional silencer. Proceedings of the National Academy of Sciences of the United States of America. 85(7):2120-4, 1988.

Diffley, J.F.X. In Molecular Biology of Saccharomyces(Grivell, L.A., ed) pp. 25-33, Kluwer Academic Publishers, London. 1992.

Dillin A. Rine J. On the origin of a silencer. [Review] Trends in Biochemical Sciences. 20(6):231-5, 1995.

DiMaio D. Nathans D. Regulatory mutants of simian virus 40. Effect of mutations at a T antigen binding site on DNA replication and expression of viral genes. Journal of Molecular Biology. 156(3):531-48, 1982.

Dobbs DL. Shaiu WL. Benbow RM. Modular sequence elements associated with origin regions in eukaryotic chromosomal DNA. Nucleic Acids Research. 22(13):2479-89, 1994.

Dodson M. Dean FB. Bullock P. Echols H. Hurwitz J. Unwinding of duplex DNA from the SV40 origin of replication by T antigen [published erratum appears in Science 1987 Dec 4;238(4832):1341]. Science. 238(4829):964-7, 1987.

Doerig C. Hirt B. Antonietti JP. Beard P. Nonstructural protein of parvoviruses B19 and minute virus of mice controls transcription. Journal of Virology. 64(1):387-96, 1990.

Doerig C. Hirt B. Beard P. Antonietti JP. Minute virus of mice non-structural protein NS-1 is necessary and sufficient for trans-activation of the viral P39 promoter. Journal of General Virology. 69 (Pt 10):2563-73, 1988.

Dornreiter I. Copeland WC. Wang TS. Initiation of simian virus 40 DNA replication requires the interaction of a specific domain of human DNA polymerase alpha with large T antigen. Molecular & Cellular Biology. 13(2):809-20, 1993.

Dornreiter I. Dehde S. Hauser M. Nasheuer H. -P. Fanning E. Unpublished data

Dornreiter I. Erdile LF. Gilbert IU. von Winkler D. Kelly TJ. Fanning E. Interaction of DNA polymerase alpha-primase with cellular replication protein A and SV40 T antigen. EMBO Journal. 11(2):769-76, 1992.

Dowell SJ. Romanowski P. Diffley JF. Interaction of Dbf4, the Cdc7 protein kinase regulatory subunit, with yeast replication origins in vivo [see comments]. Science. 265(5176):1243-6, 1994.

Dupont F. Tenenbaum L. Guo LP. Spegelaere P. Zeicher M. Rommelaere J. Use of an autonomous parvovirus vector for selective transfer of a foreign gene into transformed human cells of different tissue origins and its expression therein. Journal of Virology. 68(3):1397-406, 1994.

Ehrenhofer-Murray AE. Gossen M. Pak DT. Botchan MR. Rine J. Separation of origin recognition complex functions by cross-species complementation [see comments]. Science. 270(5242):1671-4, 1995.

Eki T. Matsumoto T. Murakami Y. Hurwitz J. The replication of DNA containing the simian virus 40 origin by the monopolymerase and dipolymerase systems. Journal of Biological Chemistry. 267(11):7284-94, 1992.

Estes HG. Robinson BS. Eisenberg S. At least three distinct proteins are necessary for the reconstitution of a specific multiprotein complex at a eukaryotic chromosomal origin of replication. Proceedings of the National Academy of Sciences of the United States of America. 89(23):11156-60, 1992.

Fanning E. Knippers R. Structure and function of simian virus 40 large tumor antigen. [Review] Annual Review of Biochemistry. 61:55-85, 1992.

Faust EA. Ward DC. Incomplete genomes of the parvovirus minute virus of mice: selective conservation of genome termini, including the origin for DNA replication. Journal of Virology. 32(1):276-92, 1979.

Forrester WC. Novak U. Gelinas R. Groudine M. Molecular analysis of the human beta-globin locus activation region. Proceedings of the National Academy of Sciences of the United States of America. 86(14):5439-43, 1989.

Forrester WC. Takegawa S. Papayannopoulou T. Stamatoyannopoulos G. Groudine M. Evidence for a locus activation region: the formation of developmentally stable hypersensitive sites in globin-expressing hybrids. Nucleic Acids Research. 15(24):10159-77, 1987.

Foss M. McNally FJ. Laurenson P. Rine J. Origin recognition complex (ORC) in transcriptional silencing and DNA replication in S. cerevisiae [see comments]. Science. 262(5141):1838-44, 1993.

Fox CA. Loo S. Dillin A. Rine J. The origin recognition complex has essential functions in transcriptional silencing and chromosomal replication. Genes & Development. 9(8):911-24, 1995.

Gardiner EM. Tattersall P. Evidence that developmentally regulated control of gene expression by a parvoviral allotropic determinant is particle mediated. Journal of Virology. 62(5):1713-22, 1988a.

Gardiner EM. Tattersall P. Mapping of the fibrotropic and lymphotropic host range determinants of the parvovirus minute virus of mice. Journal of Virology. 62(8):2605-13, 1988b.

Gavin KA. Hidaka M. Stillman B. Conserved initiator proteins in eukaryotes [see comments]. Science. 270(5242):1667-71, 1995.

Gilbert DM. Miyazawa H. DePamphilis ML. Site-specific initiation of DNA replication in Xenopus egg extract requires nuclear structure. Molecular & Cellular Biology. 15(6):2942-54, 1995.

Gossen M. Pak DT. Hansen SK. Acharya JK. Botchan MR. A Drosophila homolog of the yeast origin recognition complex [see comments]. Science. 270(5242):1674-7, 1995.

Grosveld F. van Assendelft GB. Greaves DR. Kollias G. Position-independent, high-level expression of the human beta-globin gene in transgenic mice. Cell. 51(6):975-85, 1987.

Gu Z. Plaza S. Perros M. Cziepluch C. Rommelaere J. Cornelis JJ. NF-Y controls transcription of the minute virus of mice P4 promoter through interaction with an unusual binding site. Journal of Virology. 69:239-246, 1995.

Gunther M. Tattersall P. The terminal protein of minute virus of mice is an 83 kilodalton polypeptide linked to specific forms of double-stranded and single-stranded viral DNA. FEBS Letters. 242(1):22-6, 1988.

Guo ZS. DePamphilis ML. Specific transcription factors stimulate simian virus 40 and polyomavirus origins of DNA replication. Molecular & Cellular Biology. 12(6):2514-24, 1992.

Guo ZS. Gutierrez C. Heine U. Sogo JM. Depamphilis ML. Origin auxiliary sequences can facilitate initiation of simian virus 40 DNA replication in vitro as they do in vivo. Molecular & Cellular Biology. 9(9):3593-602, 1989.

Guo ZS. Heine U. DePamphilis ML. T-antigen binding to site I facilitates initiation of SV40 DNA replication but does not affect bidirectionality. Nucleic Acids Research. 19(25):7081-8, 1991.

Gutierrez C. Guo ZS. Roberts J. DePamphilis ML. Simian virus 40 origin auxiliary sequences weakly facilitate T-antigen binding but strongly facilitate DNA unwinding. Molecular & Cellular Biology. 10(4):1719-28, 1990.

Handeli S. Klar A. Meuth M. Cedar H. Mapping replication units in animal cells. Cell. 57(6):909-20, 1989.

Harris C. Astell CR. Transcriptional activation by NS-1, the major nonstructural protein of Minute Virus of Mice. International Symposium on Nucleic Acids and Membranes in Honour of Dr. Har Gobind Khorana. Vancouver, BC., Canada. Page 42, May of 1993.

Hartwell LH. Sequential function of gene products relative to DNA synthesis in the yeast cell cycle. Journal of Molecular Biology. 104(4):803-17, 1976.

Hay RT. DePamphilis ML. Initiation of SV40 DNA replication in vivo: location and structure of 5' ends of DNA synthesized in the ori region. Cell. 28(4):767-79, 1982.

Hou Z. Umthun AR. Dobbs DL. A single-stranded DNA binding protein that specifically recognizes cis-acting sequences in the replication origin and transcriptional promoter region of Tetrahymena rDNA. Biochemistry. 34(14):4583-92, 1995.

Hsiao CL. Carbon J. High-frequency transformation of yeast by plasmids containing the cloned yeast ARG4 gene. Proceedings of the National Academy of Sciences of the United States of America. 76(8):3829-33, 1979.

Huberman JA. Cell cycle. A licence to replicate [news; comment]. Nature. 375(6530):360-1, 1995a.

Huberman JA. Prokaryotic and eukaryotic replicons. Cell. 82(4):535-42, 1995b.

Huberman JA. Spotila LD. Nawotka KA. el-Assouli SM. Davis LR. The in vivo replication origin of the yeast 2 microns plasmid. Cell. 51(3):473-81, 1987.

Hyrien O. Mechali M. Chromosomal replication initiates and terminates at random sequences but at regular intervals in the ribosomal DNA of Xenopus early embryos. EMBO Journal. 12(12):4511-20, 1993.

Ilyina TV. Koonin EV. Conserved sequence motifs in the initiator proteins for rolling circle DNA replication encoded by diverse replicons from eubacteria, eucaryotes and archaebacteria. Nucleic Acids Research. 20(13):3279-85, 1992.

Im DS. Muzyczka N. The AAV origin binding protein Rep68 is an ATP-dependent site-specific endonuclease with DNA helicase activity. Cell. 61(3):447-57, 1990.

Ishimi Y. Claude A. Bullock P. Hurwitz J. Complete enzymatic synthesis of DNA containing the SV40 origin of replication. Journal of Biological Chemistry. 263(36):19723-33, 1988.

Jindal HK. Yong CB. Wilson GM. Tam P. Astell CR. Mutations in the NTP-binding motif of minute virus of mice (MVM) NS-1 protein uncouple ATPase and DNA helicase functions. Journal of Biological Chemistry. 269(5):3283-9, 1994.

Jongeneel CV. Sahli R. McMaster GK. Hirt B. A precise map of splice junctions in the mRNAs of minute virus of mice, an autonomous parvovirus. Journal of Virology. 59(3):564-73, 1986.

Kadonaga JT. Jones KA. Tjian R. Promoter-specific activation of RNA polymerase II transcription by Sp1. Trends in Biochemical Science. 11:20-23, 1986.

Kamakaka RT. Kaufman PD. Stillman B. Mitsis PG. Kadonaga JT. Simian virus 40 origin- and T-antigen-dependent DNA replication with Drosophila factors in vitro. Molecular & Cellular Biology. 14(8):5114-22, 1994.

Kapil S. Minute virus of mice (MVM) nucleic acid production in susceptible and resistant strains of mice and F1 hybrids. Comparative Immunology, Microbiology & Infectious Diseases. 18(4):245-52, 1995.

Kelly TJ. Jallepalli PV. Clyne RK. Replication and transcription. Silence of the ORCs. [Review] Current Biology. 4(3):238-41, 1994.

Kenny MK. Lee SH. Hurwitz J. Multiple functions of human single-stranded-DNA binding protein in simian virus 40 DNA replication: single-strand stabilization and stimulation of DNA polymerases alpha and delta. Proceedings of the National Academy of Sciences of the United States of America. 86(24):9757-61, 1989.

Kilham L. Margolis G. Pathology of minute virus of mice (MVM) for rats, mice, and hamsters. Proceedings of the Society for Experimental Biology & Medicine. 133(4):1447-52, 1970.

Kitsberg D. Selig S. Keshet I. Cedar H. Replication structure of the human beta-globin gene domain [see comments]. Nature. 366(6455):588-90, 1993.

Krady JK. Ward DC. Transcriptional activation by the parvoviral nonstructural protein NS-1 is mediated via a direct interaction with Sp1. Molecular & Cellular Biology. 15(1):524-33, 1995.

Krysan PJ. Smith JG. Calos MP. Autonomous replication in human cells of multimers of specific human and bacterial DNA sequences. Molecular & Cellular Biology. 13(5):2688-96, 1993.

Labieniec-Pintel L. Pintel D. The minute virus of mice P39 transcription unit can encode both capsid proteins. Journal of Virology. 57(3):1163-7, 1986.

Lee SH. Kim DK. The role of the 34-kDa subunit of human replication protein A in simian virus 40 DNA replication in vitro. Journal of Biological Chemistry. 270(21):12801-7, 1995.

Lee SH. Kwong AD. Pan ZQ. Hurwitz J. Studies on the activator 1 protein complex, an accessory factor for proliferating cell nuclear antigen-dependent DNA polymerase delta. Journal of Biological Chemistry. 266(1):594-602, 1991.

Legendre D. Rommelaere J. Targeting of promoters for trans activation by a carboxy-terminal domain of the NS-1 protein of the parvovirus minute virus of mice. Journal of Virology. 68(12):7974-85, 1994.

Li JJ. Herskowitz I. Isolation of ORC6, a component of the yeast origin recognition complex by a one-hybrid system [see comments]. Science. 262(5141):1870-4, 1993.

Li X. Li J. Harrington J. Lieber MR. Burgers PM. Lagging strand DNA synthesis at the eukaryotic replication fork involves binding and stimulation of FEN-1 by proliferating cell nuclear antigen. Journal of Biological Chemistry. 270(38):22109-12, 1995.

Liang C. Weinreich M. Stillman B. ORC and Cdc6p interact and determine the frequency of initiation of DNA replication in the genome. Cell. 81(5):667-76, 1995.

Littlefield JW. Three degrees of guanylic acid-inosinic acid pyrophosphorylase deficiency in mouse fibroblasts. Nature. 203:1142-1144, 1964.

Liu Q. Yong CB. Astell CR. In vitro resolution of the dimer bridge of the minute virus of mice (MVM) genome supports the modified rolling hairpin model for MVM replication. Virology. 201(2):251-62, 1994.

Loo S. Fox CA. Rine J. Kobayashi R. Stillman B. Bell S. The origin recognition complex in silencing, cell cycle progression, and DNA replication. Molecular Biology of the Cell. 6(6):741-56, 1995.

Lorson C. Burger LR. Mouw M. Pintel DJ. Efficient transactivation of the minute virus of mice P38 promoter requires upstream binding of NS1. Journal of Virology. 70(2):834-42, 1996.

Lue NF. Kornberg RD. A possible role for the yeast TATA-element-binding protein in DNA replication. Proceedings of the National Academy of Sciences of the United States of America. 90(17):8018-22, 1993.

Maine GT. Sinha P. Tye BK. Mutants of S. cerevisiae defective in the maintenance of minichromosomes. Genetics. 106(3):365-85, 1984.

Marahrens Y. Stillman B. A yeast chromosomal origin of DNA replication defined by multiple functional elements. Science. 255(5046):817-23, 1992.

Marahrens Y. Stillman B. Replicator dominance in a eukaryotic chromosome. EMBO Journal. 13(14):3395-400, 1994.

Mastrangelo IA. Hough PV. Wall JS. Dodson M. Dean FB. Hurwitz J. ATP-dependent assembly of double hexamers of SV40 T antigen at the viral origin of DNA replication. Nature. 338(6217):658-62, 1989.

Masukata H. Satoh H. Obuse C. Okazaki T. Autonomous replication of human chromosomal DNA fragments in human cells. Molecular Biology of the Cell. 4(11):1121-32, 1993.

Matsumoto T. Eki T. Hurwitz J. Studies on the initiation and elongation reactions in the simian virus 40 DNA replication system. Proceedings of the National Academy of Sciences of the United States of America. 87(24):9712-6, 1990.

Maxwell IH. Spitzer AL. Maxwell F. Pintel DJ. The capsid determinant of fibrotropism for the MVMp strain of minute virus of mice functions via VP2 and not VP1. Journal of Virology. 69(9):5829-32, 1995.

McMaster GK. Beard P. Engers HD. Hirt B. Characterization of an immunosuppressive parvovirus related to the minute virus of mice. Journal of Virology. 38(1):317-26, 1981.

McWhinney C. Waltz SE. Leffak M. Cis-acting effects of sequences within 2.4-kb upstream of the human c-myc gene on autonomous plasmid replication in HeLa cells. DNA & Cell Biology. 14(7):565-79, 1995.

Melendy T. Stillman B. An interaction between replication protein A and SV40 T antigen appears essential for primosome assembly during SV40 DNA replication. Journal of Biological Chemistry. 268(5):3389-95, 1993.

Merchlinsky MJ. Tattersall PJ. Leary JJ. Cotmore SF. Gardiner EM. Ward DC. Construction of an infectious molecular clone of the autonomous parvovirus minute virus of mice. Journal of Virology. 47(1):227-32, 1983.

Metcalf JB. Bates RC. Lederman M. Interaction of virally coded protein and a cell cycle-regulated cellular protein with the bovine parvovirus left terminus ori. Journal of Virology. 64(11):5485-90, 1990.

Montag M. Spring H. Trendelenburg MF. Structural analysis of the mitotic cycle in pre-gastrula Xenopus embryos. Chromosoma. 96(3):187-96, 1988.

Morgan WR. Ward DC. Three splicing patterns are used to excise the small intron common to all minute virus of mice RNAs. Journal of Virology. 60(3):1170-4, 1986.

Murakami Y. Eki T. Hurwitz J. Studies on the initiation of simian virus 40 replication in vitro: RNA primer synthesis and its elongation. Proceedings of the National Academy of Sciences of the United States of America. 89(3):952-6, 1992.

Murakami Y. Hurwitz J. DNA polymerase alpha stimulates the ATP-dependent binding of simian virus tumor T antigen to the SV40 origin of replication. Journal of Biological Chemistry. 268(15):11018-27, 1993a.

Murakami Y. Hurwitz J. Functional interactions between SV40 T antigen and other replication proteins at the replication fork. Journal of Biological Chemistry. 268(15):11008-17, 1993b.

Myers RM. Tjian R. Construction and analysis of simian virus 40 origins defective in tumor antigen binding and DNA replication. Proceedings of the National Academy of Sciences of the United States of America. 77(11):6491-5, 1980.

Naeger LK. Cater J. Pintel DJ. The small nonstructural protein (NS2) of the parvovirus minute virus of mice is required for efficient DNA replication and infectious virus production in a cell-type-specific manner. Journal of Virology. 64(12):6166-75, 1990.

Naeger LK. Salome N. Pintel DJ. NS2 is required for efficient translation of viral mRNA in minute virus of mice-infected murine cells. Journal of Virology. 67(2):1034-43, 1993.

Nasheuer HP. von Winkler D. Schneider C. Dornreiter I. Gilbert I. Fanning E. Purification and functional characterization of bovine RP-A in an in vitro SV40 DNA replication system. Chromosoma. 102(1 Suppl):S52-9, 1992.

Nethanel T. Kaufmann G. Two DNA polymerases may be required for synthesis of the lagging DNA strand of simian virus 40. Journal of Virology. 64(12):5912-8, 1990.

Nethanel T. Reisfeld S. Dinter-Gottlieb G. Kaufmann G. An Okazaki piece of simian virus 40 may be synthesized by ligation of shorter precursor chains. Journal of Virology. 62(8):2867-73, 1988.

Newlon CS. Yeast chromosome replication and segregation. [Review] Microbiological Reviews. 52(4):568-601, 1988.

Nichols M. Weil F. Schmid W. Devack C. Kowenz-lentz E. Luckow B. Boshart M. Schütz G. Phosphorylation of CREB affects its binding to high and low affinity sites: implication for cAMP induced gene transcription. EMBO Journal. 11:3337-3346, 1992.

Nuesch JP. Cotmore SF. Tattersall P. Sequence motifs in the replicator protein of parvovirus MVM essential for nicking and covalent attachment to the viral origin: identification of the linking tyrosine. Virology. 209(1):122-35, 1995.

Nuesch JP. Tattersall P. Nuclear targeting of the parvoviral replicator molecule NS1: evidence for self-association prior to nuclear transport. Virology. 196(2):637-51, 1993.

Paradiso PR. Infectious process of the parvovirus H-1: correlation of protein content, particle density, and viral infectivity. Journal of Virology. 39(3):800-7, 1981.

Parsons R. Anderson ME. Tegtmeyer P. Three domains in the simian virus 40 core origin orchestrate the binding, melting, and DNA helicase activities of T antigen. Journal of Virology. 64(2):509-18, 1990.

Pintel D. Dadachanji D. Astell CR. Ward DC. The genome of minute virus of mice, an autonomous parvovirus, encodes two overlapping transcription units. Nucleic Acids Research. 11(4):1019-38, 1983.

Rao H. Marahrens Y. Stillman B. Functional conservation of multiple elements in yeast chromosomal replicators. Molecular & Cellular Biology. 14(11):7643-51, 1994.

Rao H. Stillman B. The origin recognition complex interacts with a bipartite DNA binding site within yeast replicators. Proceedings of the National Academy of Sciences of the United States of America. 92(6):2224-8, 1995.

Rashid MB. Shirahige K. Ogasawara N. Yoshikawa H. Anatomy of the stimulative sequences flanking the ARS consensus sequence of chromosome VI in Saccharomyces cerevisiae. Gene. 150(2):213-20, 1994.

Rowley A. Cocker JH. Harwood J. Diffley JF. Initiation complex assembly at budding yeast replication origins begins with the recognition of a bipartite sequence by limiting amounts of the initiator, ORC. EMBO Journal. 14(11):2631-41, 1995.

Rowley A. Dowell SJ. Diffley JF. Recent developments in the initiation of chromosomal DNA replication: a complex picture emerges. [Review] Biochimica et Biophysica Acta. 1217(3):239-56, 1994.

Ryder K. Silver S. DeLucia AL. Fanning E. Tegtmeyer P. An altered DNA conformation in origin region I is a determinant for the binding of SV40 large T antigen. Cell. 44(5):719-25, 1986.

Ryder K. Vakalopoulou E. Mertz R. Mastrangelo I. Hough P. Tegtmeyer P. Fanning E. Seventeen base pairs of region I encode a novel tripartite binding signal for SV40 T antigen. Cell. 42(2):539-48, 1985.

Sahli R. McMaster GK. Hirt B. DNA sequence comparison between two tissue-specific variants of the autonomous parvovirus, minute virus of mice. Nucleic Acids Research. 13(10):3617-33, 1985.

Salvino R. Skiadopoulos M. Faust EA. Tam P. Shade RO. Astell CR. Two spatially distinct genetic elements constitute a bipartite DNA replication origin in the minute virus of mice genome. Journal of Virology. 65(3):1352-63, 1991.

Sambrook J. Fritsch EF. Maniatis T. Molecular cloning , a laboratory manual. 2nd ed. Cold Spring Harbor Laboratory Press, Cold Spring Harbor, NY. 1989.

Santaren JF. Ramirez JC. Almendral JM. Protein species of the parvovirus minute virus of mice strain MVMp: involvement of phosphorylated VP-2 subtypes in viral morphogenesis. Journal of Virology. 67(9):5126-38, 1993.

Schneider C. Weisshart K. Guarino LA. Dornreiter I. Fanning E. Species-specific functional interactions of DNA polymerase alpha-primase with simian virus 40 (SV40) T antigen require SV40 origin DNA. Molecular & Cellular Biology. 14(5):3176-85, 1994.

Sclafani RA. Jackson AL. Cdc7 protein kinase for DNA metabolism comes of age. [Review] Molecular Microbiology. 11(5):805-10, 1994.

Segovia JC. Bueren JA. Almendral JM. Myeloid depression follows infection of susceptible newborn mice with the parvovirus minute virus of mice (strain i). Journal of Virology. 69(5):3229-32, 1995.

SenGupta DJ. Borowiec JA. Strand and face: the topography of interactions between the SV40 origin of replication and T-antigen during the initiation of replication. EMBO Journal. 13(4):982-92, 1994.

SenGupta DJ. Borowiec JA. Strand-specific recognition of a synthetic DNA replication fork by the SV40 large tumor antigen. Science. 256(5064):1656-61, 1992.

Shinomiya T. Ina S. Analysis of chromosomal replicons in early embryos of Drosophila melanogaster by two-dimensional gel electrophoresis. Nucleic Acids Research. 19(14):3935-41, 1991.

Simpson RT. Nucleosome positioning can affect the function of a cis-acting DNA element in vivo. Nature. 343(6256):387-9, 1990.

Skiadopoulos MH. Faust EA. Mutational analysis of conserved tyrosines in the NS-1 protein of the parvovirus minute virus of mice. Virology. 194(2):509-17, 1993.

Smith JG. Calos MP. Autonomous replication in Drosophila melanogaster tissue culture cells. Chromosoma. 103(9):597-605, 1995

Snyder RO. Samulski RJ. Muzyczka N. In vitro resolution of covalently joined AAV chromosome ends. Cell. 60(1):105-13, 1990.

Spalholz BA. Tattersall P. Interaction of minute virus of mice with differentiated cells: strain-dependent target cell specificity is mediated by intracellular factors. Journal of Virology. 46(3):937-43, 1983.

Stadlbauer F. Voitenleitner C. Bruckner A. Fanning E. Nasheuer HP. Species-specific replication of simian virus 40 DNA in vitro requires the p180 subunit of human DNA polymerase alpha-primase. Molecular & Cellular Biology. 16(1):94-104, 1996.

Stick R. Hausen P. Changes in the nuclear lamina composition during early development of Xenopus laevis. Cell. 41(1):191-200, 1985

Stillman BW. Gluzman Y. Replication and supercoiling of simian virus 40 DNA in cell extracts from human cells. Molecular & Cellular Biology. 5(8):2051-60, 1985.

Stinchcomb DT. Struhl K. Davis RW. Isolation and characterisation of a yeast chromosomal replicator. Nature. 282(5734):39-43, 1979.

Strich R. Woontner M. Scott JF. Mutations in ARS1 increase the rate of simple loss of plasmids in Saccharomyces cerevisiae. Yeast. 2(3):169-78, 1986.

Taira T. Iguchi-Ariga SM. Ariga H. A novel DNA replication origin identified in the human heat shock protein 70 gene promoter. Molecular & Cellular Biology. 14(9):6386-97, 1994.

Tam P. Astell CR. Multiple cellular factors bind to cis-regulatory elements found inboard of the 5' palindrome of minute virus of mice. Journal of Virology. 68(5):2840-8, 1994.

Tam P. Astell CR. Replication of minute virus of mice minigenomes: novel replication elements required for MVM DNA replication. Virology. 193(2):812-24, 1993.

Tam P. Cis-acting sequences found within the MVM genome required for DNA replication. PhD thesis, 1994. Dept. of Biochemistry and Molecular Biology, the University of British Columbia, Vancouver, BC., Canada.

Tattersall P. Bratton J. Reciprocal productive and restrictive virus-cell interactions of immunosuppressive and prototype strains of minute virus of mice. Journal of Virology. 46(3):944-55, 1983.

Tattersall P. Cawte PJ. Shatkin AJ. Ward DC. Three structural polypeptides coded for by minite virus of mice, a parvovirus. Journal of Virology. 20(1):273-89, 1976.

Tattersall P. Replication of the parvovirus MVM. I. Dependence of virus multiplication and plaque formation on cell growth. Journal of Virology. 10(4):586-90, 1972.

Tattersall P. Shatkin AJ. Ward DC. Sequence homology between the structural polypeptides of minute virus of mice. Journal of Molecular Biology. 111(4):375-94, 1977.

Tattersall P. Ward DC. Rolling hairpin model for replication of parvovirus and linear chromosomal DNA. Nature. 263(5573):106-9, 1976.

Theis JF. Newlon CS. Domain B of ARS307 contains two functional elements and contributes to chromosomal replication origin function. Molecular and Cellular Biology. 14:7652-7659, 1994.

Todd A. Landry S. Pearson CE. Khoury V. Zannis-Hadjopoulos M. Deletion analysis of minimal sequence requirements for autonomous replication of ors8, a monkey early-replicating DNA sequence [published erratum appears in J Cell Biochem 1995 Apr;57(4):724]. Journal of Cellular Biochemistry. 57(2):280-9, 1995.

Toyn JH. Toone WM. Morgan BA. Johnston LH. The activation of DNA replication in yeast. [Review] Trends in Biochemical Sciences. 20(2):70-3, 1995.

Tsurimoto T. Melendy T. Stillman B. Sequential initiation of lagging and leading strand synthesis by two different polymerase complexes at the SV40 DNA replication origin. Nature. 346(6284):534-9, 1990.

Tsurimoto T. Stillman B. Purification of a cellular replication factor, RF-C, that is required for coordinated synthesis of leading and lagging strands during simian virus 40 DNA replication in vitro. Molecular & Cellular Biology. 9(2):609-19, 1989.

Tsurimoto T. Stillman B. Replication factors required for SV40 DNA replication in vitro. I. DNA structure-specific recognition of a primer-template junction by eukaryotic DNA polymerases and their accessory proteins. Journal of Biological Chemistry. 266(3):1950-60, 1991a.

Tsurimoto T. Stillman B. Replication factors required for SV40 DNA replication in vitro. II. Switching of DNA polymerase alpha and delta during initiation of leading and lagging strand synthesis. Journal of Biological Chemistry. 266(3):1961-8, 1991b.

Tullis GE. Burger LR. Pintel DJ. The minor capsid protein VP1 of the autonomous parvovirus minute virus of mice is dispensable for encapsidation of progeny single-stranded DNA but is required for infectivity. Journal of Virology. 67(1):131-41, 1993.

Turchi JJ. Bambara RA. Completion of mammalian lagging strand DNA replication using purified proteins. Journal of Biological Chemistry. 268(20):15136-41, 1993.

Umek RM. Linskens MH. Kowalski D. Huberman JA. New beginnings in studies of eukaryotic DNA replication origins. [Review] Biochimica et Biophysica Acta. 1007(1):1-14, 1989.

Virta-Pearlman VJ. Gunaratne PH. Chinault AC. Analysis of a replication initiation sequence from the adenosine deaminase region of the mouse genome. Molecular & Cellular Biology. 13(10):5931-42, 1993.

Waga S. Bauer G. Stillman B. Reconstitution of complete SV40 DNA replication with purified replication factors. Journal of Biological Chemistry. 269(14):10923-34, 1994.

Waga S. Stillman B. Anatomy of a DNA replication fork revealed by reconstitution of SV40 DNA replication in vitro. Nature. 369(6477):207-12, 1994.

Walker SS. Francesconi SC. Eisenberg S. A DNA replication enhancer in Saccharomyces cerevisiae. Proceedings of the National Academy of Sciences of the United States of America. 87(12):4665-9, 1990.

Walker SS. Malik AK. Eisenberg S. Analysis of the interactions of functional domains of a nuclear origin of replication from Saccharomyces cerevisiae. Nucleic Acids Research. 19(22):6255-62, 1991.

Wang TA. Li JJ. Eukaryotic DNA replication. [Review] Current Opinion in Cell Biology. 7(3):414-20, 1995.

Ward P. Berns KI. In vitro rescue of an integrated hybrid adeno-associated virus/simian virus 40 genome. Journal of Molecular Biology. 218(4):791-804, 1991.

Weinberg DH. Collins KL. Simancek P. Russo A. Wold MS. Virshup DM. Kelly TJ. Reconstitution of simian virus 40 DNA replication with purified proteins. Proceedings of the National Academy of Sciences of the United States of America. 87(22):8692-6, 1990.

Wessel R. Schweizer J. Stahl H. Simian virus 40 T-antigen DNA helicase is a hexamer which forms a binary complex during bidirectional unwinding from the viral origin of DNA replication. Journal of Virology. 66(2):804-15, 1992.

Willwand K. Hirt B. The major capsid protein VP2 of minute virus of mice (MVM) can form particles which bind to the 3'-terminal hairpin of MVM replicative-form DNA and package single-stranded viral progeny DNA. Journal of Virology. 67(9):5660-3, 1993.

Willwand K. Hirt B. The minute virus of mice capsid specifically recognizes the 3' hairpin structure of the viral replicative-form DNA: mapping of the binding site by hydroxyl radical footprinting. Journal of Virology. 65(9):4629-35, 1991.

Willwand K. Kaaden OR. Proteins of viral and cellular origin bind to the Aleutian disease virus (ADV) DNA 3'-terminal hairpin: presentation of a scheme for encapsidation of ADV DNA. Journal of Virology. 64(4):1598-605, 1990.

Wilson GM. Jindal HK. Yeung DE. Chen W. Astell CR. Expression of minute virus of mice major nonstructural protein in insect cells: purification and identification of ATPase and helicase activities. Virology. 185(1):90-8, 1991.

Wold MS. Li JJ. Kelly TJ. Initiation of simian virus 40 DNA replication in vitro: large-tumor-antigen- and origin-dependent unwinding of the template. Proceedings of the National Academy of Sciences of the United States of America. 84(11):3643-7, 1987.

Wu C. Zannis-Hadjopoulos M. Price GB. In vivo activity for initiation of DNA replication resides in a transcribed region of the human genome. Biochimica et Biophysica Acta. 1174(3):258-66, 1993.

Yeung DE. Brown GW. Tam P. Russnak RH. Wilson G. Clark-Lewis I. Astell CR. Monoclonal antibodies to the major nonstructural nuclear protein of minute virus of mice. Virology. 181(1):35-45, 1991.